IRIDIUM CATALYZED ALKANE DEHYDROGENATION, OLEFIN ISOMERIZATION AND RELATED CHEMISTRY

by

AMLAN RAY

A Dissertation submitted to the

Graduate School-New Brunswick

Rutgers, The State University of New Jersey

in partial fulfillment of the requirements

for the degree of

Doctor of Philosophy

Graduate Program in Chemistry

written under the direction of

Professor Alan S. Goldman

and approved by

_____

_____

_____

_____

New Brunswick, New Jersey

October, 2007

ABSTRACT OF THE DISSERTATION

IRIDIUM CATALYZED ALKANE DEHYDROGENATION, OLEFIN ISOMERIZATION AND RELATED CHEMISTRY

By AMLAN RAY

Dissertation Director:

Professor Alan S. Goldman

Excellent alkane dehydrogenation activity exhibited by the pincer-ligated iridium complexes of the type – (X-^{R}PCP)IrH_2 (X-^{R}PCP = 4-X-C_6H_2-2,6-$(CH_2PR_2)_2$ with X = H, MeO; R = ^{t}Bu, ^{i}Pr) was exploited to functionalize a variety of aliphatic polyolefins *via* catalytic dehydrogenation. Of the two (MeO-^{R}PCP)IrH_2 complexes (**2** : R = ^{t}Bu and **3** : R = ^{i}Pr) used for the study, **3** was found to be an extremely active system for dehydrogenation of poly(1-hexene), giving 100% conversion with respect to the initial concentration of norbornene (acceptor) used. The catalysts exhibited selectivity for dehydrogenation of polymer branches over the backbone, with a kinetic selectivity for terminal position of the branches.

Isomerization of 1-octene conducted with iridium-pincer complexes **1** ((H-^{tBu}PCP)IrH_2) **2** and **3**, having different steric and electronic tuning, suggested that a larger alkyl group (R) on the phosphines along with a stronger π-donating group on the pincer

aryl ring (X) resulted in lower rate and higher selectivity for isomerization. In a related study, insertion of an olefin into the Ir-H bonds of the complexes (H-^{tBu}PCP)Ir(H)(Y) were investigated using *cis*-1,2-dideutero-1-octene as the substrate. In presence of the substrate octene, some (H-^{tBu}PCP)Ir(H)(Y) complexes (Y = Ph, NHPh etc) showed labile behavior in solution, being present in equilibrium with a (H-^{tBu}PCP)Ir(H)(1-octene) complex. Results of kinetic experiments suggested that π-donating Y groups enhanced the rate of olefin insertion. DFT calculations carried out on the systems predicted a slight preference for a pathway in which olefin binds to the metal center in between H and Y with a *trans* arrangement to the PCP-aryl ring. The olefin bound 14-electron complex (PCP)Ir(1-octene) was characterized by low temperature ^{1}H and ^{31}P NMR.

A new pincer complex (Me_2N-^{tBu}PCP)IrH_2 (**4d**), having π-electron rich iridium center, was synthesized and investigated for catalytic dehydrogenation. Complex **4d**, was found to exhibit better selectivity and rate, as compared to the previously reported systems **1** and **2**, for transfer dehydrogenation of branched and *n*-alkanes. It was also found to be a robust, slightly more stable and highly efficient catalyst for acceptorless dehydrogenation of cyclodecane.

Dedication

To my Parents and Teachers

Acknowledgement

This thesis is the result of five and half years of my journey as a graduate student, during which I have been accompanied and assisted by many people. It is a great feeling that now I have the opportunity to express my thankfulness to all of them.

First and foremost I would like to express my sincere gratitude to my advisor, Prof. Alan S. Goldman, who has supported me throughout my thesis with his patience and professional guidance. Without his cheerful encouragement, strong personal support and continuous financial aid over the years, this thesis would not have been completed. For the invaluable academic training and independence that I have received under his supervision, the days of my graduate study at Rutgers will remain as the most priceless years of my education.

I would like to thank my committee members, Prof. Karsten Krogh-Jespersen, Prof. Kathryn Uhrich, Prof. John B. Sheridan, and also Prof. Harvey Schugar who served on my proposal committee, for their valuable time and helpful suggestions. I would like to specially acknowledge Prof. Krogh-Jespersen, Yuriy Choliy and Dr. Patrick Achord for supplementing, some of the systems I have worked on, with the theoretical calculations. Also, my sincere thankfulness goes to Dr. Tom Emge for the crystallographic analysis and Dr. Seho Kim for his great efforts and assistance with the NMR machines.

Dated back to Fall 2001, when I joined the group, I was blessed with a warm welcome from a friendly and helpful crowd of senior colleagues. I would specially like to mention the name of Dr. Kenton B. Renkema, for his generous assistance and valuable

discussions along with his patience and sincerity in teaching me a variety of experimental techniques during the initial years. I would also like to thank all the former and current group members - Dr. Keming Zhu, Dr. Mira Kanzelberger, Dr. Margaret Czerw, Dr. Xiawei Zhang, Elizabeth Pelczar, Louis Whaley, Sabuj Kundu, Soumik Biswas, Dr. Rajsekhar Ghosh, Dr. Ritu Ahuja, Dr. Long van Dinh, Zhuo Gao and David Laviska for their friendship and cooperation.

My sincere gratitude goes to Dr. Geoffrey Coates at Cornell University for providing the polymer samples (and also for conducting their further characterization) used in my study. I would also like to thank Dr. Yuri Kissin for sharing valuable ideas and for his kind assistance related to the work described in the first chapter of this thesis.

Beyond Chemistry, I would like to mention the names of two families, Dr. Amlan Ray & Rina Ray and Dr. Ajay Kayal & Manisha Kayal, for their valuable advices and encouragement, both professionally and personally, which helped me to sustain my social life and provided energy and vitality for my research as well.

I also feel a deep sense of gratitude to my grandmother, parents and brother. Without their persistent support and encouragement for higher study, I would not have reached here. I am also very grateful to my wife Wriddhi, for her love and care throughout my pursuit of the degree. Without her patience and understanding, during some of the most difficult moments in these years, my journey would have remained incomplete.

Table of Contents

Abstract ii

Dedication iv

Acknowledgement v

Table of Contents vii

List of Tables xiii

List of Illustration xv

Chapter 1 Introduction 1

References 13

Chapter 2 Catalytic dehydrogenation of aliphatic polyolefins 16

2.1 Introduction 17

2.2 Results and Discussions 21

2.2.1 Dehydrogenation with pincer catalysts 21

2.2.1.1 Dehydrogenation of poly(1-hexene) 23

2.2.1.2 Dehydrogenation of polyethylene 30

2.2.1.3 Dehydrogenation of polyethylene-co-1-octene 33

2.2.1.4 Dehydrogenation of syndiotactic polypropylene 37

2.3 Conclusion 44

2.4 Experimental 45

2.5 References 46

Chapter 3 Isomerization of linear α-olefins catalyzed by pincer-ligated iridium dihydride complexes - (X-^{R}PCP)IrH$_2$ 49

3.1 Introduction 50

3.2 Results and Discussions 53

3.2.1 Olefin isomerization with (X-^{R}PCP)IrH$_2$ complexes 53

3.2.1.1 Steric effect on rate and selectivity – comparison between complexes with X = MeO; R = ^{t}Bu (**2**) and R = ^{i}Pr (**3**) 55

3.2.1.2 Electronic effect on rate and selectivity – comparison between complexes with R = ^{t}Bu; X = H (**1**) and R = MeO (**2**) 57

3.3 Conclusion 59

3.4 Experimental 60

3.4.1 General procedures 60

3.4.2 Isomerization experiment 60

3.5 References 62

Chapter 4 Synthesis and alkane dehydrogenation activity of a π-electron rich pincer-ligated iridium complex 63

4.1 Introduction 64

4.2 Results and Discussions 73

4.2.1 Synthesis of different pincer complexes (X-^{R}PCPIrH_2) used for the study 73

4.2.1.1 Synthesis of (H-^{tBu}PCP)IrH_4 (**1c**) 73

4.2.1.2 Synthesis of (MeO-^{tBu}PCP)IrH_4 (**2c**) (MeO-^{tBu}PCP)IrH_2 (**2d**) 73

4.2.1.3 Synthesis of (Me_2N-^{tBu}PCP)IrH_4 (**4c**) (Me_2N-^{tBu}PCP)IrH_2 (**4d**) 74

4.2.2 Comparative study of alkane transfer-dehydrogenation catalyzed by different pincer complexes (X-^{tBu}PCP)IrH_2 (X = H, MeO, Me_2N) 78

4.2.2.1 Transfer dehydrogenation of *n*-octane 81

4.2.2.2 Transfer dehydrogenation of 4-propylheptane 85

4.2.3 Comparative study of acceptorless dehydrogenation of cyclic and linear alkanes catalyzed by different pincer complexes X-^{tBu}PCPIrH_2 (X = H, MeO, Me_2N) 89

4.2.3.1 Acceptorless dehydrogenation of cyclodecane (CDA) 91

4.2.3.2 Acceptorless dehydrogenation of *n*-undecane 96

4.2.3.3 Heterogeneous transfer dehydrogenation of cyclooctane 98

4.3 Conclusion 100

4.4 Experimental 101

4.4.1 General procedures 101

4.4.2 Transfer Dehydrogenation 102

4.4.2.1 Transfer dehydrogenation of n-octane 102

4.4.2.2 Transfer dehydrogenation of 4-propylheptane 103

4.4.3 Acceptorless Dehydrogenation 103

4.4.4 Synthesis of different pincer complexes (X-^{tBu}PCPIrH_2) and their precursors 104

4.4.4.1 Synthesis of (H-^{tBu}PCP)IrH_2 (**1d**) and (MeO-^{tBu}PCP)IrH_2 (**2d**) 104

4.4.4.2 Synthesis of dimethyl 5-dimethylaminoisophthalate (**7**) 105

4.4.4.3 Synthesis of 5-dimethylamino-1,3-benzenedimethanol (**8**) 105

4.4.4.4 Synthesis of 1,3-bis(bromomethyl)-5-dimethylaminobenzene (**9**) 106

4.4.4.5 Synthesis of 1,3-bis[di(t-butyl)phosphinomethyl]-5-dimethylaminobenzene (NMe_2-^{tBu}PCP-H) (**4a**) 106

4.4.4.6 Synthesis of (NMe_2-^{tBu}PCP)IrHCl 107

4.4.4.7 Synthesis of (NMe_2-^{tBu}PCP)IrH_4 (**4c**) and (NMe_2-^{tBu}PCP)IrH_4 (**4d**) 108

4.5 References 109

Chapter 5 **Study of olefin insertion into the Ir-H bonds of pincer complexes of the type (PCP)Ir(H)(Y)** **118**

5.1 Introduction 119

5.2 Results and Discussions 129

5.2.1 Experimental Results of Olefin Insertion 129

5.2.1.1 Synthesis of (PCP)Ir(H)(Y) complexes and the olefin 129

5.2.1.2 General insertion schemes with (PCP)Ir(H)(Y) and *cis*-1,2-dideutero-1-octene 130

5.2.1.3 Labile nature of certain (PCP)Ir(H)(Y) complexes 134

5.2.1.4 Study of olefin insertion using stable (PCP)Ir(H)(Y) complexes (Y = Cl, CCPh, OH, OPh) 136

5.2.1.5 Study of olefin insertion using (PCP)Ir(H)(Ph) and 3,3-dimethyl-1-butene (TBE) 142

5.2.2 DFT Calculations for Olefin Insertion 146

5.2.3 Study of 1-olefin bound ″(PCP)Ir″ fragment – the (PCP)Ir(1-octene) complex 152

5.3 Conclusion 157

5.4 Experimental 159

5.4.1 General procedures 159

5.4.2 Synthesis of *cis*-1,2-dideutero-1-octene (*cis-1,2-d_2*) 159

5.4.3 Synthesis of (PCP)Ir(H)(Y) complexes 160

5.4.3.1 Synthesis of (PCP)Ir(H)(Y) (Y = Cl, OH, Ph, NHPh, CCPh) 160

5.4.3.2 Synthesis of (PCP)Ir(H)(OPh) 160

5.5 References 162

CURRICULUM VITAE 163

Lists of tables

Table 4.1	Distributions of octenes (in mM) from transfer dehydrogenation of *n*-octane catalyzed by **1d**, **2d** and **4d** using 0.2 M norbornene	82
Table 4.2	Distributions of octenes (in mM) from transfer dehydrogenation of n-octane catalyzed by **2d** and **4d** using 0.5 M norbornene	84
Table 4.3	Acceptorless dehydrogenation of CDA catalyzed by (X-^{tBu}PCP)IrH_2	93
Table 4.4	Acceptorless dehydrogenation of CDA catalyzed by (X-^{tBu}PCP)IrH_2. Volatiles were pumped off and fresh CDA was added every 6h	95
Table 4.5	Acceptorless dehydrogenation of *n*-undecane catalyzed by (X-^{tBu}PCP)IrH_2	97
Table 4.6	Heterogeneous dehydrogenation of cyclooctane catalyzed by (X-^{tBu}PCP)IrH_2	99
Table 4.7	Crystal data and structure refinement for complex **4a**	112
Table 4.8	Selected bond lengths [Å] and angles [°] for complex **4a**	113
Table 4.9	Crystal data and structure refinement for (Me_2N-^{tBu}PCP)Ir(CO) co-crystallized with ortho-xylene	115
Table 4.10	Selected bond lengths [Å] and angles [°] for complex (Me_2N-^{tBu}PCP)Ir(CO)	116
Table 5.1	Rates of olefin insertion into the Ir-H bonds of (PCP)Ir(H)(Y) (50°C, *p*-xylene-d_{10})	140

Table 5.2 Relative energies (kcal $mole^{-1}$) of different species involved in the insertion/alkyl-Y elimination along pathway olefin-trans. TS-I = Transition State for olefin insertion, TS-E = Transition State for alkyl-Y elimination 149

Table 5.3 Relative energies (kcal $mole^{-1}$) of different species involved in the insertion/alkyl-Y elimination along pathway olefin-cis. TS-I = Transition State for olefin insertion, TS-E = Transition State for alkyl-Y elimination 150

List of illustrations

Scheme 1.1	Mechanism of alkane transfer dehydrogenation catalyzed by (^{R}PCP)IrH_2 using norbornene (NBE) as the acceptor	10
Scheme 2.1	Rhodium catalyzed regiospecific functionalization of polyethylethylene	20
Figure 2.1	Pincer catalysts used for the study	22
Figure 2.2	Structural resemblance between poly(1-hexene)and 4-propylheptane	24
Figure 2.3	^{1}H NMR spectra of the olefinic region during transfer dehydrogenation of 4-propylheptane and subsequent isomerization of olefinic bonds using **3**	25
Scheme 2.2	Dehydrogenation and subsequent isomerization in 4-propylheptane	26
Scheme 2.3	Catalytic dehydrogenation of poly(1-hexene)by Ir-pincer complexes	26
Figure 2.4	Distribution of terminal and disubstituted olefinic bonds introduced during PH dehydrogenation by catalyst **2** as a function of time	27
Figure 2.5	Consumption of norbornene over time with **2** and **3**	28
Figure 2.6	Type and concentration of olefinic bonds introduced during PH dehydrogenation by catalyst **3** as a function of time	29

Scheme 2.4	Catalytic dehydrogenation of polyethylene by Ir-pincer complexes	30
Figure 2.7	Comparison of the total concentration of different double bonds introduced in PH (broken line ----) and PE (solid line ——) by **2** and **3** under identical conditions	31
Figure 2.8	Total concentration of different double bonds introduced in PE using higher concentrations (15 mM) of pincer complexes **2** and **3**	32
Scheme 2.5	Catalytic dehydrogenation and subsequent isomerization of polyethylene-co-1-octene by complexes **2** and **3**	34
Figure 2.9	Type and concentration of olefinic bonds introduced during EOC dehydrogenation by catalyst **2** as a function of time	35
Figure 2.10	Type and concentration of olefinic bonds introduced during EOC dehydrogenation by catalyst **3** as a function of time	36
Scheme 2.6	Catalytic dehydrogenation and sequential transformation of syndiotactic polypropylene to give multi-block polymers with different fuctionality	38
Scheme 2.7	Catalytic dehydrogenation and subsequent isomerization of syndiotactic polypropylene by Ir-pincer complex **2**	39
Scheme 2.8	Catalytic dehydrogenation and subsequent isomerization of syndiotactic polypropylene by Ir-pincer complex **3**	40
Figure 2.11	Possible dehydrogenated alkenes from 2,4-dimethylpentane	41
Scheme 2.9	Competition reaction of 2,4-dimethylpentane with n-octane	43

	towards catalytic dehydrogenation by Ir-pincer complex **3**	
Scheme 3.1	Metal hydride addition-elimination mechanism of isomerization	51
Scheme 3.2	π-allyl mechanism of isomerization	52
Scheme 3.3	Insertion/β-H elimination mechanism for isomerization of 1-olefins by (X-^{R}PCP)IrH_2 complexes	54
Scheme 3.4	Isomerization of 1-octene using (X-^{R}PCP)IrH_2 complexes. R = ^{i}Pr, ^{t}Bu; X = H, MeO	55
Figure 3.1 (a)	Isomerization of 1-octene catalyzed by (MeO-^{tBu}PCP)IrH_2 (**2**)	56
Figure 3.1 (b)	Isomerization of 1-octene catalyzed by (MeO-^{iPr}PCP)IrH_2 (**3**)	56
Figure 3.2 (a)	Isomerization of 1-octene catalyzed by (H-^{tBu}PCP)IrH_2 (**1**)	58
Figure 3.2 (b)	Isomerization of 1-octene catalyzed by (MeO-^{tBu}PCP)IrH_2 (**2**)	58
Scheme 4.1	Dehydrogenation of cyclooctane catalyzed by $L_2IrH_2(\eta^2$-$O_2CCF_3)$ by photochemical method or in the presence of a hydrogen acceptor	65
Scheme 4.2	Transfer dehydrogenation of cyclooctane catalyzed by (^{tBu}PCP)IrH_2 using tert-butylethylene as the hydrogen acceptor	67
Scheme 4.3	Thermochemical dehydrogenation of cyclodecane catalyzed by (PCP)IrH_2 without the presence of a hydrogen acceptor	68
Figure 4.1	Possible variations of the ligand backbone in (X-^{R}PCP)IrH_2 complex	68
Figure 4.2	Different pincer complexes with varying X and R used for the study	69

Figure 4.3	Pincer iridium complexes and their related precursors with the assigned reference numbers	71
Scheme 4.4	Synthesis of iridium pincer complex (NMe_2-^{tBu}PCP)IrH_2 (**4d**)	72
Scheme 4.5	Synthesis of 1,3-bis(bromomethyl)-5-dimethylaminobenzene (**9**) starting from dimethyl 5-bromoisophthalate (**5**)	74
Scheme 4.6	Attempted synthesis of dimethyl 5-dimethylaminoisophthalate (**7**) using Eschweiler-Clarke methylation	75
Scheme 4.7	Reductive methylation of amines at room temperature using formaldehyde and sodium cyanoborohydride	76
Scheme 4.8	Reductive methylation of dimethyl 5-aminoisophthalate (**6**)	77
Scheme 4.9	Transfer dehydrogenation in the presence of a sacrificial acceptor	79
Figure 4.4	Mechanism of alkane transfer dehydrogenation catalyzed by (^{R}PCP)IrH_2 using norbornene (NBE) as the acceptor	80
Scheme 4.10	Transfer dehydrogenation of *n*-octane catalyzed by (X-^{tBu}PCP)IrH_2 complexes using norbornene as the sacrificial acceptor	81
Scheme 4.11	Transfer dehydrogenation and subsequent isomerization of 4-propylheptane catalyzed by (X-^{tBu}PCP)IrH_2 complexes using norbornene as the sacrificial acceptor	86
Figure 4.5	Consumption of NBE over time during dehydrogenation of 4-propylheptane catalyzed by **2d** and **4d**. Condition: 5 mM catalyst, 0.3 M NBE, 150 °C, *p*-xylene solution.	87

Figure 4.6	Distribution of olefinic products over time during dehydrogenation of 4-propylheptane catalyzed by **2d** (*para*-MeO) and **4d** (*para*-Me_2N). Circles indicate terminal olefinic product (**A**) (see Scheme 4.11) and triangles indicate internal disubstituted 2-olefinic product (**B**). Condition: 5 mM catalyst, 0.3 M NBE, 150 °C, *p*-xylene solution.	88
Scheme 4.12	Acceptorless dehydrogenation of cyclodecane catalyzed by (X-^{tBu}PCP)IrH_2	92
Scheme 4.13	Acceptorless dehydrogenation of *n*-undecane catalyzed by (X-^{tBu}PCP)IrH_2	96
Scheme 4.14	Heterogeneous transfer dehydrogenation of cyclooctane catalyzed by (X-^{tBu}PCP)IrH_2	98
Figure 4.7	Crystal structure of complex **4a**	111
Figure 4.8	Crystal structure of complex (Me_2N-^{tBu}PCP)Ir(CO)	114
Figure 4.9	Crystal structure of complex (Me_2N-^{tBu}PCP)Ir(CO) co-crystallized with ortho-xylene	117
Scheme 5.1	Generic steps for insertion of an olefin into a M-H bond	120
Scheme 5.2	Product distribution from thermal decomposition of di-n-butyl-2,2-d_2-bis (triphenylphosphine)-platinum(II)	121
Scheme 5.3	Insertion steps and kinetic parameters for styrene insertion into the Rh-H bond of $RhH_2Cl(PPh_3)_3$ (P = PPh_3, Ar = p-X-C_6H_4 where X = Cl, H, Me, OMe)	122
Scheme 5.4	Insertion of olefins into niobium-hydride bonds	123

Scheme 5.5	Comparative binding of olefins onto the niobium center relative to ethylene	124
Scheme 5.6	Schematic representation of the transition state of olefin insertion	125
Figure 5.1	Olefin insertion rates at 318 K for unbridged niobocene ethylene hydride complexes	125
Figure 5.2	Olefin insertion rates at 318 K for various bridged niobocene ethylene hydride complexes with alkyl substituents on the Cp rings	126
Figure 5.3	Possible steric and electronic tuning of (X-PCP)Ir(H)(Y) complex	128
Scheme 5.7	Synthesis of various (PCP)Ir(H)(Y) complexes starting from the (PCP)IrH_2	129
Scheme 5.8	Synthesis of cis-1,2-dideutero-1-octene by catalytic hydrogenation	130
Scheme 5.9	Generic scheme for 1,2 insertion of cis-1,2-dideutero-1-octene (cis-1,2-d_2) into an M-H bond and product (cis-1,2-H_2) formation via subsequentβ-D elimination. R = “n-hexyl” ; for reaction with (PCP)Ir(H)(Y) complex, M = “(PCP)Ir(Y)”	131
Scheme 5.10	Generic scheme for 2,1 insertion of cis-1,2-dideutero-1-octene (cis-1,2-d_2) into an M-H bond and possible product distribution (gem-1,2-H_2 , trans-1,2-d_2 , 2-octene-d_2) via C-C/M-C bond	133

	rotation and β-H/D elimination. R = “n-hexyl” and R′ = “n-pentyl” ; for reaction with (PCP)Ir(H)(Y) complex, M = “(PCP)Ir(Y)”.	
Scheme 5.11	Distribution of products used to measure the 1,2 and 2,1 insertion rates	134
Scheme 5.12	Equilibrium between (PCP)Ir(H)(Y) and (PCP)Ir(1-octene) in solution for certain HY	135
Figure 5.4	Kinetic plot for insertion of cis-1,2-d_2 into Ir-H bond of (PCP)Ir(H)(Cl)	138
Figure 5.5	Kinetic plot for insertion of cis-1,2-d_2 into Ir-H bond of (PCP)Ir(H)(CCPh)	138
Figure 5.6	Kinetic plot for insertion of cis-1,2-d_2 into Ir-H bond of (PCP)Ir(H)(OH)	139
Figure 5.7	Kinetic plot for insertion of cis-1,2-d_2 into Ir-H bond of (PCP)Ir(H)(OPh)	139
Scheme 5.13	Possible exchanged products on reaction of 3,3-dimethy-1-butene (TBE) with (PCP)Ir(H)(Ph)	143
Scheme 5.14	Distribution of exchanged products via hydrogenation-dehydrogenation sequence through catalytic amount of (PCP)IrH_2	144
Scheme 5.15	Equilibrium between (PCP)Ir(Ph)(D) and (PCP)Ir(NBE) leading to slower rate of exchange	146
Scheme 5.16	Olefin insertion/alkyl-Y elimination with olefin trans to PCP-	

	aryl ring - pathway olefin-trans - (alkyl groups on phosphines are omitted for clarity)	147
Scheme 5.17	Olefin insertion/alkyl-Y elimination with olefin cis to PCP-aryl ring - pathway olefin-cis - (alkyl groups on phosphines are omitted for clarity)	148
Figure 5.8	(PCP)Ir(1-octene) complex – planar and perpendicular view. ^{t}butyl groups on phosphines are omitted for clarity. R = hexyl.	153
Figure 5.9	Flipping of the π-bound olefin. ^{t}butyl groups on phosphines are omitted for clarity. R = hexyl.	155
Figure 5.10	Eyring plot obtained from the ^{31}P line-shape analysis for olefin flipping (■) and a combination of flipping and rotation (▲) processes in the (PCP)Ir(1-octene) complex	156

Chapter 1

Introduction

Alkanes are by far the most abundant and cheapest organic molecules, which are available to us from natural resources. Unfortunately, despite their easy access, due to the unavailability of a suitable method for controlled conversion of these hydrocarbons into economically attractive products, vast majority of these precious raw materials are burned as simple fuels for heating and transportation. Therefore, development of a method for selective transformation of these otherwise unreactive substrates (often referred to as the "Holy Grail of chemistry") could have a huge industrial impact and potentially constitute a powerful class of reactions. There are several articles in which various aspects of this diverse area has been reviewed.[1]

High inertness of alkanes, alluded by their common name 'paraffin' (derived from the Latin *parum* meaning "barely" and *affinitas* meaning "affinity") stems from the fact that the constituent atoms of alkanes are all being held together by strong and localized C-C and C-H bonds, so unlike olefins and alkynes these molecules have no empty orbitals of low energy or filled orbitals of high energy that could readily participate in a chemical reaction.

Transition metal chemists have been trying to tackle the issue of controlled activation of small, relatively inert molecules over past 50 years and a number of observations in the 1950s and 1960s gave some early direction to this broad field. Among the various approaches available to C-H activation at metal centers, oxidative addition reaction occurs quite commonly and has been found to be one of the most promising routes. One of the earliest and best-studied case of oxidative addition, although not of an alkane C-H bond, was reported by Vaska in 1962 and involved the addition of H_2 to the 16e square planar d^8 complex, $Ir(PPh_3)_2(CO)Cl$ (eq. 1).[2]

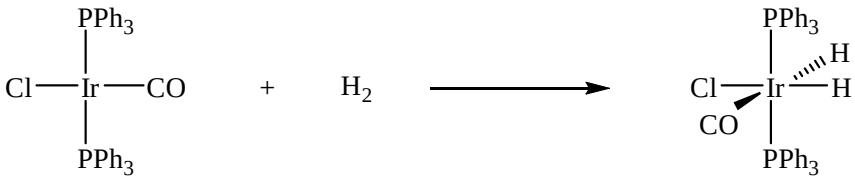

(1)

A few years later Chatt reported the first example of C-H activation by a transition metal complx. Electron rich ruthenium center of Ru(0)(dmpe) [dmpe = 1,2-bis(dimethylphosphino)ethane] was found to activate a C-H bond of a phosphinomethyl ligand of another molecule and also a C-H bond of naphthalein (eq. 2).[3] Soon thereafter Green reported that photoelimination of dihydrogen from Cp_2WH_2, in benzene, led to an aryl C-H bond activation (eq. 3).[4]

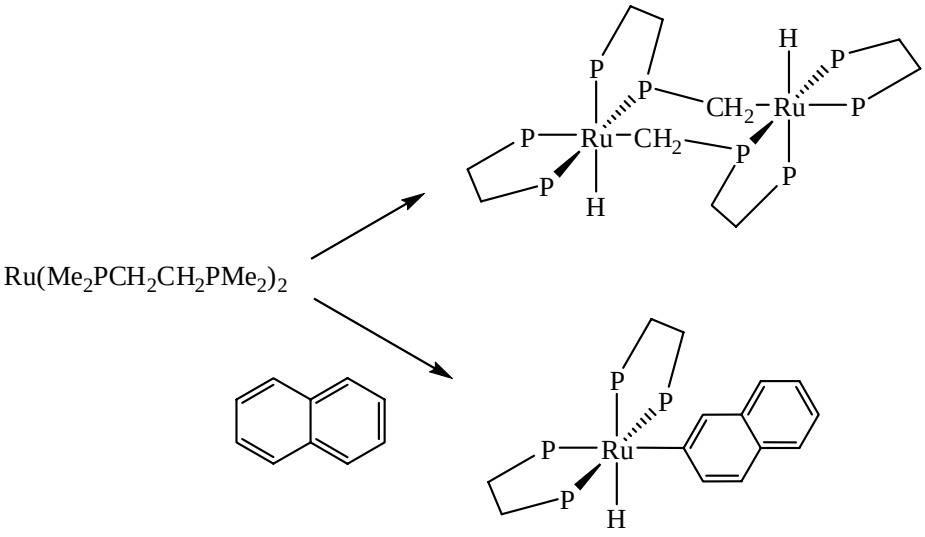

(2)

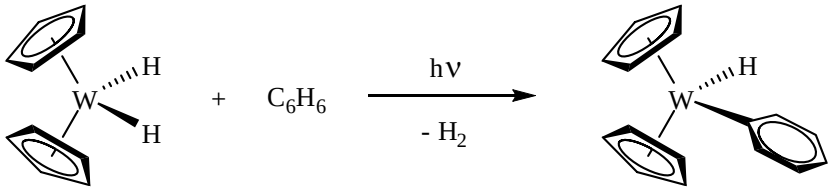

(3)

The first example of intermolecular addition of alkane C-H bonds to a transition metal complex giving a stable alkyl metal hydride was reported by Bergman (eq. 4)[5] and Graham (eq. 5)[6]. Both the reactions appreared to proceed via highly reactive d^8 Ir(I) intermediate that was generated photolytically, *in situ*, from the suitable precursors.

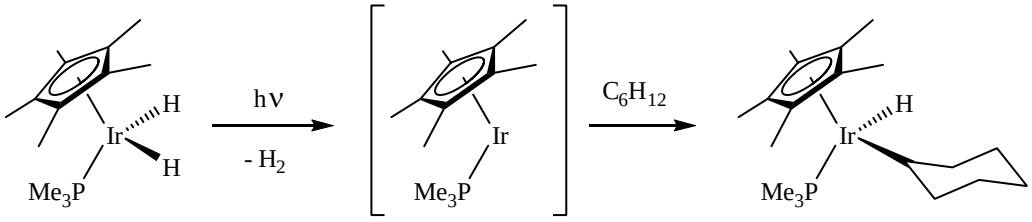

(4)

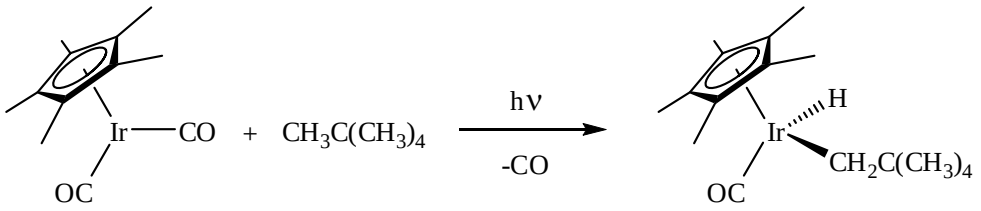

(5)

A major milestone in this field was achieved when Bergman demonstrated that besides having the ability to activate aliphatic C-H bonds, under relatively mild conditions, the $Cp^*Ir(PMe_3)$ metal center also exhibited striking selectivity by cleaving the stronger C-H bonds, preferentially (*e.g.* aryl > 1° > 2° >> 3°).[7] This discovery was a significant breakthrough since it was soon realized that transition metals, in contrast to most other reagents (*e.g.* free radicals), hold the great potential of functionalizing terminal and/or stronger C-H bonds.

A number of early (1960s and 1970s) examples of oxidative addition of C-H bonds to transition metals involved intramolecular addition of ligand C-H bonds (aryl or alkyl). For example, a few years after Chatt's discovery of the first C-H activation process using the $Ru(dmpe)_2$ system (eq. 2), cyclometalation of ligand aryl groups was reported (eq. 6).[8] Whitesides has shown that an aliphatic 'γ' C-H bond can undergo activation forming a metallacyclobutane system (eq. 7).[9]

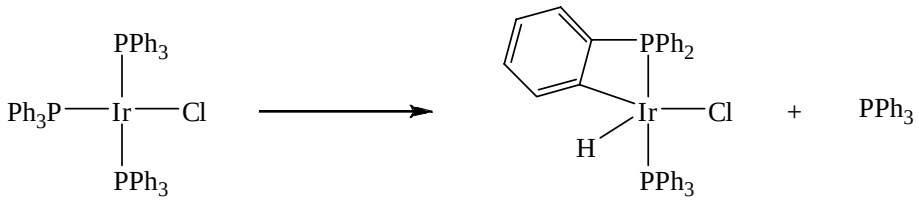

(6)

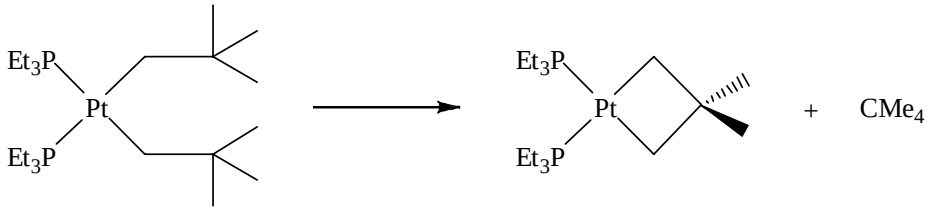

(7)

In 1976, Moulton and Shaw have demonstrated that utilizing the very favorably placed aryl C-H bond, in the ligand 1,2-bis[di-t-butylphosphino)methyl]benzene, the tridentate rhodium and iridium pincer (named after the particular coordination mode of this ligand) complexes can be synthesized (eq. 8).[10] Since then, the "pincer" system has attracted much attention and has been widely used for a variety of organometallic transformations (*e.g.* alkane dehydrogenation, Heck type coupling, activation of strong C-C and C-O bonds).[11,12]

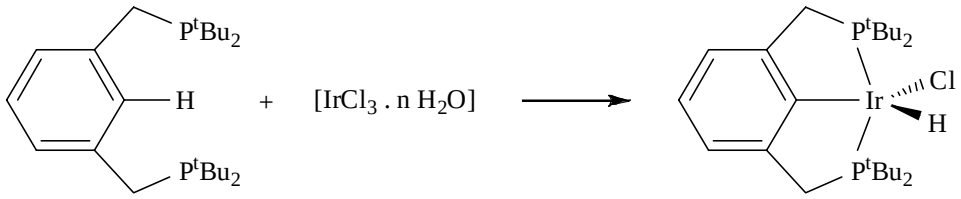

(8)

The metal "pincer" complexes besides possessing a high degree of thermal stability, exhibit a great balance of reactivity at the metal center, which can be finely adjusted, both sterically and electronically, by modification of various ligand parameters. Among the different varieties, iridium pincer complexes of the type (^{R}PCP)IrH$_2$ (where (^{R}PCP)Ir = [η^3-2,6-(CH$_2$PR$_2$)$_2$C$_6$H$_3$]Ir) have drawn much attention because of their promising activity in alkane dehydrogenation.[13]

Olefins are by far the most valuable feedstock in chemical industry because of their wide range of application in the manufacture of surfactants, synthetic rubber, lubricants, high purity commodity polymer and additives to gasoline. Several billion pounds of small aliphatic olefins like propene and isobutene are produced commercially via heterogeneous dehydrogenation of alkanes over supported chromium oxide, alumina or Pt catalysts. This process is not only energy-intensive (carried out at ~ 400°C - 700°C) but also has a significant drawback in terms of selectivity (the required high temperature often favors side reactions such as thermal cracking, hydrogenolysis, oligomerization and aromatization).[14] Therefore, development of a system for selective catalytic dehydrogenation of alkanes under relatively mild conditions could have a considerable industrial impact.

In 1979 Crabtree reported the first alkane dehydrogenation reaction, in which the cationic complex, $[(\text{acetone})IrH_2(PPh_3)_2]^+$, was found to catalyze dehydrogenation of cyclopentane and cyclooctane to give the corresponding cycloalkadiene iridium complexes.[15] 3,3-dimethyl-l-butene (*t*-butylethylene or TBE) was used as a hydrogen acceptor to overcome the large endothermicity of the dehydrogenation reaction (eq. 9).

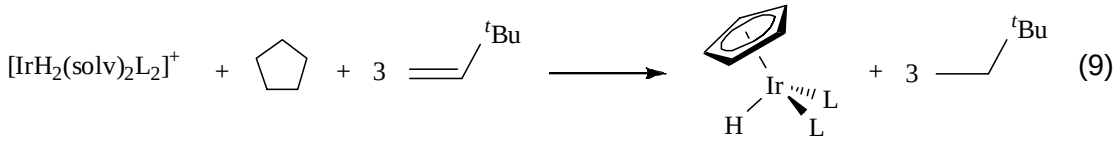

(9)

Immediately thereafter Baudry, Ephritikhine, and Felkin reported cycloalkane and *n*-pentane dehydrogenation using L_2ReH_7 (L = PPh_3, PEt_2Ph) and TBE as the acceptor.

Unfortunately, in all cases, the reactions were stoichiometric as the product olefin remained bound to the metal complex, preventing its re-entry into the catalytic cycle.[16] In 1983, the same group has shown that catalytic dehydrogenation of cycloalkanes (cyclohexane, methylcyclohexane) were possible, although catalyst decomposition limited the yield of olefin.[17]

A few years later, Crabtree reported the first catalytic alkane dehydrogenation system using $L_2IrH_2(\eta^2\text{-}O_2CCF_3)$.[18] Both cycloalkanes and *n*-alkanes were found to undergo dehydrogenation either in the presence of TBE as the sacrificial hydrogen acceptor or by activating the iridium complex photochemically. This was the first well-characterized system which had shown strong support for three-coordinate d^8 Ir(I) fragment as the intermediate, that undergoes oxidative addition with the alkanes followed by β-H elimination to give the product.

$Rh(PMe_3)_2(CO)Cl$ complex which was reported to catalyze the carbonylation of alkanes[19] was also found to be an effective photochemical alkane dehydrogenation catalyst in the absence of CO (eq. 10).[20,21] This could be considered as the first highly efficient alkane dehydrogenation catalyst, giving turnovers much higher than the previously reported systems.

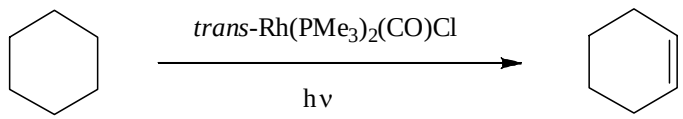

(10)

Mechanistic studies by Goldman[21] and Ford[22] have proved that 14-electron "$Rh(PMe_3)_2Cl$" fragment, formed via photo-expulsion of CO, acts as the intermediate in the catalytic cycle. However, generation of thermochemical precursor of "$Rh(PMe_3)_2Cl$" failed as it led to the formation of an inactive dimer, $[Rh(PMe_3)_2Cl]_2$. Interestingly, it was found that H_2 can break this dimer to produce $H_2Rh(PMe_3)_2Cl$, which can effect the transfer dehydrogenation.[23] Unfortunately though, the presence of H_2 led to hydrogenation of more than one equivalent of acceptor per equivalent of dehydrogenated product. In order to obviate the need of dihydrogen and keep the metal centers from dimerizing, the rhodium pincer complex (PCP)Rh was investigated; but, that was found to be a very poor dehydrogenation catalyst.[24]

Soon thereafter, Jensen and Kaska found that the iridium pincer complex however, gave very good turnover numbers for dehydrogenation of a number of cycloalkanes (eq. 11).[25] Efficient and robust nature of this catalyst was exhibited by the fact that the reactions were found to be 100% complete in terms of the amount of acceptor (TBE) used and long-term stability of the complex at temperatures as high as 200°C.

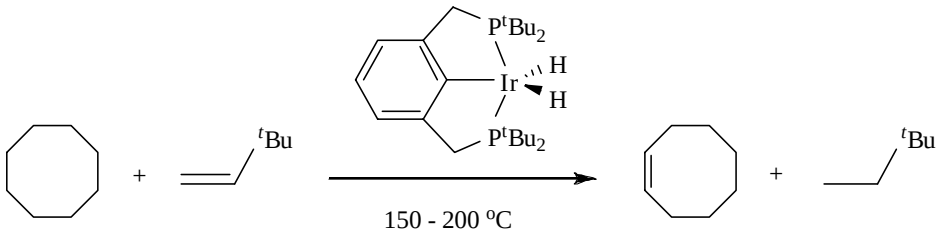

(11)

This high temperature stability of the system was a significant improvement (turnover numbers for many of the earlier dehydrogenation catalysts were limited by the ligand decomposition at elevated temperatures) and gave indication that it could be possible to overcome the barrier for alkane dehydrogenation thermally, without using a hydrogen acceptor. This was indeed found to be true when (^{tBu}PCP)IrH$_n$ has been used successfully to catalyze the acceptorless dehydrogenation of cycloalkanes. The sterically less hindered ^{i}Pr analogue was proved to be an even better catalyst, yielding turnover numbers much higher than any previously reported systems (eq. 12).[26]

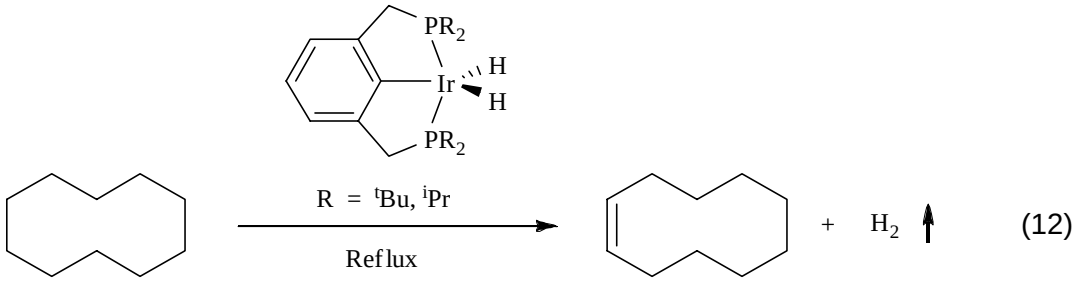

(12)

Remarkably, these catalyst systems were found to effect the regioselective dehydrogenation of *n*-alkanes giving terminal olefins as the major kinetic product.[27] The mechanisms for both transfer[28] and acceptorless[29] dehydrogenation cycles have been investigated. Scheme 1.1 depicts the catalytic cycle for transfer dehydrogenation using norbornene as the sacrificial acceptor. The 3-coordinate d^8 "(^{R}PCP)Ir" fragment is believed to be the key intermediate, which adds oxidatively to an alkane, followed by β-H elimination giving the product. The 14-electron reactive intermediate, "(^{R}PCP)Ir", has also been found to add to aryl C-H bonds[30] and the O-H bond[31] of water at room temperature.

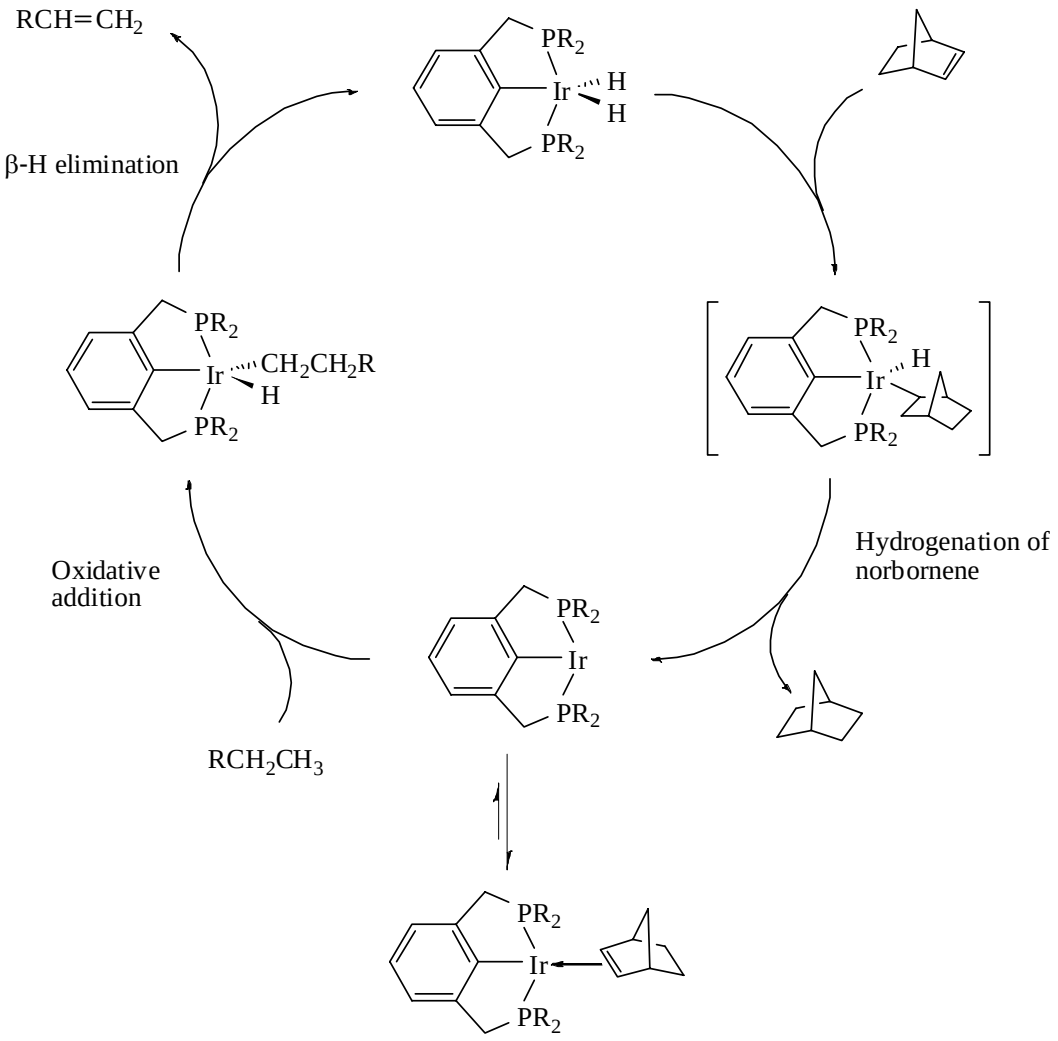

Scheme 1.1 Mechanism of alkane transfer dehydrogenation catalyzed by (^{R}PCP)IrH$_2$ using norbornene (NBE) as the acceptor

The iridium pincer complex, ($^{t\text{Bu}}$PCP)IrH$_2$, has also been found to be an effective catalyst for transfer dehydrogenation of ethylbenzene to styrene, tetrahydrofuran to furan,[32] alcohols to ketones or aldehydes,[33] secondary amines to imines[34] and tertiary amines to enamines.[35]

In this thesis, Chapter two is centered on catalytic transfer dehydrogenation of different aliphatic polyolefins to give partially unsaturated polymers. Of the two catalyst systems used to investigate the dehydrogenation, in presence of norbornene as the sacrificial acceptor, a sterically less hindered iridium-pincer complex has been found to be more active for introducing C=C double bonds into the saturated macromolecules. The catalysts have been found to exhibit selectivity for dehydrogenation of branches over backbones. Additionally, kinetic selectivity of these catalysts for terminal positions of alkanes have been exhibited by a very low activity for dehydrogenation of polyethylene compared to that of poly(1-hexene). Chapter three is focused on the steric and electronic effects exerted by different substituents on the pincer ligand backbone, towards rate and selectivity exhibited by the iridium-pincer complexes for isomerization of 1-olefins. A larger alkyl group on the phosphines along with a stronger π-electron donating group on the pincer aryl ring have been found to lower the rate of isomerization along with an increasing selectivity for 1-olefin $\rightarrow$ 2-olefin over 2-olefin $\rightarrow$ 3-olefin isomerization. Initiated by this result, a strongly π-electron donating pincer ligand and the corresponding iridium complex was synthesized, which was discussed in Chapter four. The new complex, bearing NMe_2 group on the pincer aryl ring, *para* to iridium was found to exhibit better rate and selectivity for transfer dehydrogenation of branched and *n*-alkanes, as compared to the ones previously reported. The new catalyst have also been found to be more robust and stable at a high temperature, relative to other iridium-pincer complexes, exhibiting higher rate and turnover for acceptorless dehydrogenation of cyclodecane. In the last Chapter, five, factors influencing the rate of olefin insertion into the Ir-H bonds of the complexes, (PCP)Ir(H)(Y), on varying Y are investigated. Preliminary results

suggested π-donating Y groups led to higher insertion rate. DFT calculations carried out on the (PCP)Ir(H)(Y) systems indicated a slight preference for the pathway in which olefin binds to the metal center in between H and Y with a *trans* arrangement to the PCP-aryl ring.

References:

1. (a) Sen, *A. Acc. Chem. Res.* **1998**, *31*, 550. (b) Jones, W. D. *Science* **2000**, *287*, 1942. (c) Crabtree, R. H. *J. Chem. Soc., Dalton Trans.* **2001**, *17*, 2437. (d) Labinger, J. A.; Bercaw, J. E. *Nature* **2002**, *417*, 507. (e) Kakiuchi, F.; Murai, S. *Acc. Chem. Res.* **2002**, *35*, 826. (f) Ritleng, V.; Sirlin, C.; Pfeffer, M. *Chem. Rev.* **2002**, *102*, 1731.

2. Vaska, L.; DiLuzio, J. W. *J. Am. Chem. Soc.* **1962**, *84*, 679.

3. Chatt, J.; Davidson, J. M. *J. Chem. Soc.* **1965**, 843.

4. Green, M. L. H.; Knowles, P. J. *J. Chem. Soc., Chem. Comm.* **1970**, 1677.

5. Janowicz, A. H.; Bergman, R. G. *J. Am. Chem. Soc.* **1982**, *104*, 352.

6. Hoyano, J. K.; Graham, W. A. G. *J. Am. Chem. Soc.* **1982**, *104*, 3723.

7. Bergman, R. G. *Science* **1984**, *223*, 902.

8. Bennett, M. A.; Milner, D. L. *Chem. Comm.* **1967**, 581.

9. Foley, P.; Whitesides, G. M. *J. Am. Chem. Soc.* **1979**, *101*, 2732.

10. Moulton, C. J.; Shaw, B. L. *J. Chem. Soc., Dalton Trans.* **1976**, 1020.

11. (a) van der Boom, M. E.; Milstein, D. *Chem. Rev.* **2003**, *103*, 1759. (b) Gozin, M.; Weisman, A.; Bendavid, Y.; Milstein, D. *Nature* **1993**, *364*, 699.

12. Albrecht, M.; van Koten, G. *Angew. Chem. Int. Ed. Engl.* **2001**, *40*, 3750.

13. (a) Xu, W.; Rosini, G. P.; Gupta, M.; Jensen, C. M.; Kaska, W. C.; Krogh-Jespersen, K.; Goldman, A. S. *Chem. Comm.* **1997**, 2273. (b) Liu, F.; Pak, E. B.; Singh, B.; Jensen, C. M.; Goldman, A. S. *J. Am. Chem. Soc.* **1999**, *121*, 4086.

14. Weckhuysen, B. M.; Schoonheydt, R. A. *Catalysis Today* **1999**, *51*, 223.

15. Crabtree, R. H.; Mihelcic, J. M.; Quirk, J. M. *J. Am. Chem. Soc.* **1979**,*101*, 7738.

16. Baudry, D.; Ephritikhine, M.; Felkin, H. *J. Chem. Soc., Chem. Comm.* **1980**, 1243.

17. Baudry, D.; Ephritikhine, M.; Felkin, H.; Holmes-Smith, R. *J. Chem. Soc., Chem. Comm.* **1983**, 788.

18. Burk, M. J.; Crabtree, R. H.; Parnell, C. P.; Uriarte, R. J. *Organometallics* **1984**, *3*, 816.

19. Sakakura, T.; Tanaka, M. *Chem. Lett.* **1987**, 249.

20. (a) Nomura, K.; Saito, Y. *Chem. Comm.* **1988**, 161. (b) Sakakura, T.; Sodeyama, T.; Tokunaga, M.; Tanaka, M. *Chem. Lett.* **1988**, 263.

21. Maguire, J. A.; Boese, W. T.; Goldman, A. S. *J. Am. Chem. Soc.* **1989**,*111*, 7088.

22. Spillett, C. T.; Ford, P. C. *J. Am. Chem. Soc.* **1989**, *111*, 1932.

23. Maguire, J. A.; Goldman, A. S. *J. Am. Chem. Soc.* **1991**, *113*, 6706.

24. Wang, K.; Goldman, M. E.; Emge, T. J.; Goldman, A. S. *J. Organomet. Chem.* **1996**, *518*, 55.

25. (a) Gupta, M.; Hagen, C.; Flesher, R. J.; Kaska, W. C.; Jensen, C. M. *Chem. Commun.* **1996**, 2083. (b) Gupta, M.; Hagen, C.; Kaska, W. C.; Cramer, R. E.; Jensen, C. M. *J. Am. Chem. Soc.* **1997**, *119*, 840.

26. (a) Xu, W.; Rosini, G. P.; Gupta, M.; Jensen, C. M.; Kaska, W. C.; Krogh-Jespersen, K.; Goldman, A. S. *Chem. Comm.* **1997**, 2273. (b) Liu, F.; Goldman, A. S. *Chem. Comm.* **1999**, 655.

27. Liu, F.; Pak, E. B.; Singh, B.; Jensen, C. M.; Goldman, A. S. *J. Am. Chem. Soc.* **1999**, *121*, 4086.

28. Renkema, K. B.; Kissin, Y. V.; Goldman, A. S. *J. Am. Chem. Soc.* **2003**, *125*, 7770.

29. Krogh-Jespersen, K.; Czerw, M.; Summa, N.; Renkema, K. B.; Achord, P. D.; Goldman, A. S. *J. Am. Chem. Soc.* **2002**, *124*, 11404.

30. Kanzelberger, M.; Singh, B.; Czerw, M.; Krogh-Jespersen, K.; Goldman, A. S. *J. Am. Chem. Soc.* **2000**, *122*, 11017.

31. Morales-Morales, D.; Lee, D. W.; Wang, Z. H.; Jensen, C. M. *Organometallics* **2001**, *20*, 1144.

32. Gupta, M.; Hagen, C.; Kaska, W. C. and Jensen, C. M. *J. Chem. Soc., Chem. Commun.* **1997**, 461.

33. Morales-Morales, D.; Redon, R.; Wang, Z. H.; Lee, D. W.; Yung, C.; Magnuson, K.; Jensen, C. M. *Can. J. Chem.* **2001**, *79*, 823.

34. Gu, X.-Q.; Chen, W.; Morales-Morales, D. and Jensen, C. M. *J. Mol. Cat. A*, **2002**, *189*, 119.

35. Zhang, X.; Fried, A.; Knapp, S.; Goldman, A. S. *Chem. Commun.* **2003**, 2060.

Chapter 2

Catalytic dehydrogenation of aliphatic polyolefins

Abstract

As an extension of the earlier work done in our laboratory on dehydrogenation of linear and cyclic alkanes using pincer-ligated iridium complexes, we have investigated the possibility of using the same complexes for dehydrogenation of aliphatic polyolefins. Functionalized polyolefins are a specific class of compounds with various potentially important commercial applications. There is no straightforward way to synthesize many functionalized polymeric compounds from their precursors using simple polymerization techniques. Catalytic dehydrogenation of aliphatic polyolefins presents a potential route to these functionalized polymers. Two pincer-ligated iridium complexes (4-MeO-C_6H_2-2,6-(CH_2PR_2)IrH_2 (R = ^{t}Bu **2**; R = ^{i}Pr **3**) have been used for the study and were found to cause dehydrogenation of a number of polymeric materials with varying rates. This was the first reported example of catalytic dehydrogenation of polyolefins giving partially unsaturated macromolecules. Importantly, both molecular weight and molecular weight distribution of the dehydrogenated polymers remain unchanged, indicating there was no chain scission or coupling that took place during the reaction.

2.1 Introduction

Polyolefins are a class of macromolecular alkanes produced by either homo- or co-polymerization of olefins such as ethylene and propylene. Commercially, these polymeric materials constitute a multibillion dollar per year industry with worldwide production in excess of 100 billion pounds. Despite already reaching this size and the commodity nature of the business, polyolefins are still one of the fastest-growing segments of the chemical industry.[1,2] Due to their high stability, excellent chemical resistance and broad-ranging mechanical properties, polyolefins have found widespread applications in *e.g.* lawn furniture, food packing, home appliances, automobile bumpers and medical and healthcare instruments. However, despite the successes and remarkable advances achieved in olefin polymerization over the past two decades, there are many applications for which these materials are poorly suited.[3] For example, due to the lack of polar functional groups along the backbone or the side-chain, these materials often show poor compatibility with oxygen- and nitrogen-containing polymers, polar pigments, and additives. This absence of polarity has limited the use of such polymers in applications that require, for example, good coating/adhesion characteristics.[4] Incorporation of functional groups into these otherwise nonpolar materials could alter important properties such as toughness, adhesion, barrier properties, surface properties (paintability, printability, etc.), solvent resistance (or its inverse) and miscibility with other polymers – thereby making them even more versatile.[5] Therefore, synthesis of polyolefins with specific types of functionality, with control of location and amount is an important frontier in polymer synthesis.

Of the many permutations available for incorporation of functional groups into these nonpolar materials, two main strategies are direct polymerization of functional olefins, and the post-polymerization modification of catalyst-tolerant and latent or protected functionalities (mostly limited to hindered alkenes, silyl-protected alcohols, aromatic groups, *etc.*). However, both these approaches have several drawbacks. Early transition metals, typically used in the polymerization catalysts are highly oxophilic in nature and tend to be readily deactivated by polar comonomers. Although catalysts based on late transition metals exhibit greater functional group tolerance and have been used successfully in some specific instances, smooth incorporation of various functional groups into polyolefins still remains a challenging area.[5,6] Additionally, due to the inherent difference in relative reactivity of the monomer pair with the propagating center, having a control over location and amount of functionality to be introduced also becomes a major hurdle in this approach. Moreover, most polymerization catalysts often tend to exhibit lower activities for copolymerization of olefins with polar comonomers than for homopolymerization of ethylene or other alkyl α-olefins, rendering the overall copolymerization process inefficient.[5]

A different strategy that can also be adopted to functionalize polyolefins is direct post-polymerization modification using free radicals, reactive intermediates (*e.g.* carbenes or nitrenes) or metal mediated methods.[4] The major benefits of this approach are (a) it would be possible to use any ordinary polyolefin as a starting material, (b) the degree of functional group incorporation can be adjusted as necessary (using stoichiometric amount of modification reagent) and finally, (c) transformations that are

possible to be carried out on a simple alkane could, in principle, be extrapolated to these macromolecular systems.

Historically, functionalization of alkanes has been achieved via free radical reactions.[7] Although these highly reactive species can effectively functionalize the otherwise inert alkanes, they typically tend to attack the weaker bonds in a hydrocarbon resulting in poor selectivity. Free radicals also typically initiate side reactions, such as β-scission, chain transfer and coupling, thereby reducing the efficiency of this synthetic approach.[8] These chain-coupling and chain breaking reactions can be especially detrimental to polymer modification systems, since they disrupt the molecular weight distribution of the polymer sample.

In the past, there have been attempts to functionalize polyethylene and polypropylene using UV radiation, [9a] laser ablation[9b] and various oxidants[9c-e] but most of these approaches met with limited success and often led to coupling and chain degradation.

Over the last few decades a great amount of research has been done towards developing transition-metal-based complexes for solution-phase functionalization of unreactive alkanes.[10] Very recently some of these reactions has been employed successfully into polyolefin systems for functionalization of the macromolecules. The first major breakthrough came in 2002 when Hartwig and Hillmyer showed that poly(1-butene) could be regioselectively functionalized using rhodium-catalyzed alkane

borylation to introduce boryl groups at the terminal position of branches followed by treatment with basic hydrogen peroxide in a mixture of THF and H_2O to oxidize the boronate ester groups to the corresponding alcohols (Scheme 2.1).[11] Depending on the proportion of borylating agent used, about 3-5% of functionalization was achieved per repeat unit. Polydispersity index (PDI) of the final hydroxylated materials remained largely unchanged, relative to the unfuctionalized material, except when high concentration of the borylating agent (1:1 with the polymer) was used (leading to slight increase in PDI due to chain coupling).

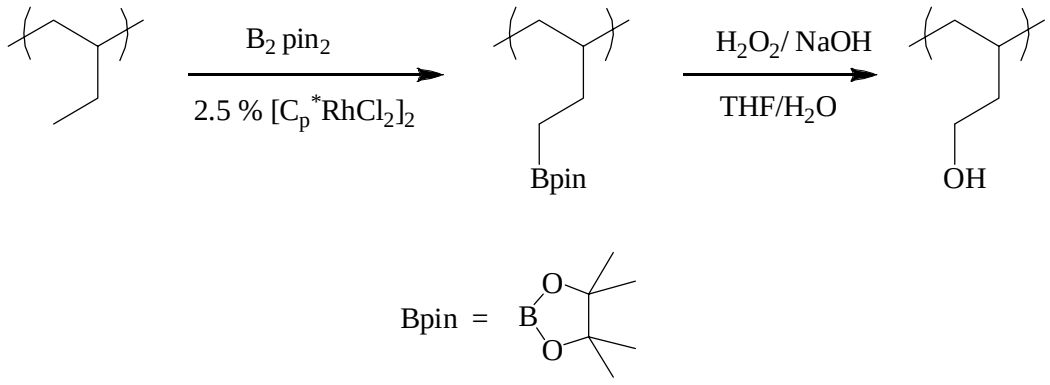

Scheme 2.1 Rhodium catalyzed regiospecific functionalization of polyethylethylene

The following year Boaen and Hillmyer reported the direct oxyfunctionalization of poly(ethylene-*alt*-propylene)(PEP) using a Mn(TDCPP)OAc (manganese *meso*-tetra-2,6-dichlorophenylporphyrin acetate)/imidazole system in the presence of Oxone (potassium peroxymonosulfate) as the oxygen donor.[12] Functionalization was found to occur preferably at the 3° carbon center giving tertiary alcohol along with some ketonic product (1-3% functionality introduced per repeat unit). Size exclusion chromatography

(SEC) of the reaction products indicated essentially no chain degradation. Recently, Hartwig and Hillmyer have demonstrated that, using the same technique as was employed for the borylation and subsequent hydroxylation of polyethylethylene, polypropylene can also be functionalized (although to a lesser extent 0.5 – 1.5%) to give hydroxymethyl side chains.[13]

Catalytic dehydrogenation of saturated polymers could also be an attractive route to functionalize polyolefins since the possibility of derivatizing the resulting unsaturation in a polymer has been well established.[14] The introduction of C-C double bonds into aliphatic polymer chains could offer a starting point for a very diverse manifold of reactivity *e.g.*, a partially unsaturated polyolefin could be cross-linked using standard techniques to give materials with enhanced mechanical properties.[15]

2.2 Results and Discussions

2.2.1 Dehydrogenation with pincer catalysts

Significant progress has been made in the past two decades toward the development of soluble transition-metal based catalysts for the dehydrogenation of alkanes.[16,17] Pincer-ligated iridium complexes, (^{R}PCP)IrH_2 , showed particularly promising activity in this context, catalyzing dehydrogenation of linear or cyclic alkanes either with or without the use of a sacrificial olefin as hydrogen acceptor.[18] The transfer-dehydrogenation cycle is

believed to proceed via the 14e "(^{R}PCP)Ir" reactive fragment, which undergoes oxidative addition to the terminal C-H bond of an alkane followed by β-H elimination to give the dehydrogenated product.[19] The iridium pincer complex, ($^{t\text{Bu}}$PCP)IrH$_2$ (**1**), has also been found to be an effective catalyst for dehydrogenation of ethylbenzene to styrene and tetrahydrofuran to furan,[20a] secondary amines to imines[20b] and tertiary amines to enamines.[20c] Recent reports from our group have suggested that the more electron rich *p*-methoxy-substituted, (MeO-^{R}PCP)IrH$_n$ (n = 2, 4) systems are even more efficient for alkane dehydrogenation.[21] Amongst these catalysts, the sterically less hindered (MeO-$^{i\text{Pr}}$PCP)IrH$_n$, has been found to be one of the best alkane dehydrogenation systems to date and has exhibited unprecedented activity for acceptorless dehydrogenation of cyclodecane. These promising results of dehydrogenation obtained with small molecules using the Ir-pincer complexes, coupled with the absence of well studied efficient catalytic systems for polymer dehydrogenation, led us to investigate the pincer complexes **2** and **3** for poly(α-olefin) dehydrogenation.

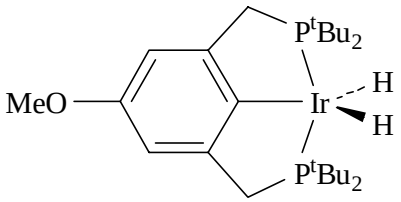

(MeO - $^{t\text{Bu}}$PCP)IrH$_2$ (**2**)

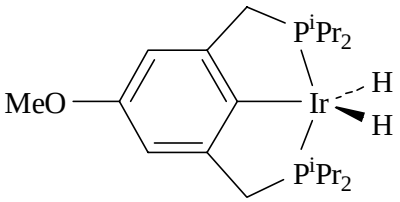

(MeO - $^{i\text{Pr}}$PCP)IrH$_2$ (**3**)

Fig 2.1 Pincer catalysts used for the study

2.2.1.1 Dehydrogenation of poly(1-hexene)

Poly(1-hexene) (PH) was synthesized in the laboratory of Prof. Geoffrey Coates, at Cornell University, using $(Cp(Me)_4Si(Me)_2N^tBu)TiCl_2$/methylaluminoxane giving a highly viscous atactic polymer with a number average molecular weight (M_n) of 6900 and polydispersity index (PDI) of 1.57.[22] *p*-Xylene solutions were prepared that were ~1 M in poly(1-hexene) repeat units, 5 mM in catalyst **2** and **3**, and approximately 0.2 M in norbornene (the sacrificial hydrogen-acceptor; NBE). Reactions were conducted in sealed tubes immersed in an oil bath maintained at 150 °C, and were periodically monitored by NMR. Trimethylphosphine in deuterated mesitylene and hexamethyldisiloxane were used as external and internal standards, respectively, for referencing and quantification purposes.

Initial ^{1}H NMR spectra of the dehydrogenated PH showed a number of peaks at different positions in the olefinic region due to dehydrogenation and subsequent isomerization. Although selectivity of the pincer complexes for the terminal position of an alkane has been reported[23] PH as a substrate contained primary, secondary and tertiary C-H bonds, any of which could theoretically be activated. Moreover, because of the broadness of ^{1}H NMR peaks it was difficult to assign them to any specific double bonds and thereby predict the type of unsaturation introduced. This led us to carry out the reaction on a simple system, one that we hoped would be more amenable to spectroscopic analysis.

We chose 4-propylheptane (Fig 2.2) as a model alkane for comparison with PH. The molecule being a simple and symmetrical one (a single 'C=C double bond' added to any position of this molecule would be unique in its nature - either terminal or disubstituted or trisubstituted) it would be expected to exhibit better resolution in the NMR spectra. The propyl group in the molecule serves as a model for the butyl branches in poly(1-hexene) and was expected to help in the study of the post-dehydrogenation isomerization kinetics in a simple branched system (Scheme 2.2).

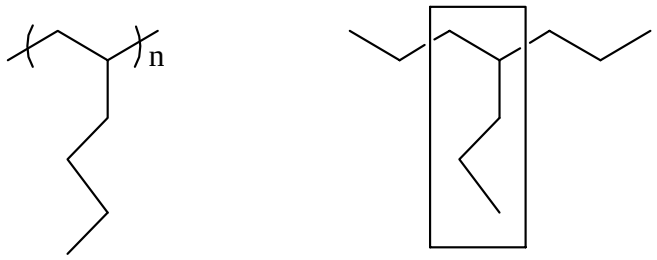

Figure 2.2 Structural resemblance between poly(1-hexene)and 4-propylheptane

Dehydrogenation carried out with 4-propylheptane in a solution of *p*-xylene-d_{10} using catalysts **2** and **3** revealed the formation of terminal alkene as the major kinetic product as indicated by multiplets at 5.1 and 5.8 ppm in ^{1}H NMR (Fig 2.3). Using (MeO-^{iPr}PCP)IrH_n (**3**) these 1-olefinic products were initially observable for only 5 min as they rapidly isomerized completely into the more stable internal olefins. With complex **2**, although similar isomerization took place, terminal double bonds were also present in the solution even after 24 h of reaction. Further heating saw the formation of trisubstituted double bonds (indicated by a triplet at 5.2 ppm in ^{1}H NMR), due to continued isomerization, after 240 min with **2** and after 40 min with **3**.

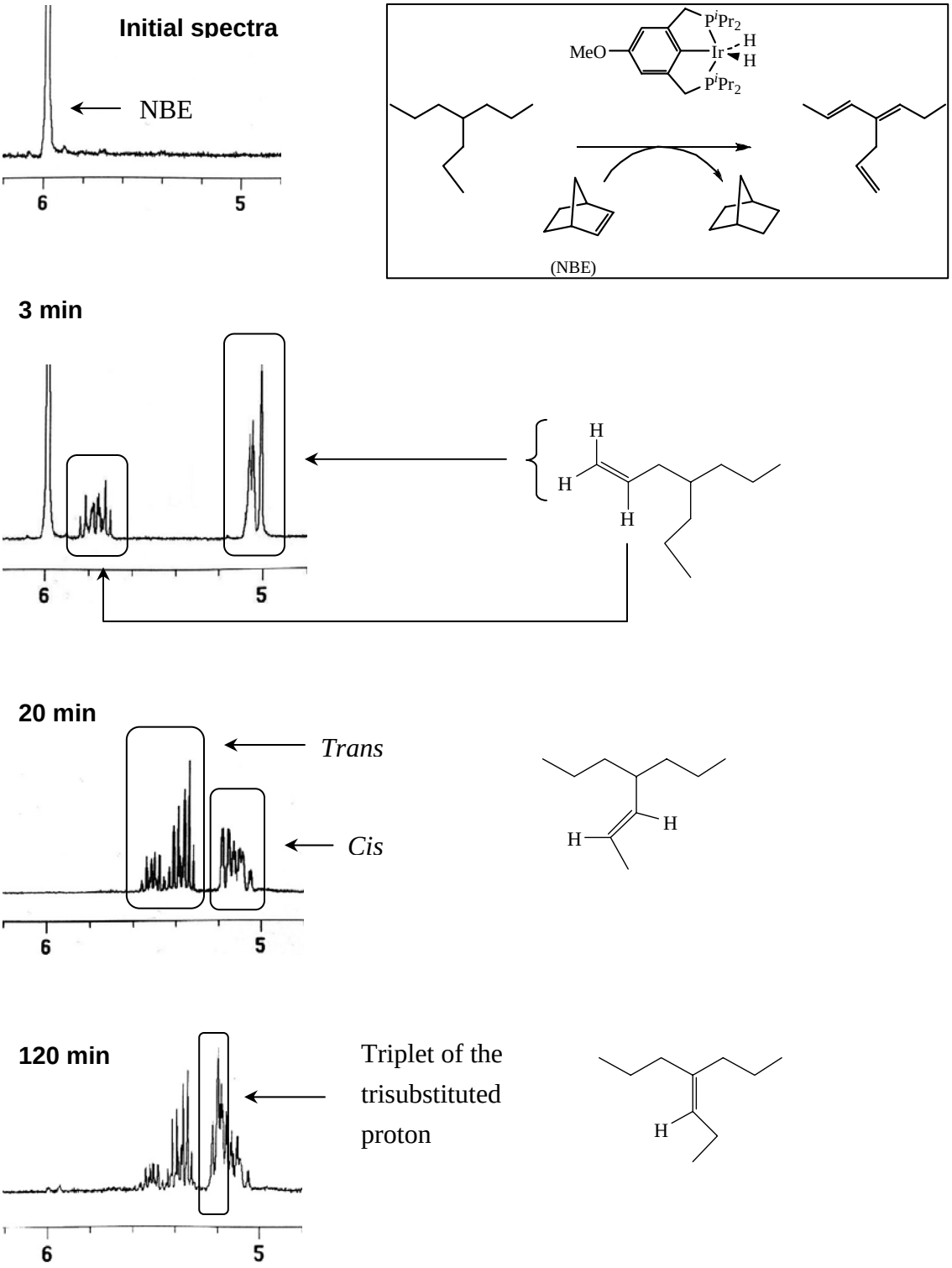

Fig 2.3 ^{1}*H NMR spectra of the olefinic region during transfer dehydrogenation of 4-propylheptane and subsequent isomerization of olefinic bonds using* ***3***

This initial comparison with 4-propylheptane helped us to establish the ^{1}H NMR peak positions in substituted olefinic compounds and thereby determine concentrations of different double bonds which were generated during the reaction with PH.

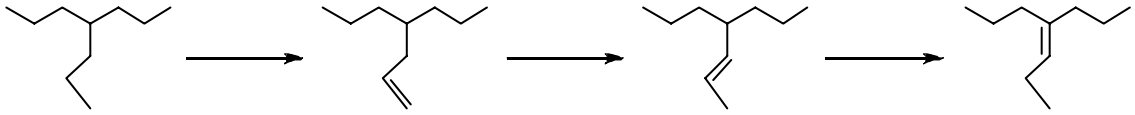

Scheme 2.2 Dehydrogenation and subsequent isomerization in 4-propylheptane

Heating a *p*-xylene solution of (MeO-^{tBu}PCP)IrH_2 (**2**; 5 mM), norbornene (0.21 M) and poly(1-hexene) (1.1 M in PH repeat units) at 150 °C for 20 minutes resulted in the loss of approximately 0.04 M norbornene. This led to commensurate appearance of terminal vinyl groups (0.01 M) and internal C-C double bonds (0.03 M) as indicated by ^{1}H spectra.

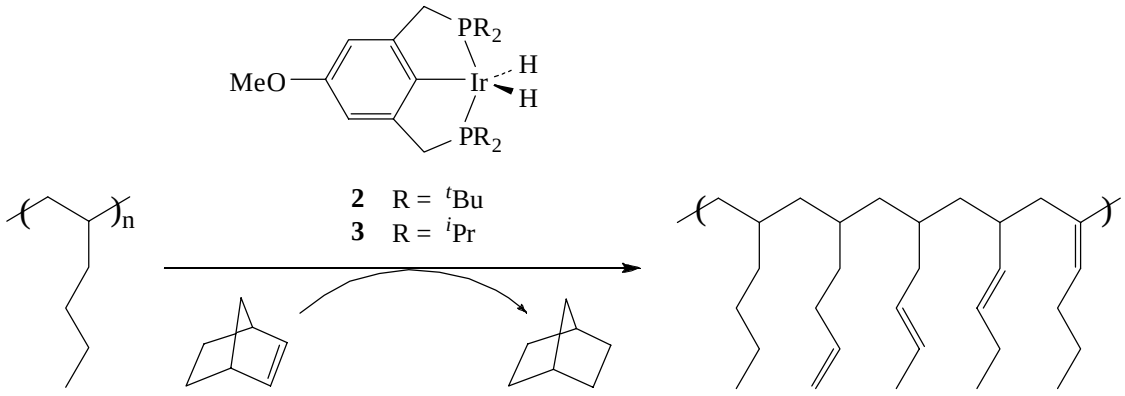

Scheme 2.3 Catalytic dehydrogenation of poly(1-hexene)by Ir-pincer complexes

Assignments of the peak positions were confirmed by results with 4-propylheptane and also by comparison with standard samples of 1-octene and cis and trans 2-octenes, respectively, under the reaction conditions. Presumably the major kinetic product was polymer dehydrogenated at the terminal position of branches, but isomerization was also fast under these conditions.

Subsequent heating resulted in an increased concentration of internal C-C double bonds with an approximate steady state concentration of terminal double bonds (Fig 2.4). After 260 min roughly 60% of the norbornene was consumed yielding 0.13 M double bonds, of which 7 mM was terminal.

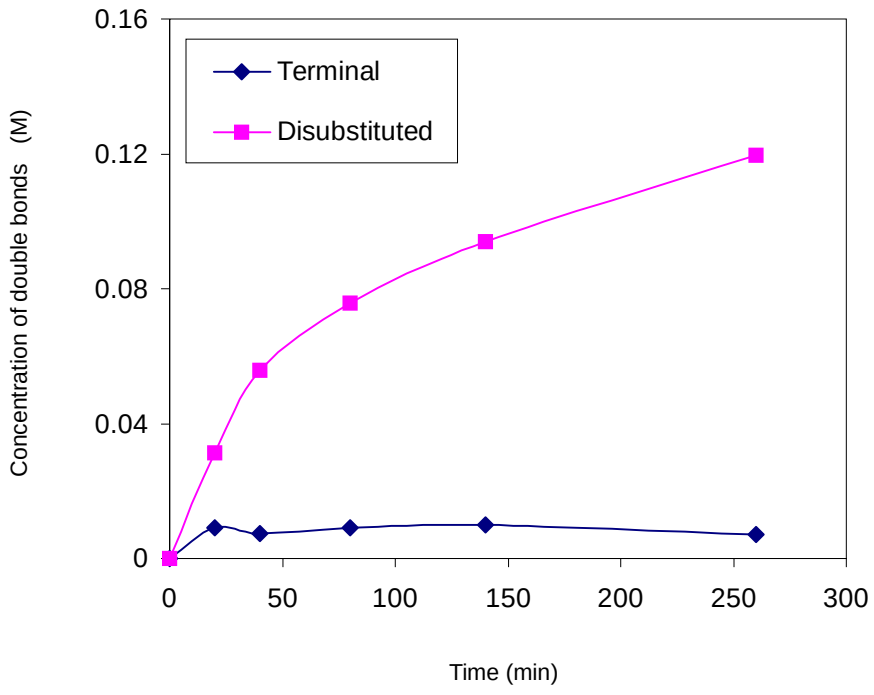

*Fig 2.4 Distribution of terminal and disubstituted olefinic bonds introduced during PH dehydrogenation by catalyst **2** as a function of time*

Further heating did not result in additional buildup of olefinic bonds indicating catalyst decomposition at this point.[24] This final concentration of total C-C double bonds, 0.13 M, represents *ca.* 14% dehydrogenation of the hexene units present in solution.

As mentioned previously, (MeO-^{iPr}PCP)IrH$_n$ (**3**) was found to be a more active catalyst for transfer-dehydrogenation of *n*-alkanes than the bis(t-butyl)phosphino analogue.[21] In agreement with that result, it has been found, under identical conditions using 0.22 M NBE, transfer-dehydrogenation of PH with **3** proceeded at a much faster rate compared to **2**; *ca.* 50% of the NBE was consumed within 10 min at 150 °C (Fig 2.5).

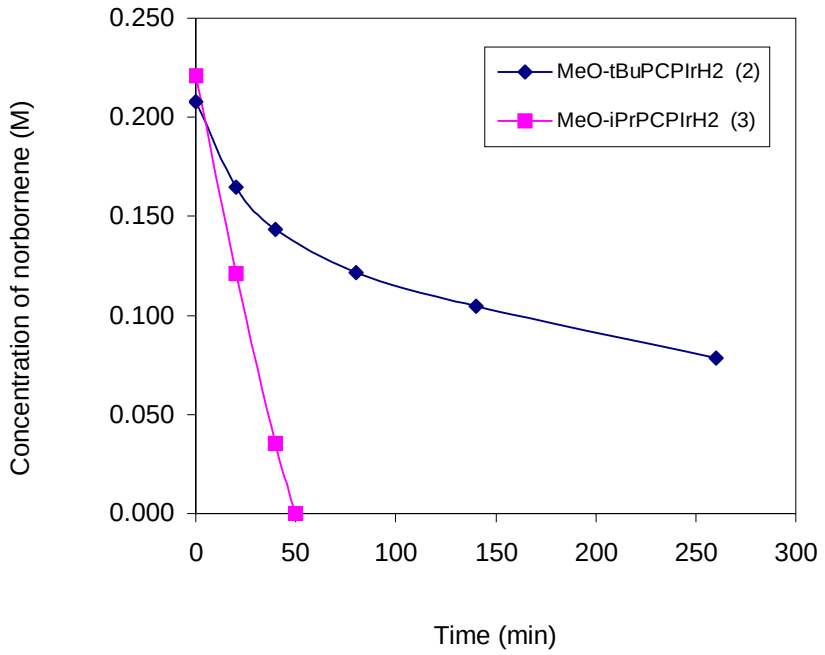

*Fig 2.5 Consumption of norbornene over time with **2** and **3***

At this point concentrations of terminal and internal double bonds produced were 0.039 M and 0.056 M respectively. After 50 min, norbornene was completely consumed and the resulting concentration of double bonds introduced into the polymer corresponded to 19% of hexene units. Isomerization, relative to dehydrogenation, is even more rapid with **3** than with **2**; no terminal vinyl groups were observed in the ^{1}H NMR spectrum after 50 min. Further, the use of complex **3**, unlike **2**, led to the formation of trisubstituted and conjugated double bonds, as confirmed by comparison with product of dehydrogenation of 4-propylheptane (vinylic proton at δ 5.19 ppm in ^{1}H NMR). Fig 2.6, below, shows the distribution of different olefinic bonds introduced in PH, on reaction with complex **3**.

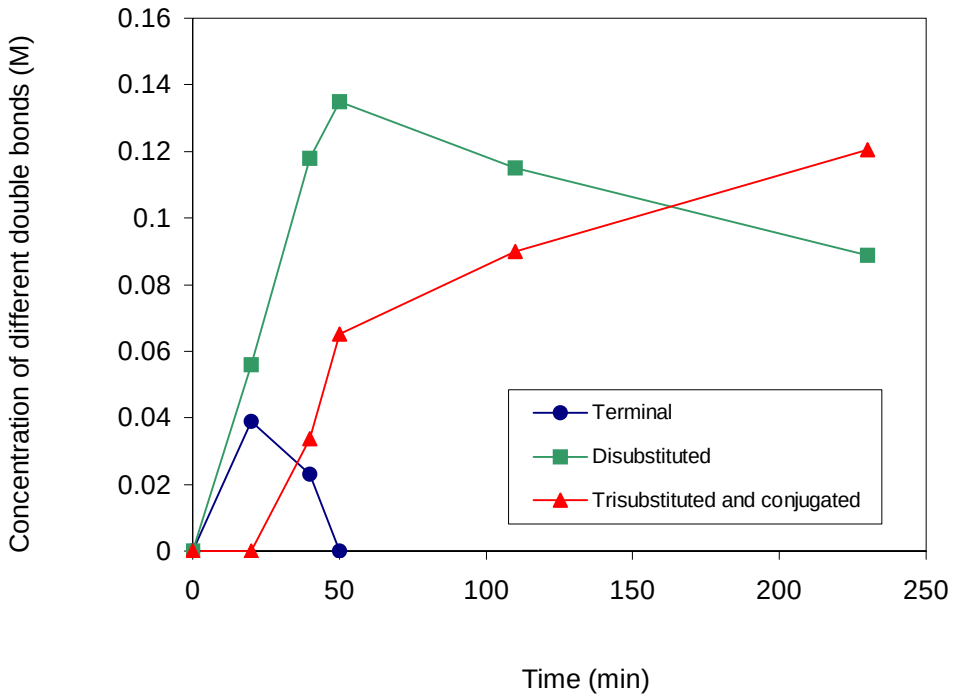

*Fig 2.6 Type and concentration of olefinic bonds introduced during PH dehydrogenation by catalyst **3** as a function of time*

Importantly, the MW of the polymer chains was unaffected by the dehydrogenation. Gel-permeation chromatography (GPC) measurements of the material before and after dehydrogenation revealed no significant difference in M_n (6540 vs. 6680) or M_w (10250 vs. 10680). Measurements on the dehydrogenated sample were made using both refractive index and UV detectors, whereas the parent saturated polymer was UV-silent; this is an indication of the possible applications of dehydrogenation with respect to polymer analysis as well as the synthesis of new materials.

2.2.1.2 Dehydrogenation of polyethylene

Linear low-density polyethylene (PE) (M_W = 4000, PDI = 2.35) was purchased from Aldrich and used without further purification. Low-MW material was used to achieve good solubility and low viscosity, conducive to reaction conditions and monitoring by NMR.

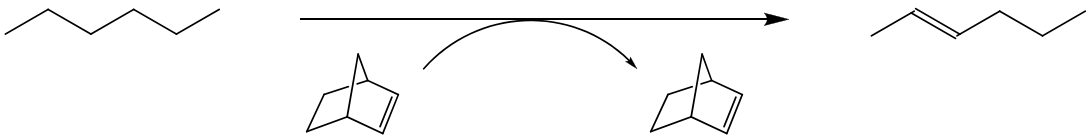

Scheme 2.4 Catalytic dehydrogenation of polyethylene by Ir-pincer complexes

Polyethylene was found to be a much less reactive substrate than poly(1-hexene) towards dehydrogenation. Heating a solution of **2** (5 mM), NBE (0.21 M) and PE (3.2 M repeat units) for 260 min at 150 °C resulted in formation of 0.02 M concentration of double bonds incorporated into polyethylene (see Fig 2.7) and commensurate loss of NBE (longer reaction times did not result in improved yield indicating catalyst decomposition[24]). Under identical reaction condition with **3**, 0.05 M olefinic bonds were introduced, corresponding to dehydrogenation of 1.6% of the PE C–C linkages.

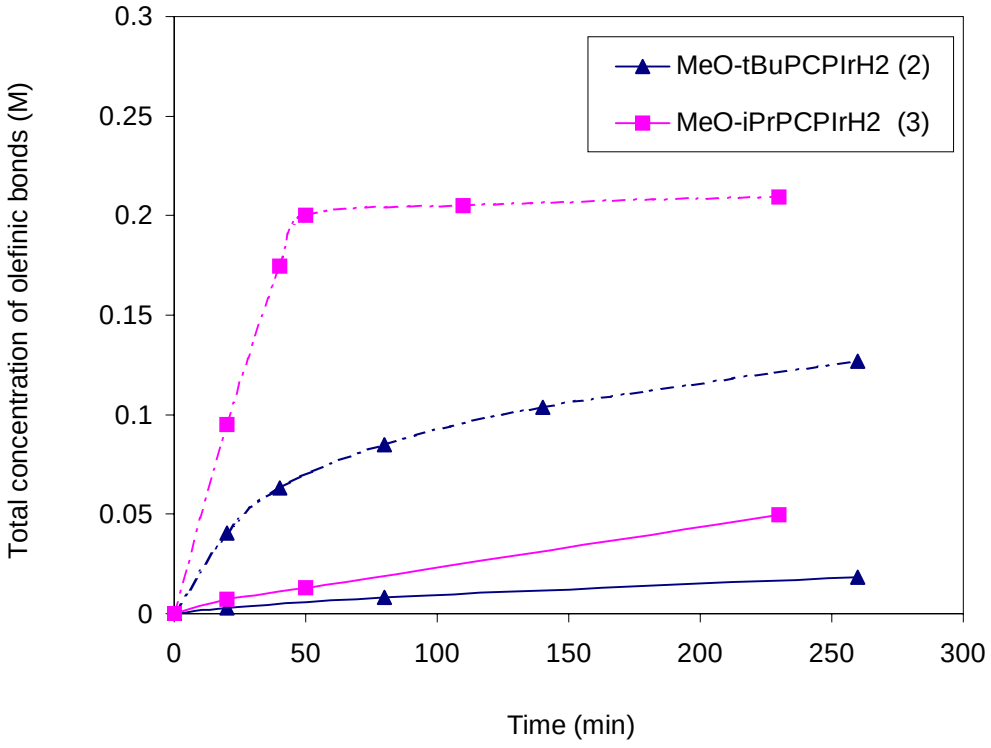

*Fig 2.7 Comparison of the total concentration of different double bonds introduced in PH (broken line ----) and PE (solid line ——) by **2** and **3** under identical conditions*

Using a higher concentration of catalyst (15 mM). after 230 min the degree of dehydrogenation achieved were 1.6% and 4.4% (0.042 M and 0.14 M double bonds) with **2** and **3** respectively (Fig 2.8). As in the case of PH, no indication of chain scission was noted; molecular weight distributions as determined by GPC before and after dehydrogenation were as follows (0, 2, 8 h reaction time using **3**): M_n (606, 696, 599), M_w (3000, 3121, 2974), PDI (4.95, 4.48, 4.96).

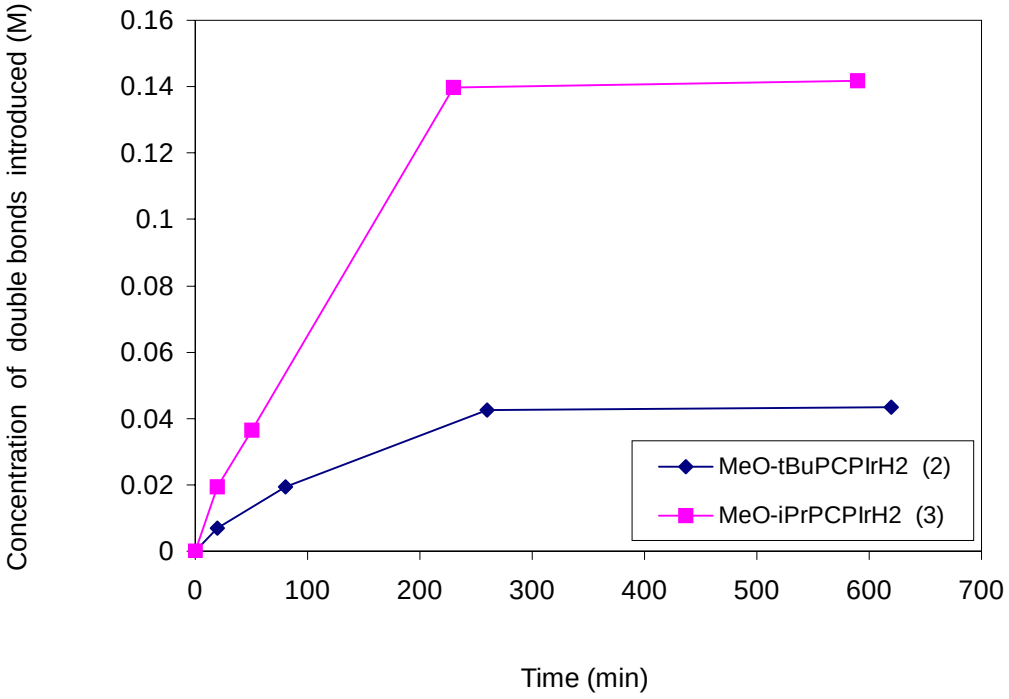

*Fig 2.8 Total concentration of different double bonds introduced in PE using 15 mM of pincer complexes **2** and **3***

This lower activity of PE compared to PH was presumably due to much greater reactivity of terminal ethyl groups, present only in very low concentration in the case of

PE and is consistent with the high selectivity exhibited by the pincer complexes for terminal positions of *n*-alkanes, in similar dehydrogenation reactions.[23]

2.2.1.3 Dehydrogenation of polyethylene-co-1-octene

Polyethylene-co-1-octene (EOC) was synthesized in the laboratory of Prof. Geoffrey Coates, at Cornell University, following the same method as was reported earlier for the synthesis of PH, to give a highly viscous atactic co-polymer (containing roughly 34% 1-octene) with a number average molecular weight (M_n) of 7800 and polydispersity index (PDI) of 2.11. The sample was dissolved in *p*-xylene, precipitated from methanol and was dried overnight *in vacuo* at 80 °C before being used for the dehydrogenation.

Different types of double bonds introduced into EOC, over time, on reaction with **2** and **3** are shown in Scheme 2.5. Dehydrogenation with both catalysts took place primarily at the terminal position of hexyl branches (polymer side chain) followed by migration of the double bond into internal positions through isomerization. Due to higher isomerization activity of **3**, on reaction with this catalyst, migration of a terminal double bond further into the hexyl branches opened up the previous terminal position for another catalytic attack – resulting in the formation of a conjugated double bond. With **2**, the terminal double bond was present even after two hours of reaction and was never fully isomerized to completion.

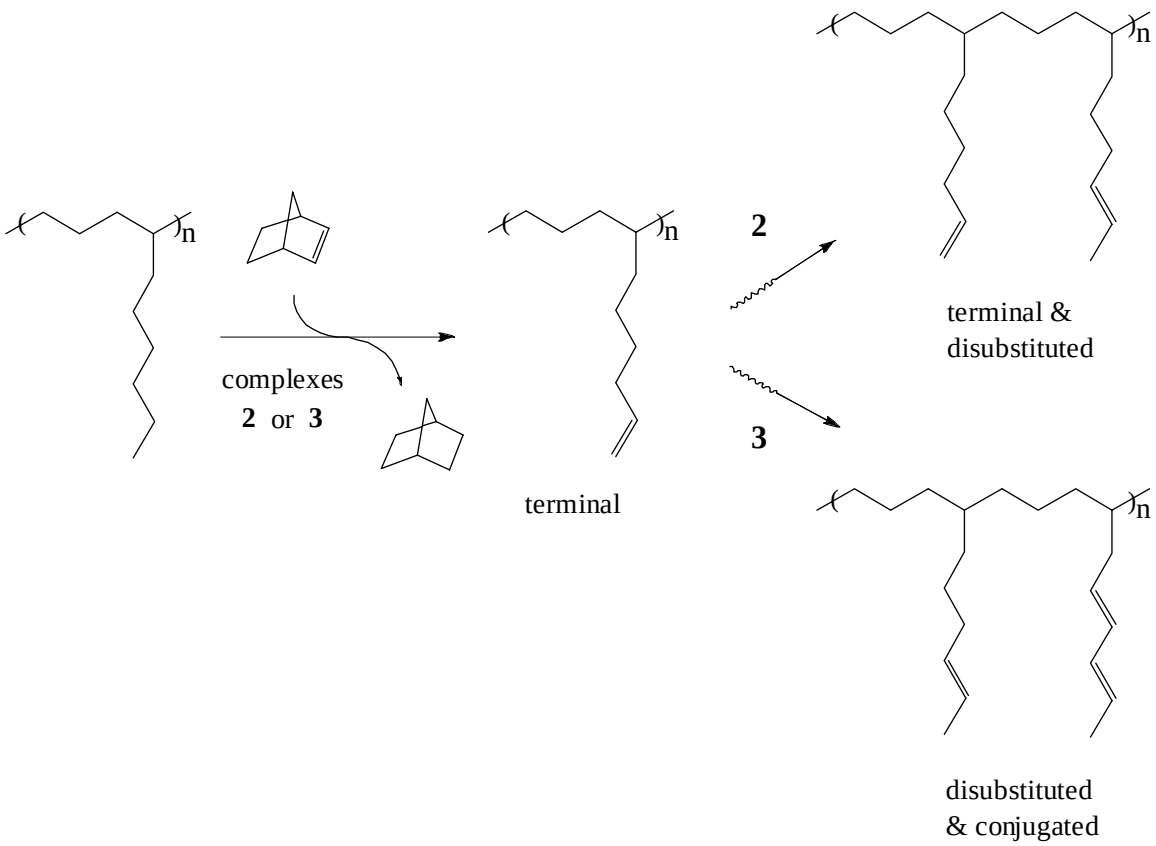

*Scheme 2.5 Catalytic dehydrogenation and subsequent isomerization of polyethylene-co-1-octene by complexes **2** and **3***

Heating a *p*-xylene solution of EOC (~ 0.61 M side chain concentration) and NBE (0.26 M) in the presence of **2** (5 mM) at 150 °C resulted in loss of about 15% NBE, after 20 min, along with commensurate appearance of 0.015 M terminal and 0.023 M internal double bonds. On continued heating, after 140 min the total concentration of double bond introduced into the polymer was roughly 0.1 M, of which about 20% was terminal (Fig. 2.9 below). Only a very modest increase in yield was observed upon heating the reaction mixture overnight indicating probable decomposition of the catalyst. At this point, total

double bond concentration introduced into the polymer was roughly 0.11 M, which corresponds to *ca*. 7% dehydrogenation of hexyl side chains.

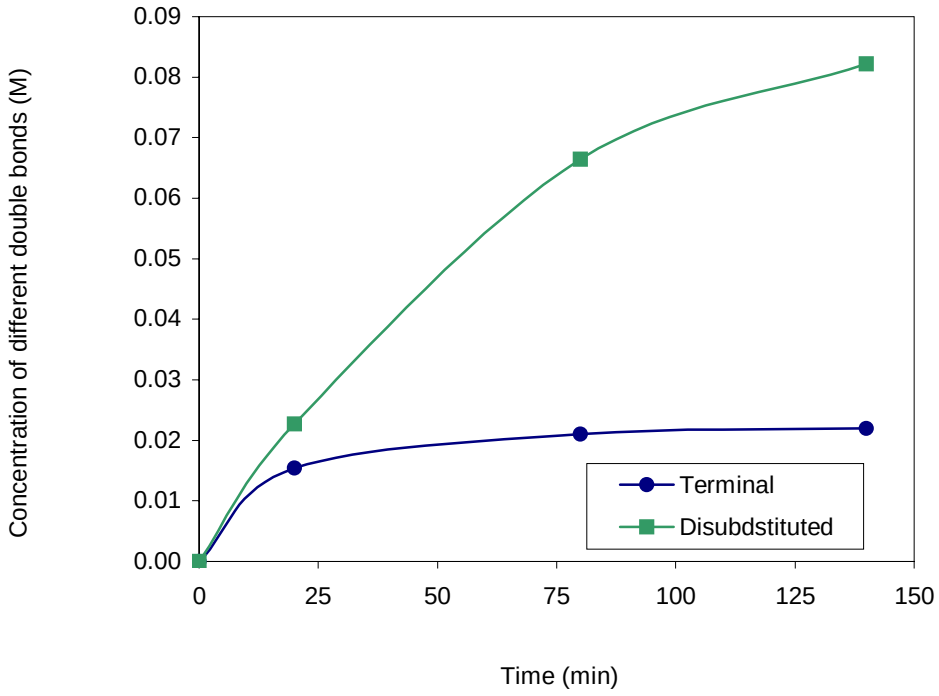

*Fig 2.9 Type and concentration of olefinic bonds introduced during dehydrogenation of EOC by catalyst **2** as a function of time*

In accordance with the results mentioned earlier, (MeO-^{iPr}PCP)IrH$_n$ (**3**) has been found to be a more active catalyst also for this system. Accordingly, under the same conditions, after 20 min of reaction about 30% of NBE was consumed on reaction with **3** and a slightly over 50% of the total double bond introduced at this point was terminal (Fig. 2.10 below). However, due to high isomerization activity of **3**, after one hour of reaction the terminal double bonds produced were all converted into internal disubstituted

ones. Additionally, as mentioned earlier, use of **3** led to the formation of conjugated double bonds, indicated by the presence of multiplets around δ 6.1 in the ^{1}H NMR spectrum.[26] NBE was completely consumed after 80 min and about 0.25 M double bond was introduced into the polymer, corresponding to about 15 double bonds per 100 hexyl side chains.

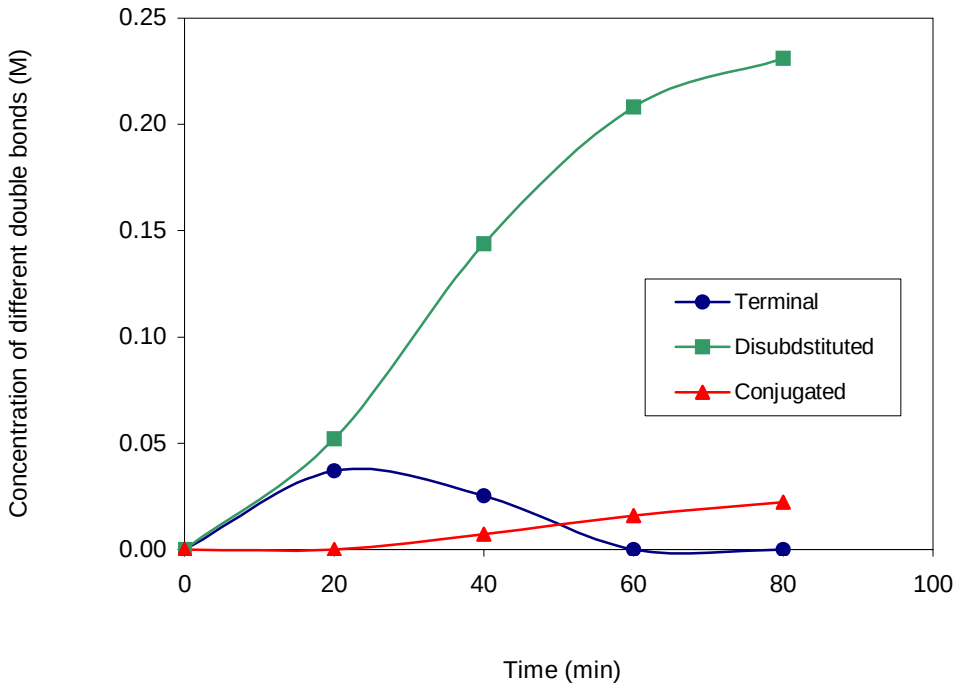

*Fig 2.10 Type and concentration of olefinic bonds introduced during EOC dehydrogenation by catalyst **3** as a function of time*

Overall, the sequence of double bond formation and also the reaction kinetics with EOC was fairly similar to that observed for PH. For both systems, use of **3**, led to complete isomerization of terminal double bond with the formation of conjugated double

bond on continued heating. However, the shorter length of branches in case of PH (butyl) as compared to EOC (hexyl), allowed the formation of trisubstituted double bond with the former. Additionally due to the presence of fewer branches available with EOC (a 34% 1-octene copolymer) relative to PH (a 1-hexene homopolymer) the reaction was faster with the later substrate (*e.g.* using complex **3** *ca.* 0.2 M NBE was completely consumed after 50 and 80 min with PH and EOC, respectively). This served as an indirect evidence that the reaction primarily proceeded through an attack at the terminal position of branches rather than at the backbone (again demonstrating the selectivity exhibited by these catalysts for the terminal C-H bonds of paraffinic substrates).

2.2.1.4 Dehydrogenation of syndiotactic polypropylene

Linear type long chain alcohol or carbonyl compounds with functionality only at the two ends of the chain are very rare. It is a synthetic challenge to prepare these compounds by traditional organic transformations. Selectivity of iridium-pincer complexes towards the terminal position of a hydrocarbon prompted us to investigate the dehydrogenation of polypropylene. If a linear polypropylene can be dehydrogenated only at the two ends of the chain, it would be possible to carry out further transformation the said double bonds to give polyolefins with functional group at the two ends. This would then allow the use of these terminal functionalized polyolefins as mid-segments for other polymers, which has significant potential to give unprecedented polymers (Scheme 2.6).

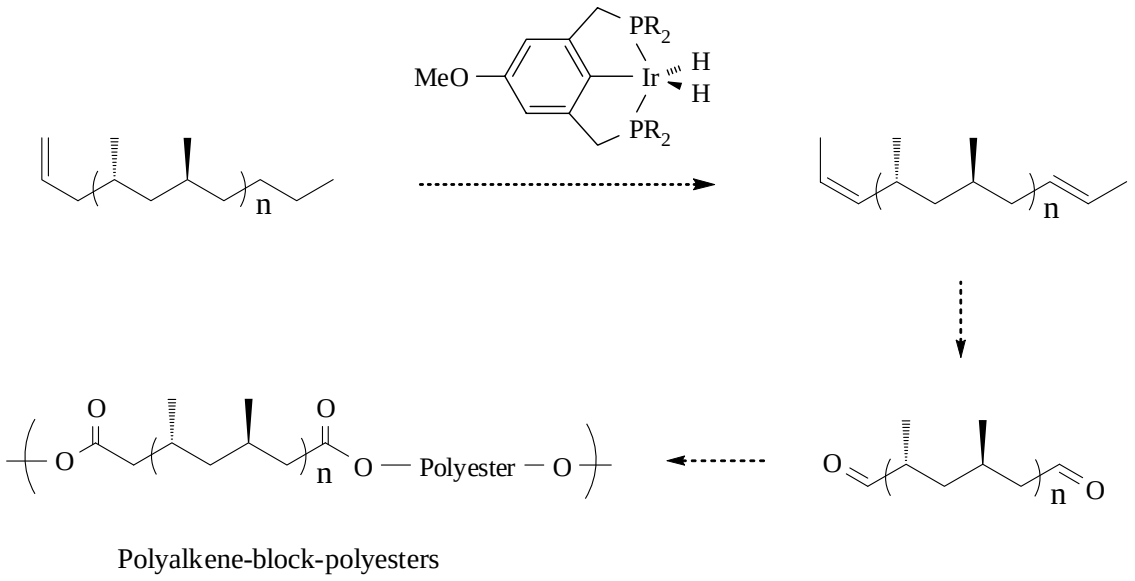

Polyalkene-block-polyesters

Scheme 2.6 Catalytic dehydrogenation and sequential transformation of syndiotactic polypropylene to give multi-block polymers with different functionality

Syndiotactic polypropylene (PP) (M_n = 11446 and PDI = 1.94) was synthesized in the laboratory of Prof. Geoffrey Coates, at Cornell University. The sample was subjected to Soxhlet extraction in refluxing toluene and the extract was precipitated with copious methanol. The precipitate was dried overnight *in vacuo* at 70 °C to give a white powder that was soluble in aromatic solvents at elevated temperature (80-90 °C).

Under the same reaction conditions as noted above (5 mM catalyst, 0.3 M NBE, *p*-xylene, 150 °C) a solution of PP (2.1 M repeat unit) was found to react at an extremely slow rate with **2**. The only dehydrogenated product that was observed by NMR, after overnight heating, was **A** (~ 10 mM) formed through catalytic attack at the only terminal alkyl group present at the end of the polymer chain, followed by isomerization (Scheme

2.7). The terminal double bond that was present initially in the polymer (formed via chain termination through β-H elimination during the polymerization) was isomerized into internal position during the reaction.

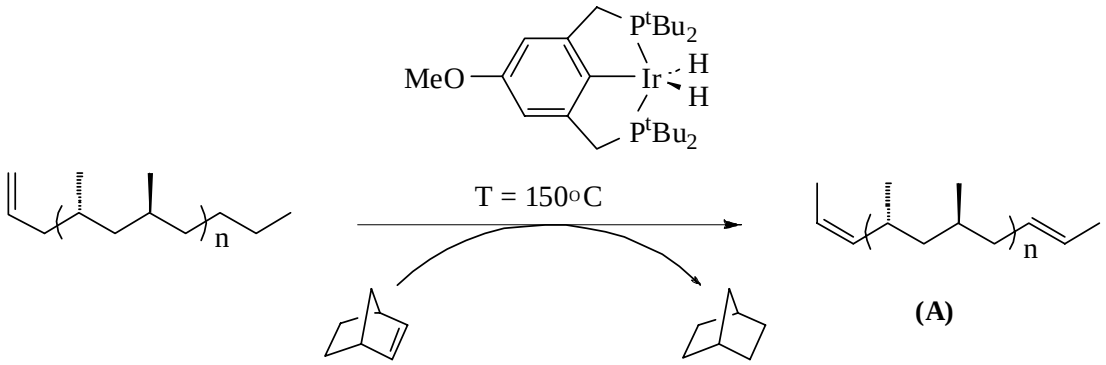

*Scheme 2.7 Catalytic dehydrogenation and subsequent isomerization of syndiotactic polypropylene by Ir-pincer complex **2***

Apparently a double bond concentration of only 10 mM might seem very little and not a practical approach to the functionalization. However, a solution repeat unit concentration of 2.1 M indicates a total of 15 mM concentration of the terminal double bond if only the terminal position of every molecule in the solution is dehydrogenated. Therefore a 10 mM concentration of terminal double bonds indicated that the catalyst successfully produced the desired unsaturated product with about high selectivity (80-100%) and yield (70%).

Dehydrogenation using **3** was slightly faster but was still sluggish compared to the rates observed for other polyolefins using this catalyst. After reaction at 150 °C for 18 h,

15 mM of **A** was observed along with roughly 10 mM of **B** (Scheme 2.8). Possible trisubstituted olefinic product **C**, which could have been formed through direct dehydrogenation of the polymeric backbone, was not observed. Considering the maximum possible concentration of terminal double bonds could only be 15 mM, these results indicate a very high selectivity (>100:1) and complete dehydrogenation of end groups.

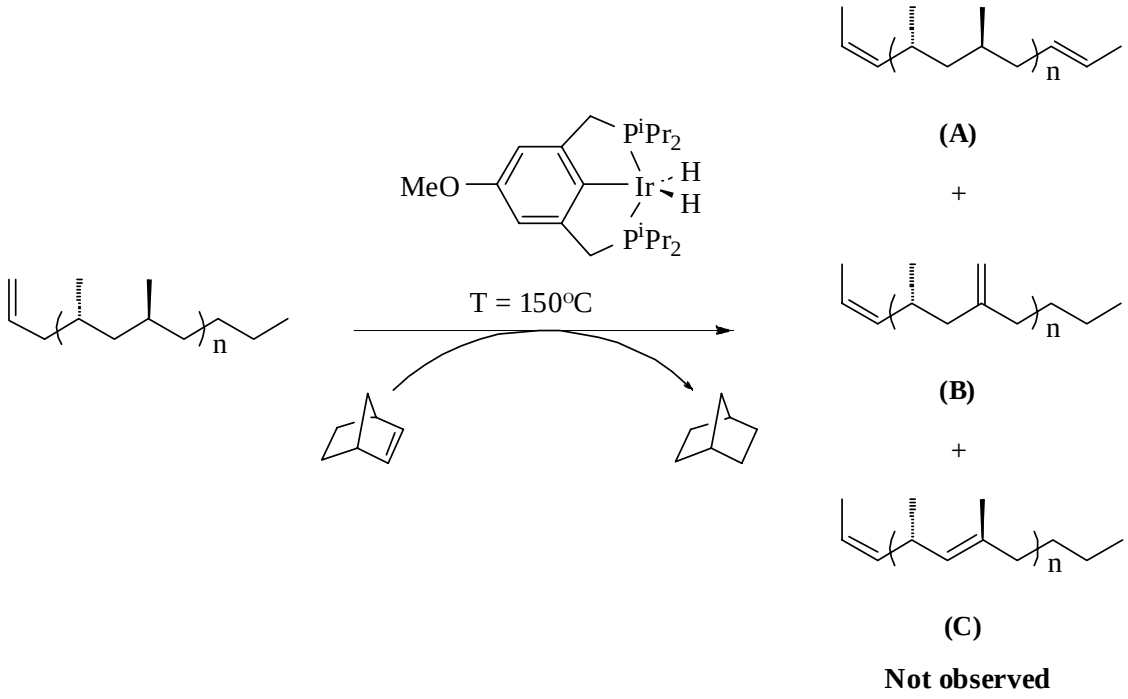

*Scheme 2.8 Catalytic dehydrogenation and subsequent isomerization of syndiotactic polypropylene by Ir-pincer complex **3***

Extreme unreactivity of syndiotactic PP towards dehydrogenation of the polymeric backbone led us investigate the effect of sterics on alkane dehydrogenation by the iridium-pincer complexes, using a simple molecular substrate: 2,4-dimethylpentane.

This alkane could be viewed as a small model of polypropylene, which we felt would help us to compare and interpret the results with PP. Being a symmetrical system only two types of double bonds could be introduced into this molecule, thereby giving a well resolved ^{1}H NMR spectra (Fig 2.11).

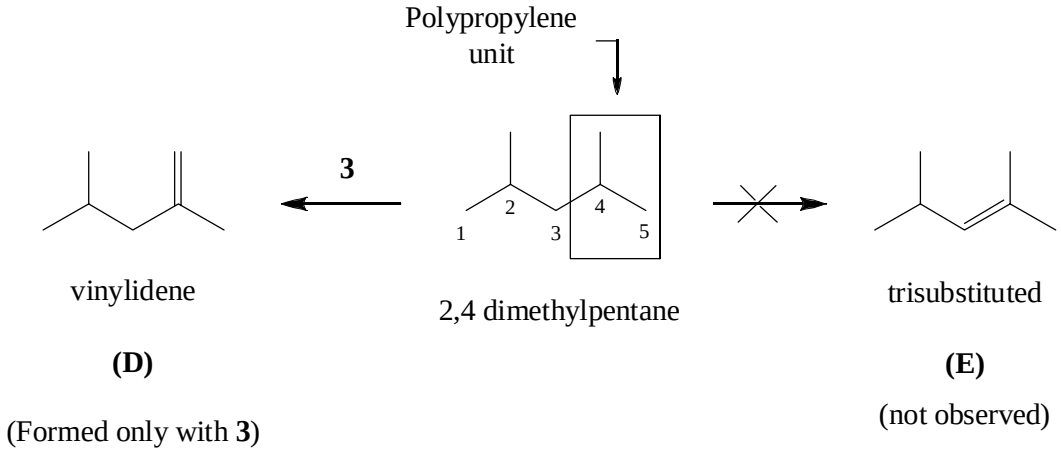

Fig 2.11 Possible dehydrogenated alkenes from 2,4-dimethylpentane

Under similar reaction conditions (5 mM of catalyst, 0.3 M NBE, 150 °C) on heating a 2.3 M solution of 2,4-dimethylpentane in *p*-xylene-d_{10}, in presence of complex **2**, no dehydrogenated product was observed after two hours of reaction. Use of the more active catalyst **3** led to the formation of only a very small amount (~20 mM) of the vinylidene product (**D**) after 120 min.

Although iridium-pincer complexes have been found to exhibit selectivity for the terminal position of alkanes, in the complete absence (*e.g.* dehydrogenation of cycloalkanes) or very low availability (*e.g.* reaction with linear polyethylene) of the

primary C-H bonds, activation of a secondary C-H bond leading to the direct formation of an internal olefinic product can occur with these catalysts. Therefore, in the reactions with 2,4-dimethylpentane, complete lack of formation of the trisubstituted product (**E**) with either of the catalysts could not be simply ascribed to the absence of ethyl groups. Presumably, due to substitution at both C2 and C4 positions, the central carbon of the molecule (C3) is too crowded to give a tri-substituted olefin via dehydrogenation. Similar argument also holds for formation of the vinylidene product (**D**) with only the sterically less hindered bis(i-propyl)phosphino complex (**3**). Because of the bulky t-butyl groups in **2**, the transition state for β-H elimination from the trisubstituted center, leading to (**D**) is strongly disfavored.

Competition reaction carried out to compare the effect of sterics towards selectivity in dehydrogenation has shown that under the same condition dehydrogenation of an *n*-alkane is much faster than that of 2,4-dimethylpentane. A solution of 5 mM **3**, 0.3 M NBE, 0.083 M hexamethyldisiloxane (for quantification purpose) and *n*-octane to 2,4-dimethylpentane 1:1 proportion (v/v) (molar ratio = 1:1.1) was prepared in *p*-xylene-d_{10}. The solution was heated at 150 °C in a sealed tube and periodically monitored by both ^{1}H and ^{31}P NMR. After 30 min of reaction, 50 mM of octenes (mixture of terminal and internal) were formed but concentrations of both **E** and **D** were undetectable by NMR (< 2 mM).

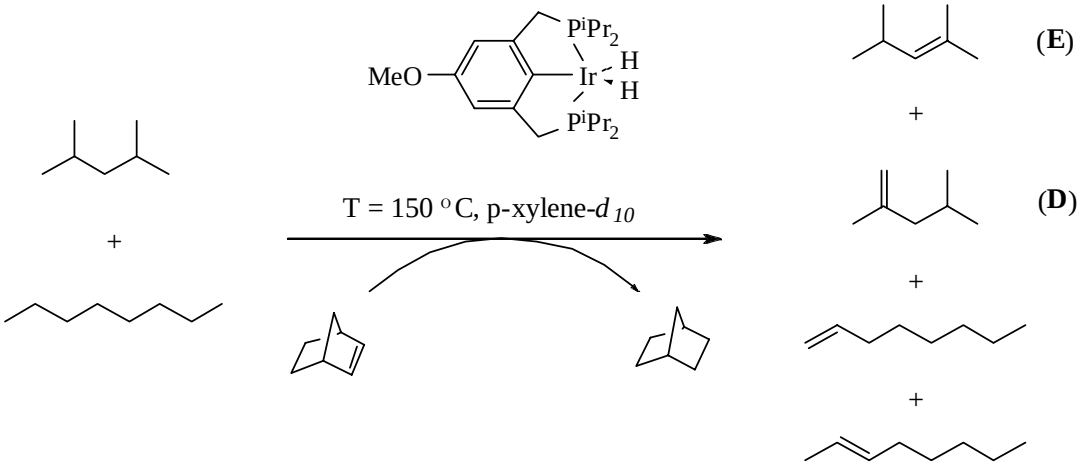

*Scheme 2.9 Competition reaction of 2,4-dimethylpentane with n-octane towards catalytic dehydrogenation by Ir-pincer complex **3***

After 90 min of heating roughly 100 mM octenes were present in the solution, which was ten times the concentration of only dehydrogenated product, **D** (~10 mM), that was observed from 2,4-dimethylpentane. There was no evidence for formation of the trisubstituted product, **E**, by NMR. Considering the initial molar ration of alkanes was (1:1.1 *n*-octane to 2,4-dimethylpentane), selectivity of complex **3**, towards terminal positions of *n*-octane *vs*. the methyl groups of 2,4-dimethylpentane was found out to be about 22:1.

2.3 Conclusion

In summary, pincer-ligated iridium complexes **2** and **3** were found to be efficient systems for the incorporation of double bonds into saturated polyolefins. This was the first example of catalytic dehydrogenation of aliphatic polyolefins to give partially unsaturated hydrocarbon polymers. The catalysts appeared to be highly selective for branches *vs.* backbone (with kinetic selectivity for the terminal positions). This was evident from the nature of the product of dehydrogenation of poly(1-hexene) and from the lower activity exhibited by catalysts for dehydrogenation of polyethylene compared to that of poly(1-hexene). For dehydrogenation of both PH and EOC, using complex **3**, the reactions were 100% complete with respect to norbornene (*i.e.* the sacrificial acceptor was completely consumed in both cases).

Due to the higher isomerization activity of **3** relative to **2**, even relative to the faster dehydrogenation activity of **3**, olefinic bonds introduced into the branches (*e.g.* with PH and EOC) on reaction with **3** move to the internal positions and no terminal double bond was present with either polymer beyond one hour of reaction. In contrast, with **2**, terminal olefinic bonds were never completely isomerized for either polymer. Dehydrogenation of syndiotactic polypropylene (PP) was found to be extremely sluggish with both catalyst systems. Further exploration of the reaction with a model alkane, 2,4-dimethylpentane, having structural resemblance to that of the PP repeat unit revealed that the extreme unreactivity was due to steric effects.

Notably, the molecular weights and molecular weight distributions of the polymer samples remained unaffected by the reaction. The degree of unsaturation achieved (without extensive effort at optimization) could allow the controlled modification of saturated polyolefins by introducing alkene functionality for further reactions.

2.4 Experimental

All routine manipulations were performed at ambient temperature in an argon-filled glove box or under argon using standard Schlenk techniques. Dehydrogenation reactions were carried out in NMR tubes sealed under vacuum and was heated either in an oil bath or a GC oven maintained at a constant temperature. All NMR solvents (protiated or deuterated) were distilled from sodium/potassium alloy, vacuum transferred under argon and stored in an argon-filled glove box. ^{1}H, $^{31}P\{^{1}H\}$ and $^{13}C\{^{1}H\}$ NMR spectra were obtained on a 400-MHz, Varian Inova-400 spectrometer or on a 300-MHz, Varian Mercury-300 spectrometer. ^{1}H chemical shifts were reported in ppm downfield from tetramethylsilane and were referenced to residual (^{1}H) or deuterated solvent. ^{31}P NMR chemical shifts were referenced to PMe_3. Catalysts **2**[25] and **3**[21] were prepared according to literature procedures. Norbornene was purchased from Sigma-Aldrich, sublimed under vacuum and was stored in an argon-filled glove box. All other chemicals were used as received from commercial suppliers.

2.5 References

1. Thayer, A. M. *Chem. Eng. News* **1995**, *73* (Sept 11), 15.

2. Schumacher, J. In *Chemical Economics Handbook*; SRI International: Menlo Park, CA, 1994; p 530.

3. Patil, A. O. *Chem. Innovation* **2000**, *30(5)*, 19.

4. Boaen, Nicole K. and Hillmyer, Marc A. *Chem. Soc. Rev.* **2005**, *34*, 267.

5. Boffa, L. S. and Novak, B. M. *Chem. Rev.* **2000**, *100 (4)*, 1479.

6. Ittel, S. D.; Johnson, L. K. and Brookhart M. *Chem. Rev.* **2000**, *100 (4)*, 1169.

7. Dumas, J. B. *Liebigs Ann.* **1840**, *33*, 187-191.

8. Lu, B.; Chung, T. C. *J. Polym. Sci. Part A* **2000**, *38*, 1337.

9. (a) Kagiya, Tsutomu; Hagiwara, Miyuki; Kagiya, Tsukasa; Takemoto, Katsuo. (Japan Atomic Research Institute). Japanese Patent 48067376 (**1973**). (b) L. Torrisi, S. Gammino, A.M. Mezzasalma, A.M. Visco, J. Badziak, P. Parys, J. Wolowski, E. Woryna, J. Krása, L. Láska, M. Pfeifer, K. Rohlena, F.P. Boody, *Applied Surface Science* **2004**, 227, 164. (c) Stefanovskaya, N. N.; Gavrilenko, I. F.; Markevich, I. V.; Sandomirskaya, N. D.; Shmonina, V. L.; Tinyakova, E. I.; Dolgoplosk, B. A. *European Polymer Journal* **1969**, 479. (d) De Andres, Jaime; Aguilar, Antonio; Domenech, Jorge. *Journal of Macromolecular Science* **1990**, *A27(2)*, 213. (e) DeLaMare, H.E. *Journal of Polymer Science, Part B: Polymer Letters* **1965**, *3(10)*, 809.

10. "Organometallic C-H Bond Activation : An Introduction" Goldman, A. S. and Goldberg, K. I. in *Activation and Functionalization of C-H Bonds;* K. I. Goldberg and A. S. Goldman, Eds. **2004**; ACS Symposium Series 885; 1-44.

11. Kondo, Y.; Garcia-Cuadrado, D.; Hartwig, J. F.; Boaen, N. K.; Wagner, N. L.; Hillmyer, M. A. *J. Am. Chem. Soc.* **2002**, *124*, 1164.

12. Boaen, N. K and Hillmyer, M. A. *Macromolecules* **2003**, *36*, 7027.

13. Bae, C.; Hartwig, J. F.; Boaen Harris, N. K.; Long, R. O.; Anderson, K. S. and Hillmyer, M. A. *J. Am. Chem. Soc.* **2005**, *127*, 767.

14. Schulz, D. N.; Turner, S. R. and Golub, M. A. *Rubber Chem. Tech.* **1982**, *55*, 809.

15. T. Ho and J. M. Martin, in *Structure, properties and applications of polyolefin elastomers produced by constrained geometry catalysts*, ed. J. Scheirs and W. Kaminsky, John Wiley & Sons, New York, **2000**.

16. (a) Burk, M. J.; Crabtree, R. H; Parnell, C. P.; Uriarte, R. J. *Organometallics* **1984**, *3*, 816-817 (and references therein for stoichiometric dehydrogenations). (b) Burk, M. J.; Crabtree, R. H. *J. Am. Chem. Soc.* **1987**, *109*, 8025. (c) Felkin, H.; Fillebeen-Khan, T.; Holmes-Smith, R.; Lin, Y. *Tetrahedron Lett.* **1985**, *26*, 1999.

17. A. S. Goldman, 'Dehydrogenation, Homogeneous', in *The Encyclopedia of Catalysis*, ed. I. T. Horvath, Volume 3, John Wiley & Sons, New York, 2003, pp. 25–34.

18. (a) Gupta, M.; Hagen, C.; Flesher, R. J.; Kaska, W. C.; Jensen, C. M. *Chem. Commun.* **1996**, 2083. (b) Xu, W.; Rosini, G. P.; Gupta, M.; Jensen, C. M.; Kaska, W. C.; Krogh-Jespersen, K.; Goldman, A. S. *Chem. Commun.* **1997**, 2273. (c) Göttker-Schnetmann, I.; White, P. and Brookhart, M. *J. Am. Chem. Soc.*, **2004**, *126*, 1804.

19. Renkema, K. B.; Kissin, Y. V.; Goldman, A. S. *J. Am. Chem. Soc.* **2003**, *125*, 7770.

20. (a) Gupta, M.; Hagen, C.; Kaska, W. C. and Jensen, C. M. *J. Chem. Soc., Chem. Commun.* **1997**, 461. (b) Gu, X.-Q.; Chen, W.; Morales-Morales, D. and Jensen, C. M. *J. Mol. Cat. A*, **2002**, *189*, 119. (c) Zhang, X.; Fried, A.; Knapp, S.; Goldman, A. S. *Chem. Commun.* **2003**, 2060.

21. Zhu, K.; Achord, P. D.; Zhang, X.; Krogh-Jespersen, K.; Goldman, A. S. *J. Am. Chem. Soc.* **2004**, *126*,13044.

22. McKnight, A. L. and Waymouth, R. M. *Chem. Rev.* **1998**, 98, 2587.

23. Liu, F.; Pak, E. B.; Singh, B.; Jensen, C. M.; Goldman, A. S. *J. Am. Chem. Soc.* **1999**, *121*, 4086.

24. At room temperature, the reactions of **2** and **3** with NBE (in either the presence or absence of polymer, and in both alkane and arene solvents) give complexes that have been tentatively identified as "(MeO–^{R}PCP)Ir(NBE)" (R = t-Bu and i-Pr) (^{31}P NMR resonances at δ 62.6 and δ 53.3 respectively). These species have been found to act as precursors of the corresponding 14-electron fragments, "(MeO–^{R}PCP)Ir". In the reaction of **3** and PH/NBE this remains a major species in solution throughout the course of the reaction. In addition, species are formed to which dehydrogenated polymer is apparently bound, "(MeO–^{R}PCP)Ir(olefin)" (δ 48.7, 46.8 and 44.7), identified by comparison with the reaction of **3** with linear octenes. Similar behavior is observed in the case of **3** and PE/NBE; however in

this case one major, catalytically inactive product ultimately forms with a peak at δ 67.8. In the case of **2** and either PH or PE, a number of minor products are also observed, presumably the analogous "(MeO–^{R}PCP)Ir(olefin)" complexes (δ 59.2, 57.1 and 55.1). Loss of both polymer- and norbornene-bound species is observed upon further heating, with the appearance of a number of minor peaks (δ 95.3, 92.8, 81.9 and 81.1) which correlates with the eventual loss of catalytic activity.

25. Krogh-Jespersen, K.; Czerw, M.; Zhu, K.; Singh, B.; Kanzelberger, M.; Darji, N.; Achord, P. D.; Renkema, K. B.; Goldman, A. S. *J. Am. Chem. Soc.* **2002**, *124*, 10797.

26. Positions of the peaks were confirmed comparing ^{1}H NMR shifts of the reaction mixture with authentic samples of 2,4-hexadiene.

Chapter 3

Isomerization of linear α-olefins catalyzed by pincer-ligated iridium dihydride complexes - (X-^{R}PCP)IrH$_2$

Abstract

During alkane dehydrogenation catalyzed by Ir-pincer complexes, along with the formation of terminal olefins as the kinetic product, a large buildup of internal olefins is always observed, over time. These internal olefins are presumably formed through isomerization of terminal olefins *via* an insertion/*β*-H elimination mechanism. Using 1-octene as the substrate, we probed into the steric and electronic effects, which would have an influence on the isomerization activity of iridium pincer dihydride complexes - (X-^{R}PCP)IrH$_2$. The presence of large alkyl groups (R) on the phosphine ligands and/or π-donating groups on the phenyl ring attached *para* to the iridium center led to lower rate of isomerization. The same effects were also found to result in selectivity in isomerization exhibited by these complexes.

3.1 Introduction

The chemistry of olefin coordination to transition metal complexes covers a large field of organometallic chemistry and homogeneous catalysis. Olefin isomerization is perhaps amongst one of the oldest and most widespread reactions that involve interaction between an olefin and a catalyst. Many commercially vital transition-metal-catalyzed reactions such as hydrozirconation,[1] hydroformylation,[2] hydrosilylation[3] and hydrocyanation[4] involve olefin isomerization as one or more of the key steps.

The two established pathways for transition-metal-catalyzed olefin isomerization are the π-allyl metal hydride mechanism and the metal hydride addition-elimination mechanisms.[5] The metal hydride addition-elimination mechanism (Scheme 3.1) is the more prevalent pathway for transition metal catalysts which have an M–H bond. In this mechanism, free olefin coordinates to a kinetically long-lived metal hydride species, followed by insertion in either 1,2 or 2,1 fashion. The 1,2 insertion pathway is a non-productive one, in which *β*-H elimination gives the same olefin (double bond in the identical position) back. A 2,1 insertion of the olefin into the metal-hydride bond yields a secondary metal alkyl, which can undergo *β*-H elimination from the internal *β*-carbon to give isomerized olefin and regenerate the initial metal hydride.

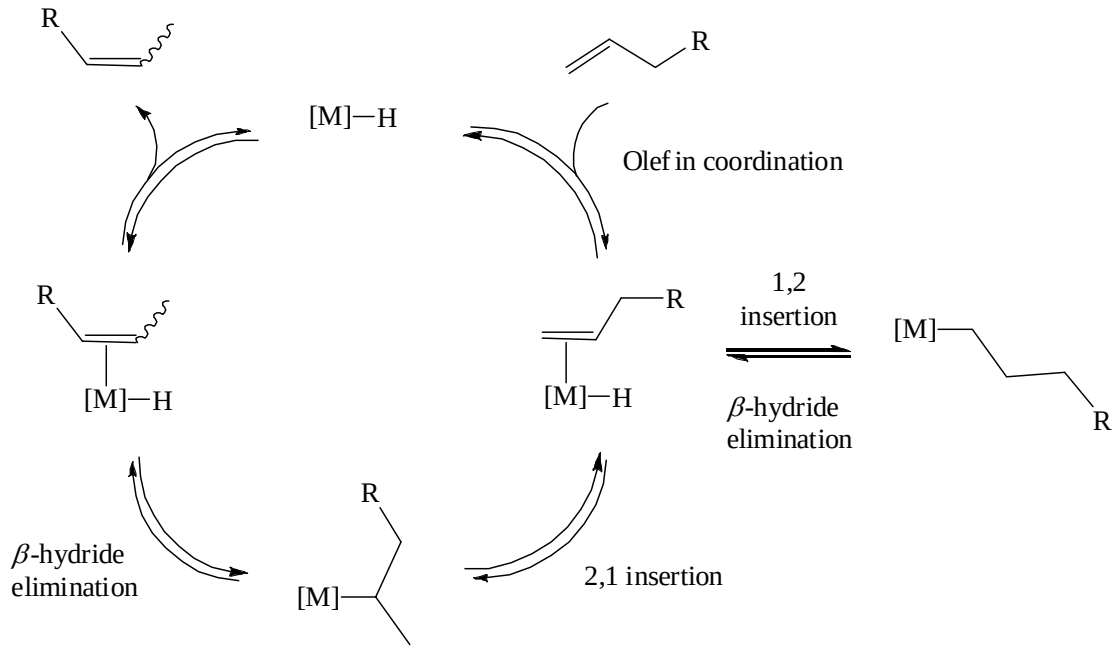

Scheme 3.1 Metal hydride addition-elimination mechanism of isomerization

The π-allyl hydride mechanism (Scheme 3.2) is the less commonly observed pathway for olefin isomerization (generally known for some metal carbonyl catalysts *e.g.* $Fe_3(CO)_{12}$ or metal complexes in low-oxidation states having no hydride ligand).[2b] In this mechanism, free olefin coordinates to a transition metal fragment followed by oxidative addition of an activated allylic C-H bond to the metal giving a π-allyl metal hydride. Transfer of the coordinated hydride to the opposite end of the allyl group yields isomerized olefin.

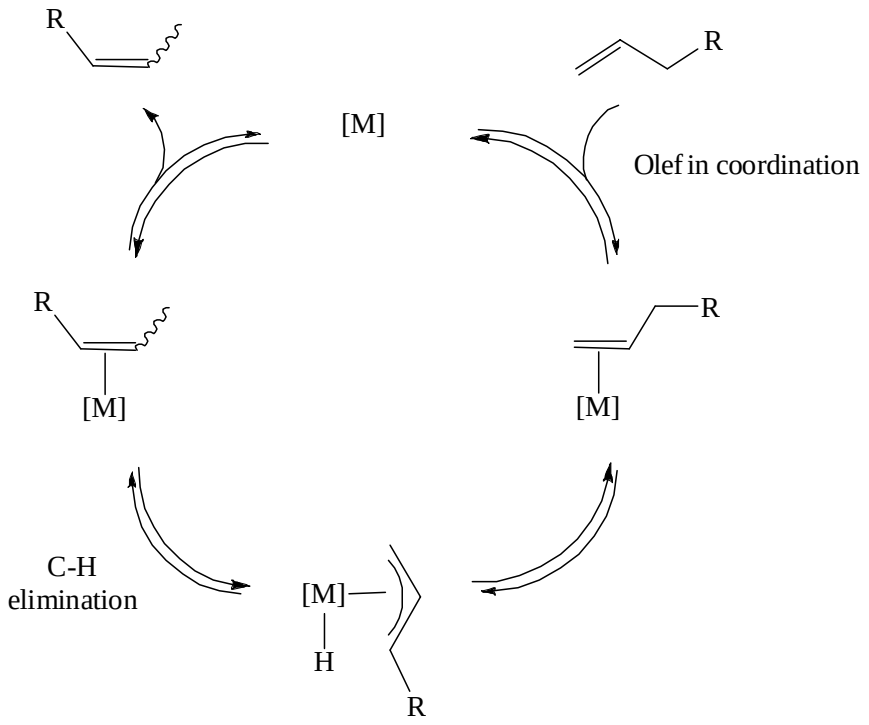

Scheme 3.2 π-allyl mechanism of isomerization

Although isomerization of olefins is a key intermediate step in many catalytic processes due to a lack of catalysts for selective isomerization, there have been few applications of olefin isomerization as an individual reaction. Consequently, although there are quite a few reports in the parent literature studying the mechanism leading to isomerization,[6] there are not many examples of investigation of steric and electronic effects that control the rate as well as selectivity of isomerization.

Earlier studies on alkane dehydrogenation with Ir-pincer complexes (**1**, **2** and **3**) revealed that in spite of high kinetic regioselectivity exhibited by these catalysts to

produce terminal olefins, the final concentration of terminal olefinic products were low due to subsequent isomerization to more stable internal ones.[7] A study of the isomerization process was undertaken with several aims in mind, including –

1. To elucidate the factors (steric, electronic) controlling isomerization rates. In addition to isomerization we felt that this would shed light on other reactions involving olefin insertion and β-H elimination.

2. To develop catalysts that could be useful in isomerizing a terminal alkene selectively to 2- (β) olefins.

3. Understanding such factors would help in developing a catalyst that would favor dehydrogenation over isomerization.

3.2 Results and Discussions

3.2.1 Olefin isomerization with (X-^{R}PCP)IrH$_2$ complexes

As shown in Scheme 3.3 Pincer-ligated iridium dihydride complexes presumably cause olefin isomerization through an insertion/β-H elimination mechanism.[7]

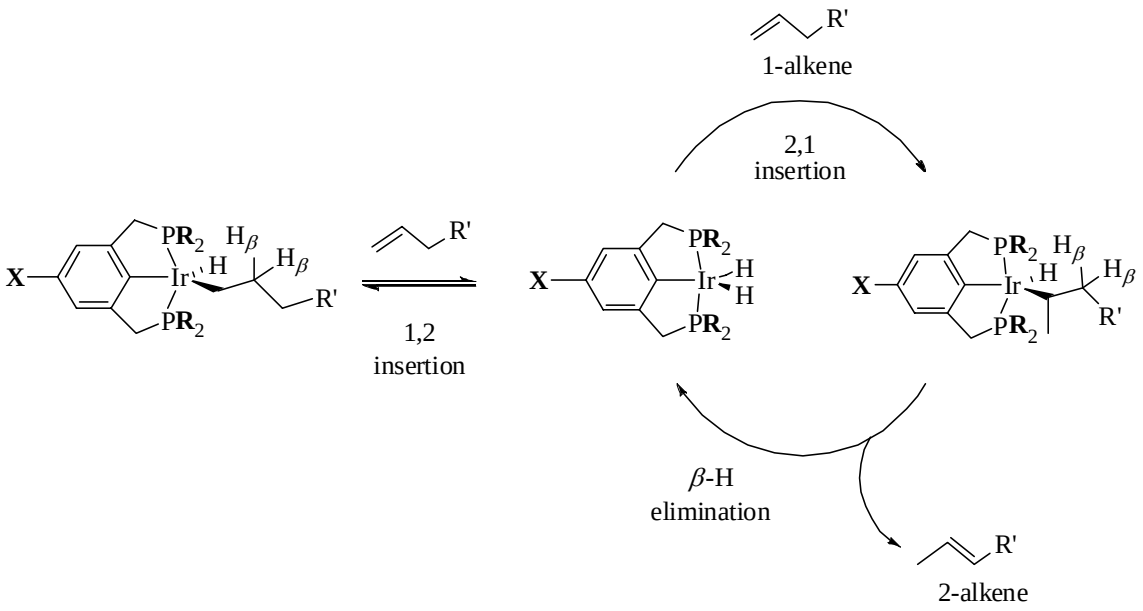

Scheme 3.3 Insertion/β-H elimination mechanism for isomerization of 1-olefins by (X-^{R}PCP)IrH$_2$ complexes

As suggested by the mechanism, both steric (exerted by the 'R' groups on phosphines) and electronic (due to substituent 'X') tuning of the catalysts would influence the rate of isomerization as well as the selectivity in terms of the final product ratios. In order to investigate these effects, experimentally, isomerization of 1-octene was carried out using three iridium-pincer complexes in which the R and X groups were varied separately to study their effects (Scheme 3.4). In a typical reaction, a 1.0 M solution of 1-octene in *p*-xylene containing 5 mM of a catalyst (**1**, **2** or **3**) was heated at 120 °C under argon atmosphere and samples were taken out periodically for GC analysis. The results are illustrated by comparing rates and selectivity from different catalysts (Fig 3.1 and 3.2).

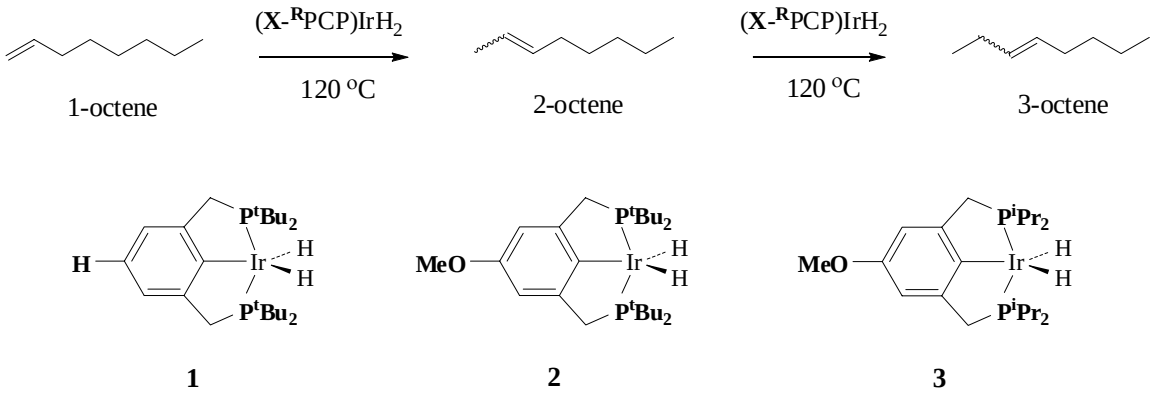

Scheme 3.4 Isomerization of 1-octene using (X-^{R}PCP)IrH$_2$ complexes.

R = ^{i}Pr, ^{t}Bu; X = H, MeO

*3.2.1.1 Steric effect on rates and selectivity – comparison between complexes with X = MeO; R = ^{t}Bu (**2**) and R = ^{i}Pr (**3**)*

Comparison of the rate of consumption of 1- and 2-octene and also the rate of formation of the 3- isomer showed that the overall kinetics was much faster with **3** compared to **2** (figs. 3.1). The bulky ^{t}Bu groups on (MeO-^{tBu}PCP)IrH$_2$ (**2**) appeared to hinder 2,1 insertion of the olefin, leading to a much slower rate of isomerization than was found for (MeO-^{iPr}PCP)IrH$_2$ (**3**). Isomerization of 1-octene to 2-octene by **3** is followed by appreciable buildup of the 3-octene isomer, which of course was also slowed by the bulky ^{t}Bu groups in **2**. The relative rates of 1-octene → 2-octene *vs.* 2-octene → 3-octene isomerization would determine the maximum yield of 2-octene. Presumably the transition state for 2-octene → 3-octene isomerization is *slightly* more crowded. Accordingly the more bulky (MeO-^{tBu}PCP)IrH$_2$ (**2**) appears to be slightly more selective for the first isomerization and gives a slightly higher maximum yield: 85% (**2**) *vs.* 78% (**3**).

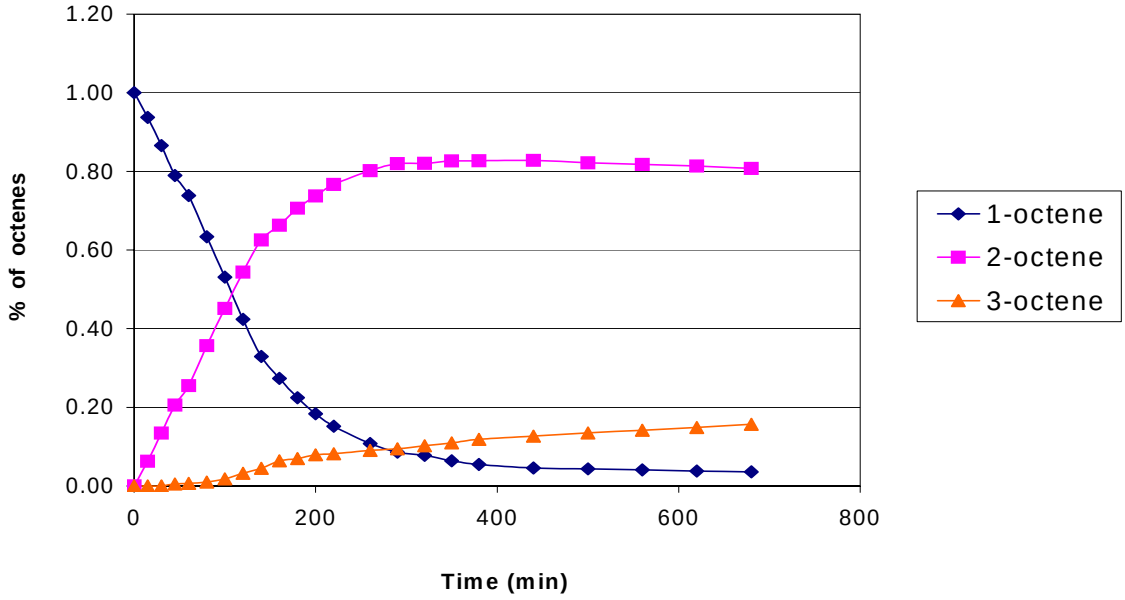

*Fig 3.1(a) Isomerization of 1-octene catalyzed by (MeO-^{tBu}PCP)IrH_2 (**2**)*

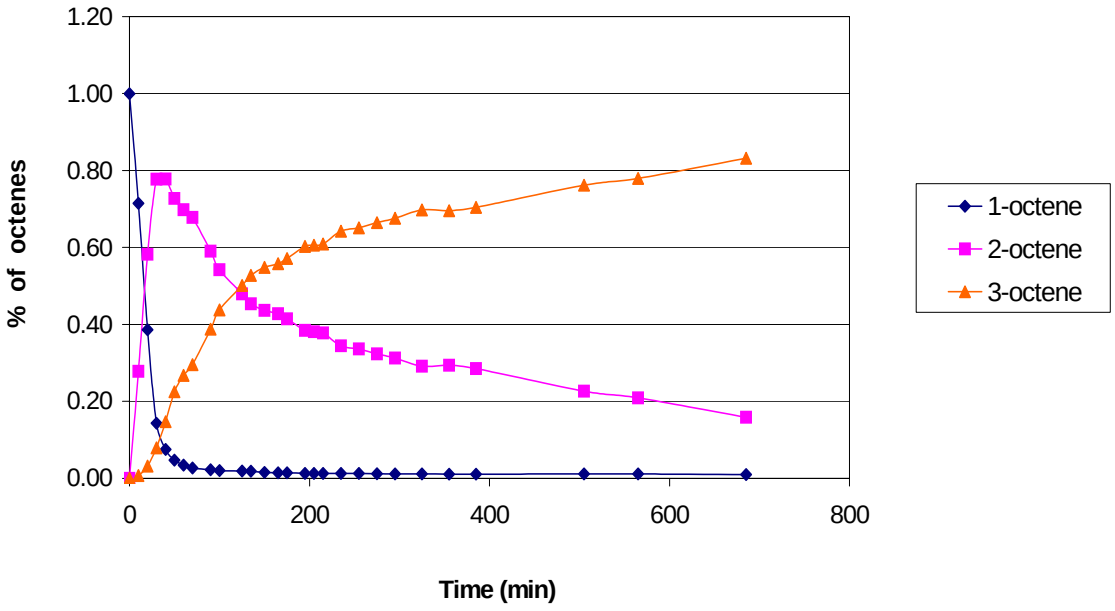

*Fig 3.1(b) Isomerization of 1-octene catalyzed by (MeO-^{iPr}PCP)IrH_2 (**3**)*

*3.2.1.2 Electronic effect on rate and selectivity – comparison between complexes with R = ^{t}Bu; X = H (**1**) and R = MeO (**2**)*

Comparison of the Figs 3.2(a) and 3.2(b) revealed the difference in rate of isomerization by the catalysts (H-^{tBu}PCP)IrH_2 **(1)** and (MeO-^{tBu}PCP)IrH_2 (**2**) due to electronic tuning. Enhanced π-donation of MeO- group in (MeO-^{tBu}PCP)IrH_2 led to increased electron density on Ir. Previous studies showed that π-donation disfavors coordination of an olefin to the 16-electron species.[8] Accordingly, π-donation appeared to also disfavor the insertion of olefins into the Ir-H bond, resulting in an overall slower rate of isomerization of both 1-octene and 2-octene by complex **2** compared to the parent complex, **1**. Additionally, just as it is slightly more crowded, the transition state for 2-octene → 3-octene isomerization is expected to be *slightly* more electron-rich than the TS for 1-octene → 2-octene isomerization. Accordingly a slightly higher maximum concentration of 2-octene is obtained with (MeO-^{tBu}PCP)IrH_2 (85%) *vs.* (H-^{tBu}PCP)IrH_2 (78%).

DFT calculations (P. Achord and K. Krogh-Jespersen) have shown that the π-donating MeO-group in the para position disfavors insertion of propene into the Ir-H bond of (H-^{tBu}PCP)IrH_2 *vs.* (MeO-^{tBu}PCP)IrH_2 by 1.7 kcal/mol. This is consistent with the slower rate of isomerization observed with (MeO-^{tBu}PCP)IrH_2.

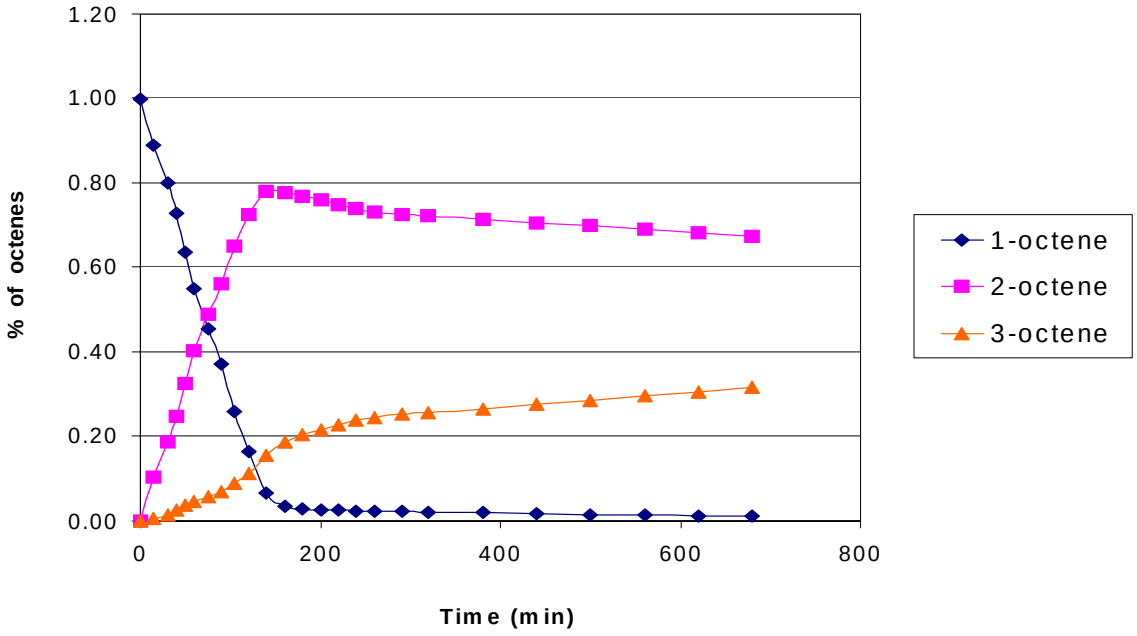

*Fig 3.2 (a) Isomerization of 1-octene catalyzed by (H-^{tBu}PCP)IrH_2 (**1**)*

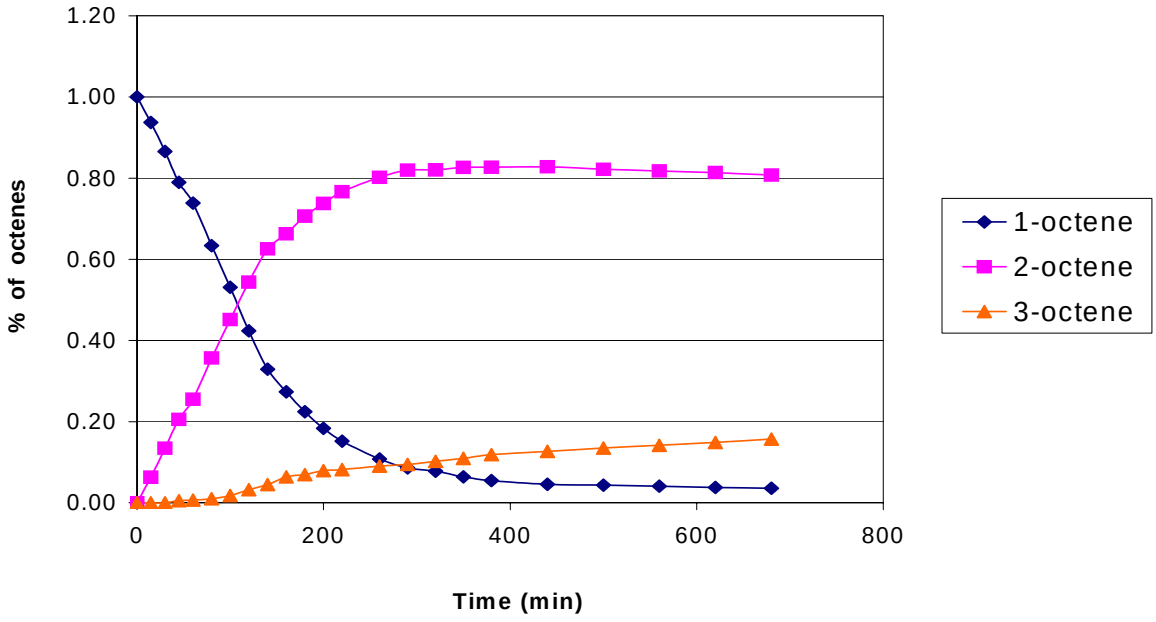

*Fig 3.2 (b) Isomerization of 1-octene catalyzed by (MeO-^{tBu}PCP)IrH_2 (**2**)*

3.3 Conclusion

The effects of steric and electronic tuning on the rate and selectivity of isomerization of 1-olefin, by a series of pincer-ligated iridium dihydride complexes were investigated. Isomerization of 1-octene was conducted in a solution of *p*-xylene using three different iridium pincer complexes of the type (X-^{R}PCP)IrH_2 (**1** : X = H, R = ^{t}Bu; **2** : X = MeO, R = ^{t}Bu; **3** : X = MeO, R = ^{i}Pr).

A comparison between complexes **2** and **3** has indicated that the presence of larger alkyl groups on phosphines in **2** has resulted in a slower rate of isomerization by this complex relative to **3**. Considering there are two steps in the conversion of 1-octene to 3-octene *via* the isomerization process (1-octene $\rightarrow$ 2-octene followed by 2-octene $\rightarrow$ 3-octene), selectivity was measured by a comparison between the relative rates of those two steps. With the more bulky ^{t}Bu groups, complex **2** has exhibited a relatively lower rate for the second step (2-octene $\rightarrow$ 3-octene) than the first one (1-octene $\rightarrow$ 2-octene) as compared to complex **3**. Therefore, the overall rate with **2** was lower but selectivity for 2-octene formation was slightly better with this catalyst relative to catalyst **3**.

Between **1** and **2**, the iridium center in case of the latter is more π-electron rich. Since increase in π-electron density at the metal center for a 16-electron pincer complex, (X-^{R}PCP)IrH_2, results in a lower tendency to bind an olefin, the rate of isomerization was found to be lower with **2**, relative to complex **1**. Additionally, due to the same electronic factors, **2** exhibited a lower rate for the 2-octene $\rightarrow$ 3-octene isomerization than the 1-

octene → 2-octene isomerization relative to **1** (presumably the iridium center is slightly more electron rich in the 2 → 3 TS as compared to the one in the latter). This has resulted in a higher buildup of 2-octene, during the overall isomerization, with **2** than with **1** – thus indicating its better selectivity towards formation of 2-olefinic products.

3.4 Experimental

3.4.1 General procedures

All routine manipulations were performed at ambient temperature in an argon-filled glove box or under argon using standard Schlenk techniques. *p*-xylene and 1-octene were distilled from sodium/potassium alloy, vacuum transferred under argon and stored in an argon-filled glove box. Complexes **1**, **2** and **3** were prepared according to the literature reported procedures.[9]

3.4.2 Isomerization experiment

A 1-mL reactor vessel was fitted with a Kontes high-vacuum stopcock, which allows freeze-pump-thaw cycling and addition of argon, and an Ace Glass "Adjustable Electrode Ace-Thred Adapter", which allows removal of 0.2-μL samples. In the argon-atmosphere glovebox, 0.15 mL of 1-octene, 0.75 mL of *p*-xylene and 0.05 mL of

hexamethyldisiloxane (HMDS, used as internal standard) were mixed together to give a resulting solution of 1.0 M in 1-octene and 0.25 M in HMDS. Required amount of **1**, **2** or **3** was added to this solution to make it 5 mM with respect to the catalyst. The charged apparatus was removed from the glovebox, and additional argon was added on a vacuum line to give a total pressure of 800 Torr. The reactor was put into a GC oven at 120 °C and samples were periodically taken out to analyze the product concentrations by GC.

GC Method: Analysis of octenes was carried out with a Varian 3400 gas chromatograph using SUPELCO SPB™-5 capillary column (60 m length x 0.32 mm ID) with FID detector. Calibration curves were prepared using authentic samples. A method file (Inlet temperature: 250 °C, Detector temperature: 250 °C) having a start temperature of 35 °C, 5 °C/min ramp and 250 °C final temperature was used.

3.5 References

1. (a) Schwartz, J. *Pure Appl. Chem.* **1980**, *52*, 733. (b) Schwartz, J.; Labinger, J. A. *Angew. Chem., Int. Ed. Engl.* **1976**, *15*, 333.

2. (a) Tkatchenko, I. In *Comprehensive Organometallic Chemistry;* Wilkinson, G.**;** Stone, F. G**.** A., Abel, E. W., Eds.; Pergamon Press: New York, **1982;** Vol. 8, pp 101-223**.** (b) Casey, C. P.; Cyr, C. R. *J. Am. Chem. Soc*. **1973,** *95***,** 2240**.** (c) Heck, R. F.; Breslow, D. S. *J. Am. Chem. Soc*. **1961,** *83*, 4023**.**

3. (a) Chalk, A. J. *J. Organomet. Chem.* **1970**, *21*, 207. (b) Chalk, A. J.; Harrod, J. F. J. *Am. Chem. Soc.* **1966**, *87*, 16. (c) Ryan, J. W.; Speier, J. L. *J. Am. Chem. Soc.* **1964**, *86*, 895.

4. (a) McKinney, R. J. *Organometallics* **1986**, *4*, 1142. (b) James, B. R. In *Comprehensive Organometallic Chemistry;* Wilkinson, G.**,** Stone, F. G. A., Abel, E. W., Eds.**;** Pergamon Press: New York, **1952;** Vol. 8, pp 285-369**.** (c) Tolman, C. A.; Seidel, *W.* C. *J. Am. Chem. Soc*. **1974**, *96*, 2774**.**

5. (a) Parshall, G. W. *Homogeneous Catalysis;* Wiley: New York, **1980**, pp 31-35; (b) Crabtree, R. H. *The Organometallic Chemistry of the Transition Metals;* Wiley: New York, **2001**; pp 226-227.

6. (a) Cramer, R. *J. Am. Chem. Soc.* **1966**, *88*, 2272. (b) McGrath, D. V.; Grubbs, R. H. *Organometallics* **1994**, *13*, 224.

7. Liu, F.; Pak, E. B.; Singh, B.; Jensen, C. M.; Goldman, A. S. *J. Am. Chem. Soc.* **1999**, *121*, 4086.

8. Krogh-Jespersen, K.; Czerw, M.; Zhu, K.; Singh, B.; Kanzelberger, M.; Darji, N.; Achord, P. D.; Renkema, K. B.; Goldman, A. S. *J. Am. Chem. Soc.* **2002**, *124*, 10797.

9. (a) Gupta, M.; Hagen, C.; Flesher, R. J.; Kaska, W. C.; Jensen, C. M. *Chem. Commun.* **1996**, 2083. (b) Zhu, K.; Achord, P. D.; Zhang, X.; Krogh-Jespersen, K.; Goldman, A. S. *J. Am. Chem. Soc.* **2004**, *126*, 13044.

Chapter 4

Synthesis and alkane dehydrogenation activity of a π-electron rich pincer-ligated iridium complex

Abstract

It has been found that an increase in π-electron density at the iridium center of (X-^{R}PCP)IrH_2 complexes leads to a catalyst with higher thermal stability and also superior alkane dehydrogenation activity. Earlier success in this regard on changing the X group (*para*-to iridium on the PCP aryl ring) from 'H' to 'MeO' prompted us to investigate any possible improvement in dehydrogenation activity the activity of iridium-pincer complexes by replacing MeO with an even more π-electron donating group 'NMe_2'. When tested for transfer dehydrogenation of linear and branched alkanes, the new catalyst, (NMe_2-^{tBu}PCP)IrH_2, was indeed found to exhibit higher activity and also slightly better selectivity (to give higher fraction of terminal olefinic products through dehydrogenation). Results obtained with the acceptorless dehydrogenation of cyclodecane were also found to be promising. However, no significant improvement in catalytic activity was observed on conducting the acceptorless dehydrogenation of *n*-undecane; presumably the linear olefinic products, obtained from *n*-undecane dehydrogenation, remained bound very strongly to the iridium centers, which ultimately led to fast decomposition of the catalysts.

4.1 Introduction

Selective catalytic dehydrogenation of alkanes has the potential for considerable industrial impact. Using low-cost saturated hydrocarbons as feedstock this process may be used to generate compounds with C-C double bonds that are useful precursors for commodity- and fine chemical synthesis. Heterogeneous dehydrogenation of alkanes over supported chromium oxide, alumina or Pt catalysts is carried out widely in industry for commercial production of a number of small aliphatic olefins like propene and isobutene. These molecules have large-scale industrial applications *e.g.* synthetic rubber, high purity commodity polymer, gasoline additives.[1]

Commercial processes (steam-thermal-cracking with or without heterogeneous catalyst) currently used to generate valuable olefins from the corresponding cheap alkanes have a number of inherent limitations. Since alkane dehydrogenation is an endothermic process, in industry, relatively high temperatures (~400 °C – 700 °C) are employed to obtain significant yields of alkenes; this makes the overall process significantly energy-intensive.[2] Moreover, under heterogeneous conditions, the required high temperatures often favor side reactions like thermal cracking, hydrogenolysis, oligomerization and aromatization, as well as the formation of unreactive carbon residues. With increasing chain length these side reactions, particularly the thermal cracking, becomes progressively more prevalent. For these reasons heterogeneous dehydrogenation of aliphatic alkanes, for commercial purpose, is still mostly limited to compounds containing up to five carbon atoms. Homogeneous dehydrogenation catalysts,

by contrast, not only offer the promise of much greater selectivity but also have the potential of effecting the reaction under milder conditions.

In the late 1970s Crabtree discovered the first solution phase transition metal system for alkane dehydrogenation.[3] Although a few more systems were reported soon thereafter, most of the early examples of alkane dehydrogenation were found to be stoichiometric (the dehydrogenated olefin remained bound to the metal complex rendering it catalytically inactive).[4] In 1984 Crabtree reported the first well-characterized alkane dehydrogenation system using $L_2IrH_2(\eta^2\text{-}O_2CCF_3)$ (L = PPh_3) (scheme 4.1).[5]

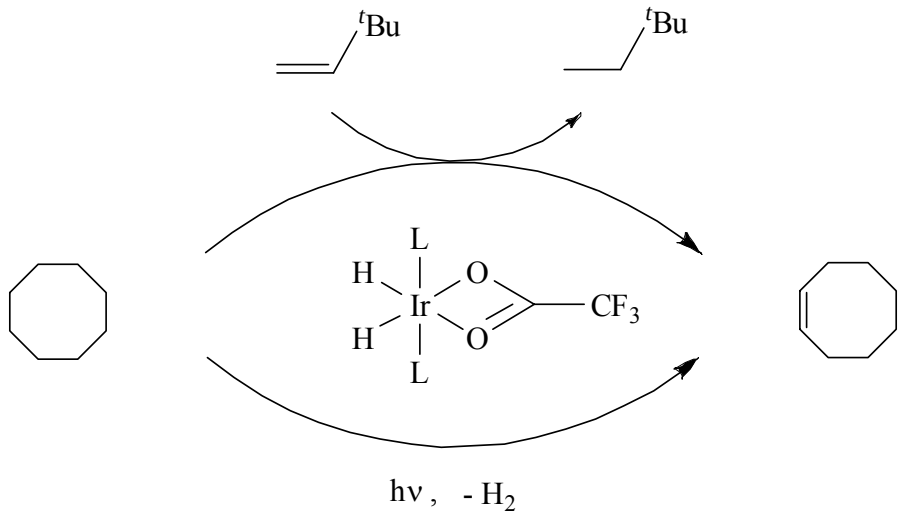

Scheme 4.1 Dehydrogenation of cyclooctane catalyzed by $L_2IrH_2(\eta^2\text{-}O_2CCF_3)$ by photochemical method or in the presence of a hydrogen acceptor

Both cycloalkanes and *n*-alkanes were found to undergo catalytic dehydrogenation by this complex, either in the presence of *t*-butylethylene (TBE) as the

sacrificial hydrogen acceptor, or photochemically (scheme 4.1). It was proposed that hydrogenation of the acceptor (TBE) followed by dechelation of the carboxylate ligand (η^2 to η^1) generated a three-coordinate 14-electron metal fragment, which was believed to be the key intermediate of the reaction.

Although the system, mentioned above, was recognized as the first example of catalytic alkane dehydrogenation, the turnover numbers were low (~ 40) as the catalyst was plagued by ligand decomposition. The first catalytic, highly efficient organometallic alkane dehydrogenation system was reported in the late 1980s. $Rh(PMe_3)_2(CO)Cl$ was found to give unprecedented turnovers (~ 1000) under photochemical conditions.[6,7] It was proposed that the role of photon was to generate the reactive intermediate "$Rh(PMe_3)_2Cl$", again indicating the importance of 3-coordinate d^8 systems for these type of reactions.[7,8] Interestingly, it was found that to drive the reaction thermochemically using a hydrogen acceptor (*e.g.* TBE), H_2 atmosphere was required. The proposed role of hydrogen was to cleave the inactive dimer, $[Rh(PMe_3)_2Cl]_2$, or displace a ligand L from $Rh(PMe_3)_2L$, through the formation of $H_2Rh(PMe_3)_2Cl$ intermediate.[9]

Although the $Rh(PMe_3)_2(CO)Cl$ system has shown promising dehydrogenation activity, the presence of H_2 led to the hydrogenation of more than one mole of acceptor per mole of olefin produced. To obviate the need for dihydrogen and to keep the metal centers from dimerizing, rhodium pincer complex, $(PCP)RhH_2$ was investigated. However, this was found to be a very poor dehydrogenation catalyst.[10] The same year, however, Jensen and Kaska reported that the iridium pincer complex, $(PCP)IrH_2$, gave

very good turnover numbers for transfer-dehydrogenation of a number of cycloalkanes (scheme 4.2).[11]

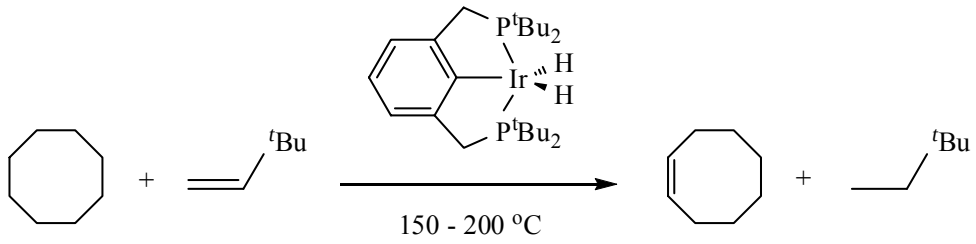

Scheme 4.2 Transfer dehydrogenation of cyclooctane catalyzed by (^{tBu}PCP)IrH$_2$ using tert-butylethylene as the hydrogen acceptor

Most importantly, prolonged stability of these complexes at high temperatures led to the discovery of first, efficient acceptorless dehydrogenation system (scheme 4.3). On refluxing a 1 mM solution of (^{tBu}PCP)IrH$_2$ in cyclodecane, 360 turnovers are obtained after 24 h. Under the same condition, sterically less bulky ^{i}Pr analogue was found to be an even better system, producing about 850 turnovers after 20 h of heating.[12] These catalyst systems were also found to dehydrogenate *n*-alkanes, regioselectively, to give terminal olefins as the major kinetic product[13] and have been found to be an effective system for transfer dehydrogenation of a variety of other substrates like ethylbenzene, tetrahydrofuran, alcohols, and secondary and tertiary amines.[14]

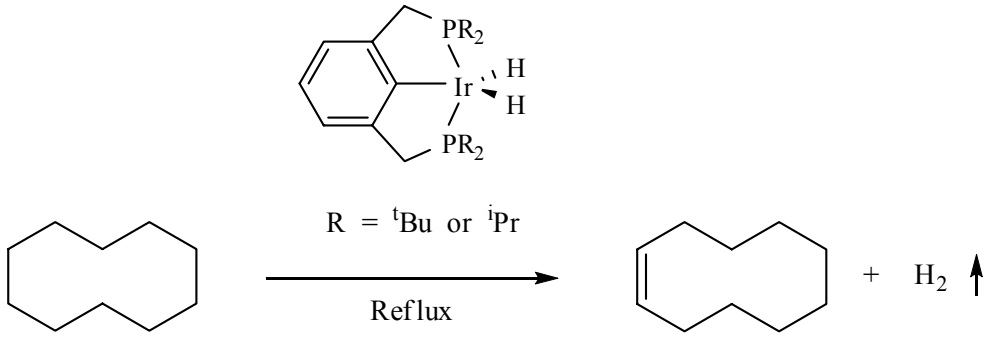

Scheme 4.3 Thermochemical dehydrogenation of cyclodecane catalyzed by (PCP)IrH_2 without the presence of a hydrogen acceptor

The rigid nature of the pincer (η^3- P,C,P,) backbone allows for modification of various ligand parameters to finely tune the steric and electronic properties of the complexed metal center. For example, by varying the **R** groups (to adjust steric factors) on phosphorus atoms and the **X** group (to adjust electronic factors) on pincer phenyl ring, it could be possible to systematically tune the reactivity pattern of the metal center (Fig 4.1).

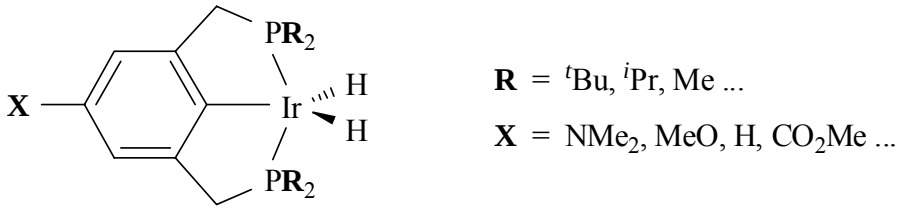

Fig 4.1 Possible variations of the ligand backbone in (X-^{R}PCP)IrH_2 complex

DFT calculations have shown that additions of C-H bonds and H_2 to the 14-electron fragments "(**X**-PCP)Ir" are favored by π-donating **X** groups.[15] Since the dehydrogenation cycle is known to operate via C-H oxidative addition to this "(X-PCP)Ir" fragment, strong π-donating groups attached to the phenyl ring might improve the performance of these catalysts. This was indeed found to be the case for (**X**-^{R}PCP)IrH_n (X = MeO, R = ^{t}Bu or ^{i}Pr) complexes as compared to the parent systems (X = H), for both acceptorless and transfer-dehydrogenation.[16]

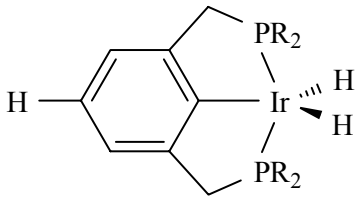

(H - ^{R}PCP)IrH_2

R = ^{t}Bu or ^{i}Pr

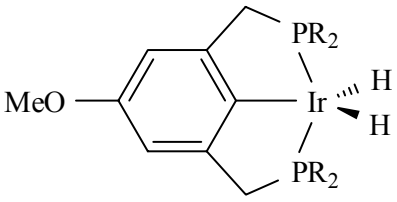

(MeO - ^{R}PCP)IrH_2

R = ^{t}Bu or ^{i}Pr

Fig 4.2 Different pincer complexes with varying X and R used for the study

In this chapter we report the synthesis and catalytic activity (both transfer and acceptorless dehydrogenation) of a new pincer complex with -NMe_2 substitution on the PCP-aryl ring *para* to the iridium. DFT calculations have predicted that both H_2 and benzene additions to the "(**X**-PCP)Ir" fragment are favored by changing **X** from -OMe to -NH_2 for **X**.[15] Additionally, it has been found that the same substitution also reduced the rate of isomerization of 1-octene by (X-PCP)IrH_2.[17] Replacement of H by MeO has also resulted in significant improvement of catalytic activity exhibited by these complexes

towards acceptorless dehydrogenation, presumably, due to increased thermal stability of these complexes.[16] Accordingly, we decided to pursue the synthesis of the *p*-dimethylamino-substituted pincer complex (**4d**) which should be even more electron rich than the "(**MeO**-^{R}PCP)IrH_2" analogue.

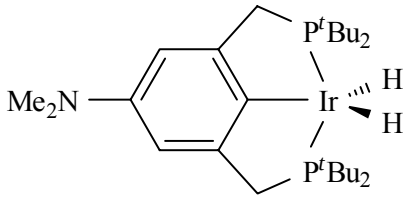

(Me$_2$N - ^{tBu}PCP)IrH_2 (**4d**)

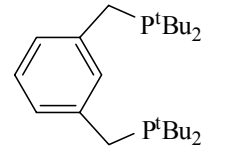

1a

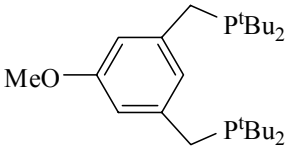

2a

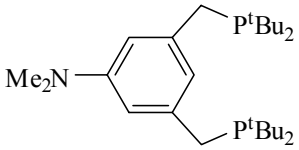

4a

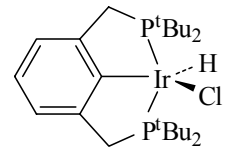

1b

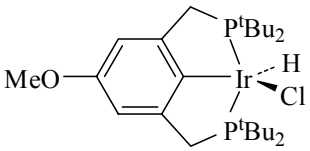

2b

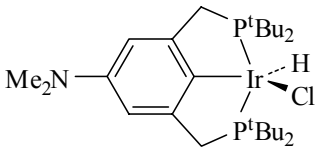

4b

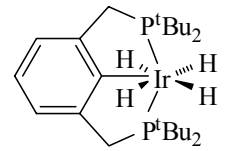

1c

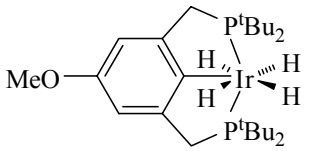

2c

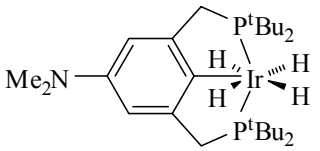

4c

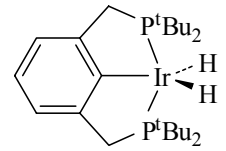

1d

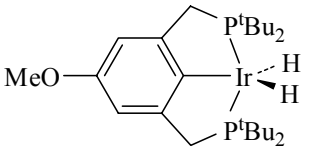

2d

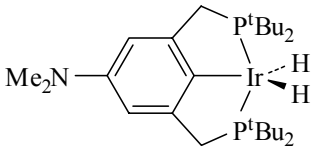

4d

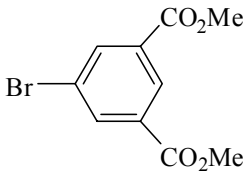

5

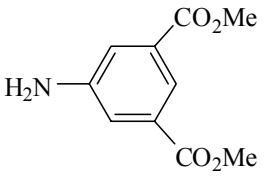

6

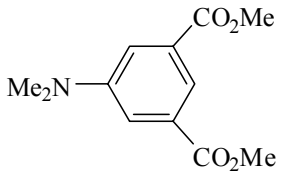

7

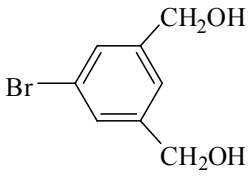

8

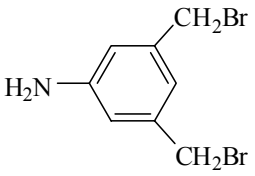

9

Fig 4.3 Pincer iridium complexes and their related precursors with the assigned reference numbers

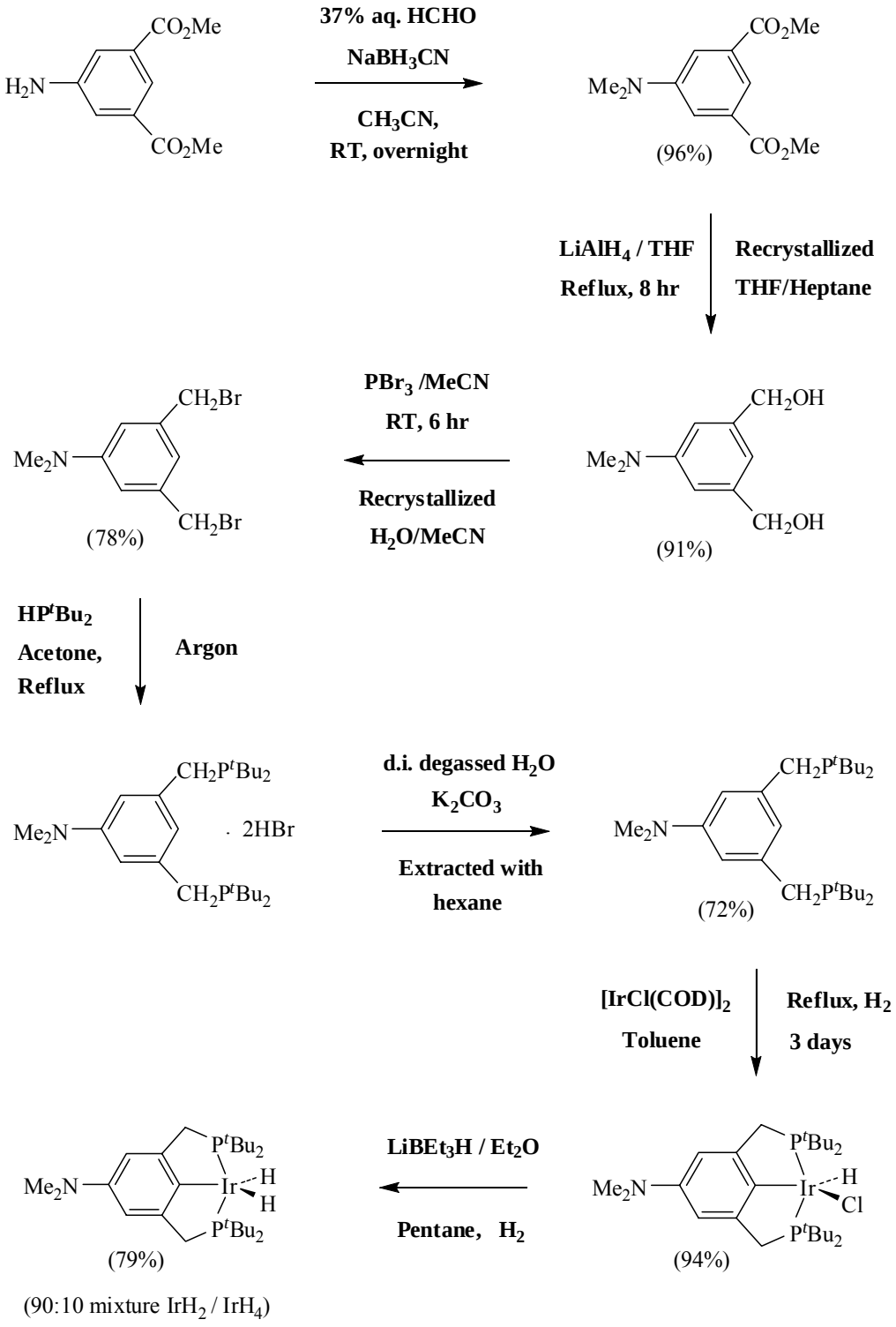

*Scheme 4.4 Synthesis of iridium pincer complex (NMe_2-^{tBu}PCP)IrH_2 (**4d**)*

4.2 Results and Discussions

4.2.1 Synthesis of different pincer complexes (X-^{R}PCPIrH$_2$) used for the study

*4.2.1.1 Synthesis of (H-^{tBu}PCP)IrH$_4$ (**1c**)*

In 1976 Moulton and Shaw reported the pincer ligand, ^{tBu}PCP-H (**1a),** and the corresponding iridium hydrido chloride complex (**1b**).[18] The latter can be reduced by LiBEt$_3$H at room temperature under hydrogen atmosphere to give the (H-^{tBu}PCP)IrH$_4$ catalyst (**1c**).[19] Upon heating at 130 °C under vacuum the tetrahydride complex (**1c**) loses a molecule of hydrogen to give the dihydride complex (**1d**). At room temperature both **1c** and **1d** react with acceptors (norbornene or *tert*-butylethylene) to act as the precursors of the 14-electron fragment "(H-^{tBu}PCP)Ir", presumably the active species in the dehydrogenation cycle.

*4.2.1.2 Synthesis of (MeO-^{tBu}PCP)IrH$_4$ (**2c**) (MeO-^{tBu}PCP)IrH$_2$ (**2d**)*

The complexes **2c** and **2d** were synthesized according to the literature reported procedure.[15] Reduction of the corresponding hydrido chloride complex (**2b**) with LiBEt$_3$H at room temperature under hydrogen atmosphere gives a mixture of **2c** and **2d** in roughly 3:1 proportion.

*4.2.3.3 Synthesis of (Me_2N-^{tBu}PCP)IrH_4 (**4c**) (Me_2N-^{tBu}PCP)IrH_2 (**4d**)*

Synthesis of both complexes **4c** and **4d** requires synthesis of the corresponding pincer phosphine ligand Me_2N-^{tBu}PCP-H (**4a**) via 1,3-bis(bromomethyl)-5-dimethylaminobenzene (**9**). Since **9** was not commercially available it was first necessary to synthesize it from an easily accessible precursor.

Synthesis of **9** was first attempted *via* **7** and **8** from the commercially available dimethyl 5-bromoisophthalate (**5**) and dimethylamine using the *Buchwald-Hartwig* C-N coupling route (scheme 4.5).[20]

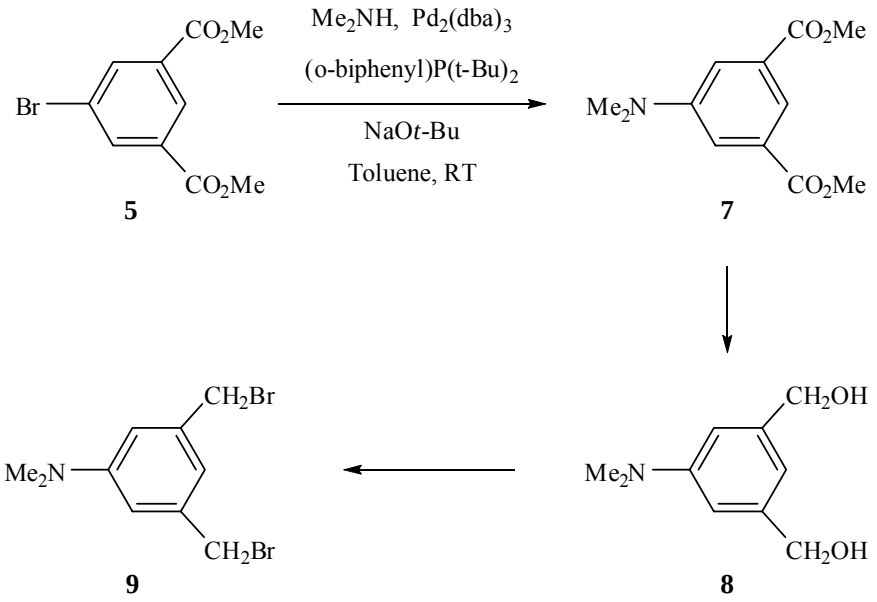

*Scheme 4.5 Synthesis of 1,3-bis(bromomethyl)-5-dimethylaminobenzene (**9**) starting from dimethyl 5-bromoisophthalate (**5**)*

Although the expected product (**7**) was obtained in fair yield (~ 72%) via this route, it was mixed with some unknown impurity even after the standard workup procedure. This route was finally abandoned due to high cost of the starting material and because of the problem associated with separation of the impurity while scaling up the reaction.

Next, entry into the above scheme was attempted via **7** using the easily available and inexpensive dimethyl 5-aminoisophthalate (**6**) as the starting material. However, *Eschweiler-Clarke* methylation with formaldehyde and formic acid did not yield the expected product, **7**. The starting compound (**6**) was found to get polymerized under the reaction conditions (acidic) due to the presence of strongly electron withdrawing (-CO_2Me) and donating groups (-NH_2) (which can underwent intermolecular condensation) on the ring (scheme 4.6).

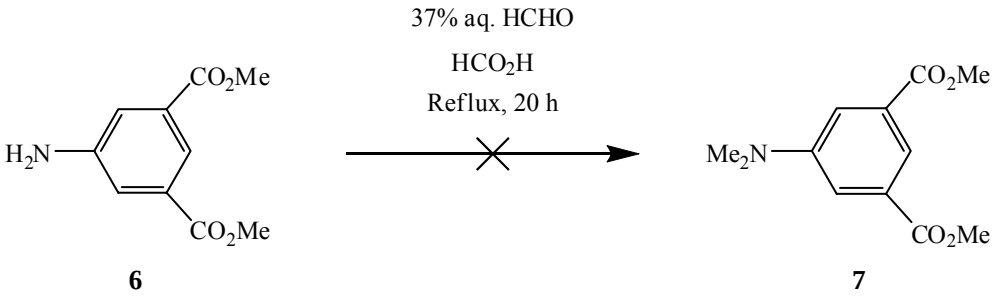

6 **7**

Scheme 4.6 Attempted synthesis of dimethyl 5-dimethylaminoisophthalate (7) using Eschweiler-Clarke methylation

A new procedure was then adopted to carry out the alkylation (**6** → **7**) under relatively milder conditions. Borch and Hassid have reported that it is possible to methylate aromatic amines using aqueous formaldehyde and sodium cyanoborohydride ($NaBH_3CN$) at room temperature.[21] The key point of the reaction was the finding that reduction of an imminium moiety (*i.e.* $>C=\overset{\oplus}{N}R_2$ or $>C=\overset{\oplus}{N}HR$) with $NaBH_3CN$ was rapid at pH 6-7, whereas reduction of aldehydes or ketones was negligible under this condition. Although, the initial equilibrium step (first step of scheme 4.7) is known to be unfavorable with aromatic amines (R = Ar), using an excess of the aldehyde it is possible to drive the reaction forward.

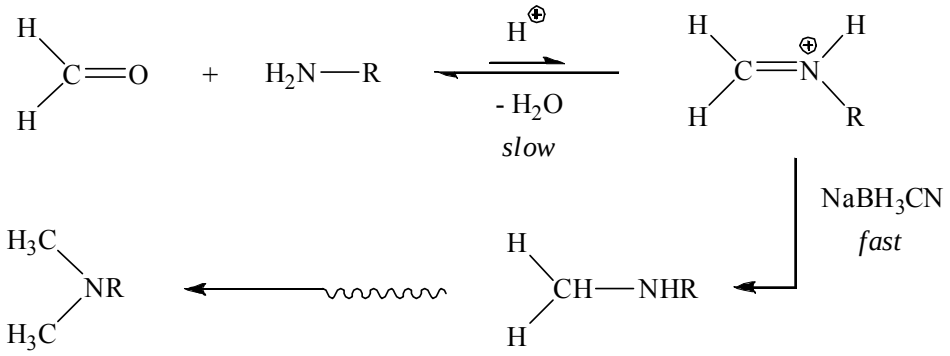

Scheme 4.7 Reductive methylation of amines at room temperature using formaldehyde and sodium cyanoborohydride

After several attempts with various proportions of formaldehyde and dimethyl 5-aminoisophthalate (**6**), a ratio of 10:1 was found to work well, giving a clean conversion with about 97% yield (scheme 4.8). Lower ratios resulted in a mixture of various proportions of dimethylated and monomethylated products.

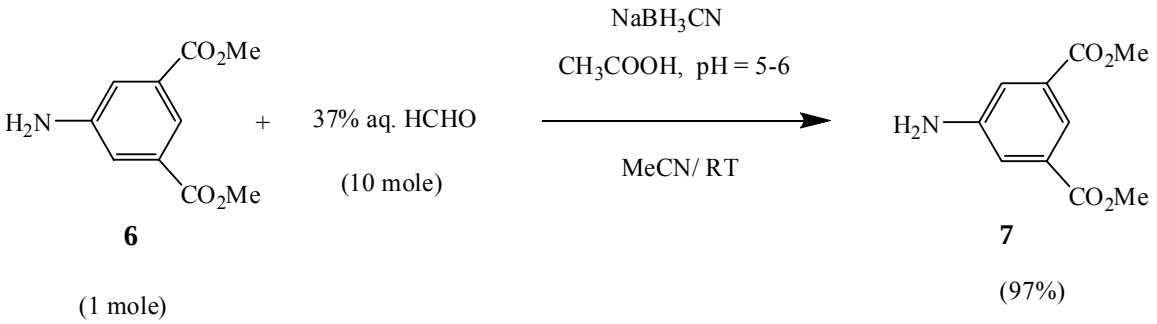

*Scheme 4.8 Reductive methylation of dimethyl 5-aminoisophthalate (**6**)*

The diester **7** was reduced to 5-dimethylamino-1,3-benzenedimethanol (**8**) by lithium aluminum hydride in THF.[22] Initially, the yield was not found to be satisfactory (40-50%) and the product was hard to recover in absolute purity. Although a similar problem has been reported in the literature for related systems containing heteroatom in the phenyl ring,[23] this was found to be mainly associated with incomplete reduction of the diester **7**, causing improper separation by recrystallization. Increasing the reaction time resulted in efficient conversion (91%) to the product **8**, after recrystallization from THF/heptane. The diol (**8**) was then reacted with PBr_3 in acetonitrile and the pure product **9** was recrystallized out in 77% yield from acetonitrile/water system.[24]

The synthesis of iridium pincer complexes, **4c** and **4d**, was similar to that of the complexes **2c** and **2d,**[16] but some changes were made for preparation of the corresponding phosphine ligand (**4a**). An earlier procedure involved dissolving the ligand salt, (X-^{tBu}PCP).2HBr, in water, and liberating the free phosphine using NaOAc as base, followed by extraction with diethyl ether. Due to the stronger basicity of NMe_2-^{tBu}PCP moiety relative to the acetate anion, K_2CO_3 was used instead of NaOAc. Secondly, due to

the miscibility of diethyl ether with water (~7% w/w) the extraction process often used to transfer some unknown impurities into the phosphine, taken up from the water layer. To avoid this problem, extraction was performed using hexane, and the ligand NMe_2-^{tBu}PCP (**4a**) was isolated in 72% yield with very high purity. In the crystal structure of complex **4a** (Fig 4.7), sum of the angles around nitrogen atom of NMe_2 was found to be 352°, strongly indicating a planar arrangement and significant π-donation from the nitrogen into the aryl ring. Cyclometalation of **4a** with $[Ir(COD)Cl]_2$ to give the corresponding hydrido chloride **4b** was not successful initially, until carried out under hydrogen atmosphere. Several attempts to obtain the expected product under argon failed – giving unidentified compounds with inequivelent, strongly coupled phosphorus atoms. However, after refluxing in hydrogen for 3 days the complex **4b** was obtained in high purity and in nearly quantitative yield (94%). Reduction of **4b** with $LiBEt_3H$ under hydrogen in pentane gave a dark red solid containing **4c** and **4d** in roughly 1:9 proportion. Either **4c** or **4d** completely turns into a four coordinate monocarbonyl complex (Me_2N-^{tBu}PCP)IrCO, with the evolution of hydrogen. Crystal structure of (Me_2N-^{tBu}PCP)IrCO is shown in Fig 4.8.

4.2.2 Comparative study of alkane transfer-dehydrogenation catalyzed by different pincer complexes (X-^{tBu}PCP)IrH_2 (X = H, MeO, Me_2N)

The dehydrogenation reaction of a typical organic substrate to give a C-C double bond and H_2 is generally quite endothermic (approximately 23 – 30 kcal/mole) process.

In general, to offset endothermicity, one of the commonly used strategies is to use a hydrogen acceptor (*e.g.* norbornene or tert-butylethylene) having a high negative enthalpy of hydrogenation (-30 to -33 kcal/mol). From the point of view of "atom-economy" a transfer dehydrogenation reaction might not seem to be an efficient process; however, if the product olefin has a higher value compared to the one hydrogenated, the overall reaction would be economical. Additionally, homogeneous catalytic transfer dehydrogenations are carried out at a relatively lower temperature and offer more control over product selectivity (for alkanes $>C_5$) compared to the heterogeneous counterpart thereby making the process more cost-effective.

Scheme 4.9 Transfer dehydrogenation in the presence of a sacrificial acceptor

Figure 4.4 below shows the catalytic cycle for alkane transfer dehydrogenation with iridium-pincer complexes, (X-^{R}PCP)IrH_2, using norbornene as the hydrogen acceptor. The 3-coordinate d^8 "(^{R}PCP)Ir" fragment is believed to be the key intermediate, which preferentially undergoes oxidative addition to the terminal position of an alkane, followed by β-H elimination to give a terminal olefin.

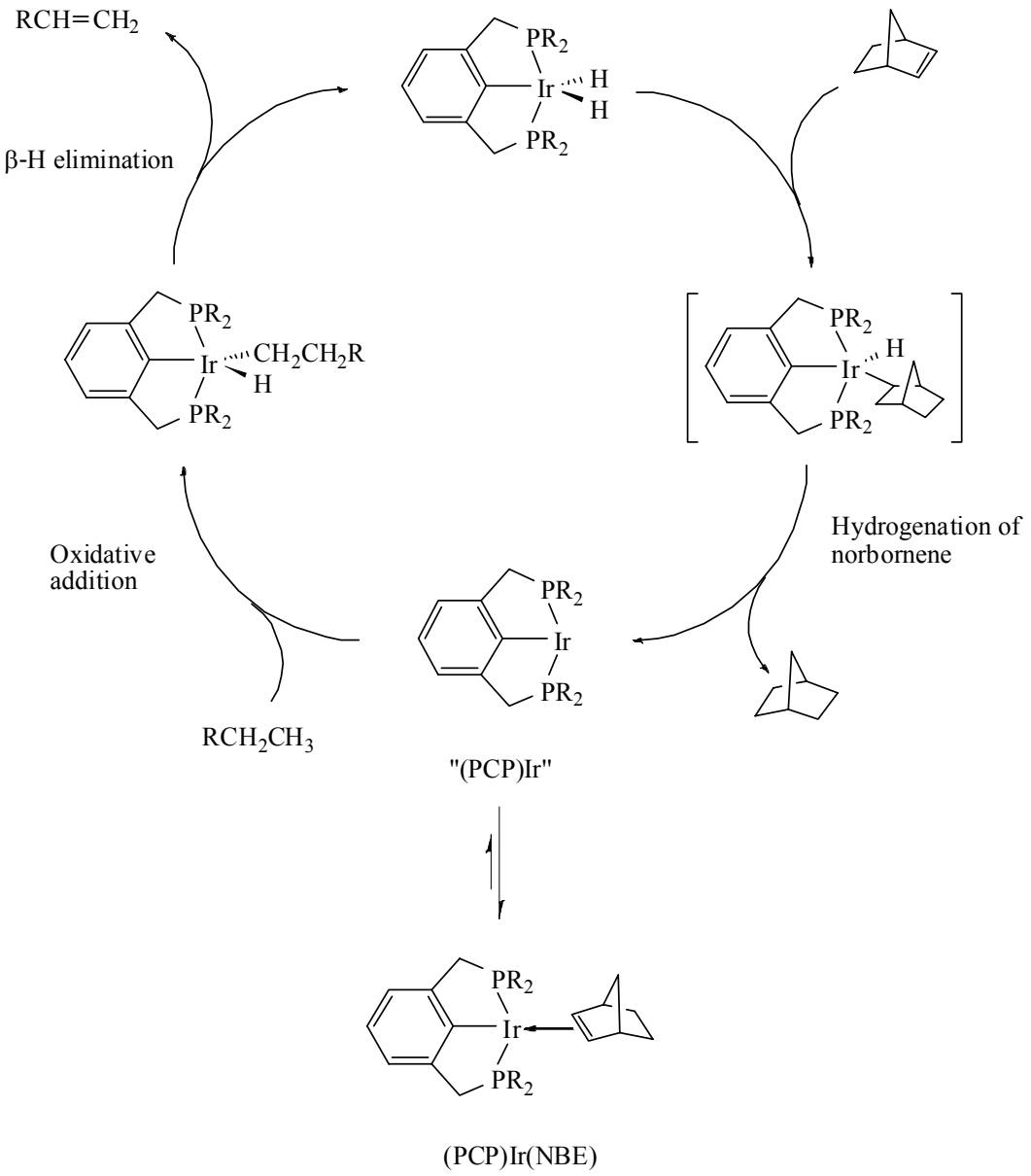

Fig 4.4 Mechanism of alkane transfer dehydrogenation catalyzed by (^{R}PCP)IrH$_2$ using norbornene (NBE) as the acceptor

Herein we report the transfer dehydrogenation activity (using *n*-octane and 4-propylheptane as substrates) of a new iridium pincer complex **4d**, having the strong π-donating group Me_2N on the pincer phenyl ring *para* to the iridium, and compare the

results, with the ones, obtained using complexes **1d** (H in the *para* position) and **2d** (MeO in *para* position).

4.2.2.1 Transfer dehydrogenation of n-octane

Earlier reports of *n*-octane dehydrogenation using iridium pincer complexes have indicated that these complexes show remarkable kinetic selectivity towards formation of 1-octene.[13]

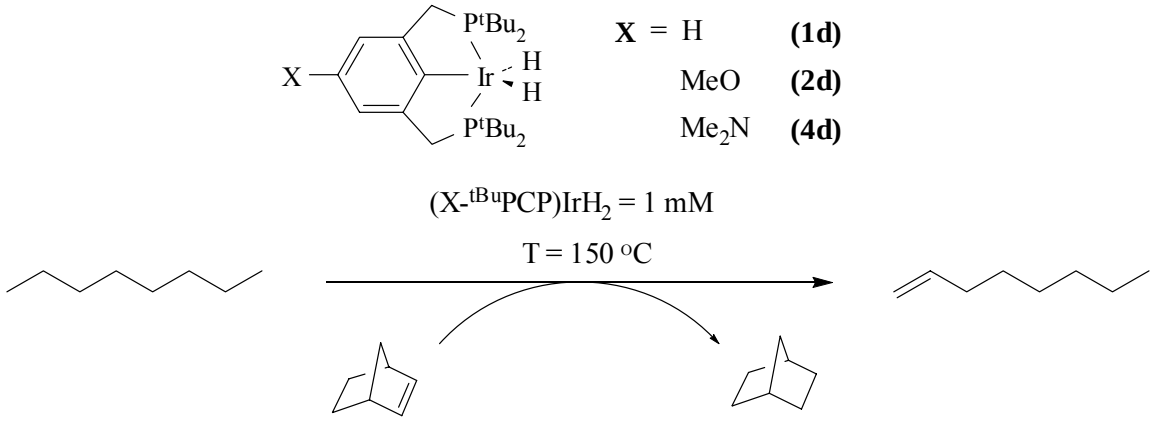

Scheme 4.10 Transfer dehydrogenation of n-octane catalyzed by (X-^{tBu}PCP)IrH$_2$ complexes using norbornene as the sacrificial acceptor

However, as these complexes also catalyze the isomerization of linear olefins, the terminal olefin initially produced in the reaction is converted to internal isomers over time. We have investigated the relative dehydrogenation rates and also the isomerization behavior of different iridium pincer complexes with *n*-octane as the substrate. Table 4.1 lists the results of dehydrogenation obtained using complexes **1d**, **2d** and **4d**.

*Table 4.1 Distributions of octenes (in mM) from transfer dehydrogenation of n-octane catalyzed by **1d**, **2d** and **4d** using 0.2 M norbornene*

Catalyst	Time (min)	NBE	1-octene	(*cis* + *trans*) 2-octene	Total	% of 1-octene	Rate
1d (X = H)	0	202	0	0	0	0	0
	5	184	11	5	16	68	192
	15	176	9	16	25	37	101
	30	166	7	27	34	20	69
	60	154	5	41	46	10	45
2d (X = MeO)	0	205	0	0	0	0	0
	5	185	15	3	18	84	217
	15	165	21	17	38	55	152
	30	148	17	38	55	31	110
	60	125	11	56	77	14	77
4d (X = NMe_2)	0	202	0	0	0	0	0
	5	181	19	2	21	90	251
	15	156	30	16	46	65	183
	30	131	26	43	69	38	138
	60	104	16	80	96	16	96

All runs were conducted at 150℃ using 1 mM of catalysts in neat n-octane.

All concentrations are reported in mM.

Rate = mM of octenes/h/mM of catalyst

In a typical experiment, an *n*-octane solution with 1 mM pincer complex and *ca.* 0.2 M norbornene (NBE) was charged into a sealed reactor under approximately 800 Torr of argon pressure. The reactor was heated in an oven at 150 °C; concentrations of the octenes and NBE were monitored by GC using hexamethyldisiloxane as the internal standard.

After five minutes of reaction although the difference in total yield between three catalysts were not significant, **2d** and **4d** showed slightly better selectivity (higher fraction of 1-octene in the solution). Complex **4d** had a slightly higher initial rate compared to the other two, catalysts and the difference became even more pronounced after 30 minutes into the reaction. At this point, **4d** showed an overall rate and selectivity which were 50% and 25% higher than **1d** and **2d**, respectively. This was indicative of a catalyst which was not only more active in terms of dehydrogenation but also had a lower isomerization rate. After one hour of reaction, roughly 50% of the initial NBE was consumed with **4d**, while the amount of NBE left with the other two catalysts, **1d** and **2d**, were 76% and 61% respectively.

Overall it was apparent that replacement of MeO- by Me_2N- led to a catalyst with slightly higher dehydrogenation activity and also exhibiting slightly better regioselectivity towards formation of 1-olefin. On heating a solution of 15 mM of the catalysts in presence of 100 mM of 1-octene at 150 °C it was found that both **2d** and **4d** had a longer lifetime compared to **1d**, with **4d** being marginally better compared to **2d**, as was indicated by ^{31}P NMR.

Results obtained from reactions carried out with a higher NBE concentration (0.5 M, Table 4.2) gave dehydrogenation rates slightly lower than those obtained with 0.2 M NBE.

*Table 4.2 Distributions of octenes (in mM) from transfer dehydrogenation of n-octane catalyzed by **2d** and **4d** using 0.5 M norbornene.*

Catalyst	Time (min)	NBE	1-octene	(*cis* + *trans*) 2-octene	Total	% of 1-octene	Rate
2d (X = MeO)	0	510	0	0	0	0	0
	5	493	13	2	15	89	179
	15	468	25	14	39	65	156
	30	446	28	33	61	46	122
	60	408	28	69	97	29	97
4d (X = NMe_2)	0	503	0	0	0	0	0
	5	483	16	1	17	94	204
	15	453	33	14	47	71	188
	30	419	42	38	80	52	159
	60	364	46	87	133	36	133

All runs were conducted at 150 ℃ using 1 mM of catalysts in neat n-octane.

All concentrations are reported in mM.

Rate = mM of octenes/h/mM of catalyst

The drop in initial rate of the reaction suggested that there is a slight NBE inhibition during the earlier phase of the reaction (217 *vs.* 179 with **2d** and 251 *vs.* 204 with **4d**). However, presence of higher concentrations of NBE led to lower isomerization activity by both **2d** and **4d**. It has been proposed that (X-^{R}PCP)IrH_2 is the active isomerizing catalyst; a higher concentration of acceptor leads to a lower steady-state concentration of this species and thus reduced isomerization rate.[13]

As has been found previously (with 0.2 M NBE) complex **4d** again demonstrated a slightly higher overall activity at every stage compared to **3d**. Although higher concentration of NBE resulted in better selectivity exhibited by both catalysts, apparently, complex **4d** had a slight advantage over **3d** – as evident from the % of 1-octene after 60 min of reaction - 14% (**2d**) *vs*. 16% (**4d**) with 0.2 M NBE compared to 29% (**2d**) *vs*. 36% (**4d**) with 0.5 M NBE.

4.2.2.2 Transfer dehydrogenation of 4-propylheptane

Dehydrogenation of 4-propylheptane has been investigated earlier for the comparative study with dehydrogenation of poly(1-hexene). As mentioned in chapter two, due to the symmetrical nature of the molecule and better resolution of its ^{1}H NMR spectra, it was easy to follow the dehydrogenation of this alkane and subsequent isomerization of the olefinic bonds by ^{1}H NMR alone. As shown in scheme 4.11 below, each olefinic product from this molecule was unique in its nature and also the ^{1}H NMR signal of different double bonds were widely separated and therefore easy to assign and quantify.

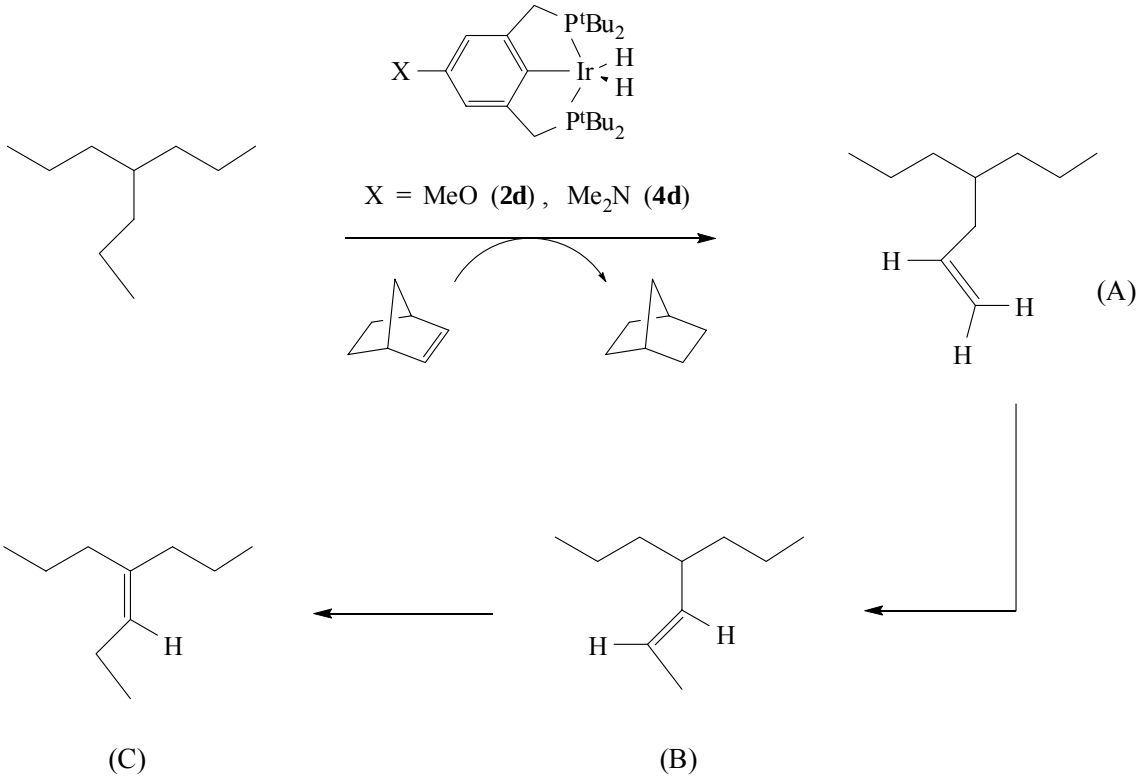

Scheme 4.11 Transfer dehydrogenation and subsequent isomerization of 4-propylheptane catalyzed by (X-^{tBu}PCP)IrH$_2$ complexes using norbornene as the sacrificial acceptor

A *p*-xylene-d_{10} stock solution of 4-propylheptane (~ 2 M) was prepared in, having approximately 0.3 M NBE and 0.086 M hexamethyldisiloxane (HMDS). To this solution required quantities of complexes **2d** or **4d** were added to give solutions 5 mM in catalyst. The solutions were heated in a sealed tubes immersed in an oil bath maintained at 150 °C and periodically monitored by both ^{1}H and ^{31}P NMR. PMe$_3$/mesitylene-d_{12} in a capillary and HMDS were used as internal and external standard, respectively, for quantification and referencing purposes.

After 60 min of reaction, *ca.* 70% of NBE was consumed with both **2d** and **4d**. As seen in Fig 4.5 there is a very slight difference between the rates, with **4d** being marginally better than **2d**. This small difference in initial rates observed here as compared to *n*-octane dehydrogenation was not completely unusual as the dehydrogenation in this case were carried out in a diluted solution (*p*-xylene) , rather than in neat alkane.

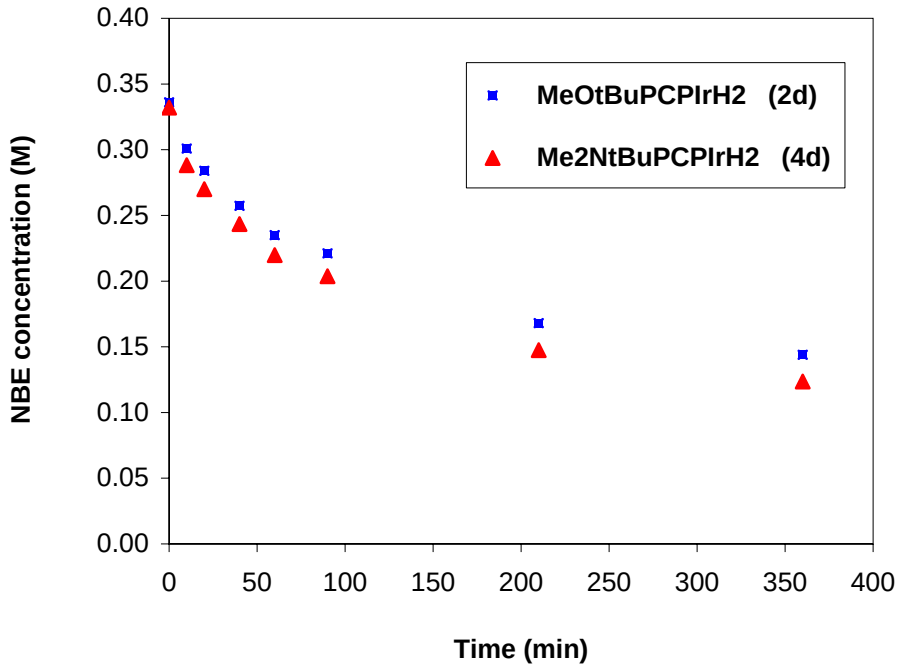

*Fig 4.5 Consumption of NBE over time during dehydrogenation of 4-propylheptane catalyzed by **2d** and **4d**. Condition: 5 mM catalyst, 0.3 M NBE, 150 ℃, p-xylene solution.*

The lower isomerization behavior of **4d** as compared to **2d** was also manifested in this reaction, although to a lesser extent than seen with *n*-octane dehydrogenation. As seen in Fig 4.6 at every point of the reaction, terminal olefinic product (indicated by solid

circle) with **4d** was always slightly higher in concentration as compared to the one produced with **2d**.

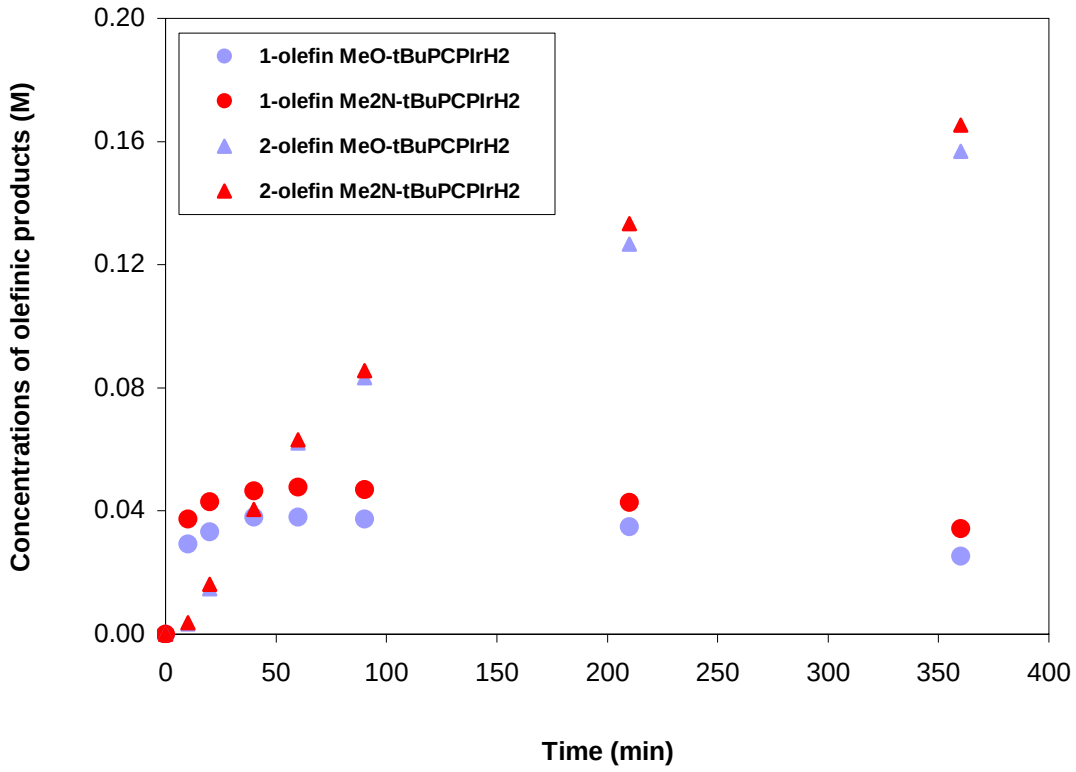

*Fig 4.6 Distribution of olefinic products over time during dehydrogenation of 4-propylheptane catalyzed by **2d** (para-MeO) and **4d** (para-Me_2N). Circles indicate terminal olefinic product (**A**) (see Scheme 4.11) and triangles indicate internal disubstituted 2-olefinic product (**B**). Condition: 5 mM catalyst, 0.3 M NBE, 150 ℃, p-xylene solution.*

^{31}P NMR data indicated there was no significant catalyst decomposition during the reaction. After six hours, the major species present in solution for both **2d** and **4d** were the NBE bound 14-electron intermediate, (X-PCP)Ir(NBE) complex.

In conclusion the Me_2N-PCP pincer ligated catalyst **4d** shows slightly greater activity than complex **2d** (which in turn is more active than the parent **1d**). For transfer dehydrogenation of both *n*-octane and 4-propylheptane higher turnover numbers are achieved with complex **4d** than with the other two pincer systems. The dimetylamino-pincer also exhibited slightly better selectivity towards formation of terminal olefins, which was believed to be a combination of both higher dehydrogenation activity coupled with lower isomerization rates.

4.2.3 Comparative study of acceptorless dehydrogenation of cyclic and linear alkanes catalyzed by different pincer complexes X-^{tBu}PCPIrH_2 (X = MeO, Me_2N)

Unlike transfer dehydrogenation, where the hydrogenation enthalpy of the acceptor is used to compensate the endothermicity of the overall process, in the case of acceptorless dehydrogenation, the reaction is driven thermochemically to overcome the energy barrier of alkane dehydrogenation (eq. 1).

$$\text{Alkane} \xrightarrow[\text{reflux}]{\text{catalyst}} \text{Alkene} + H_2 \qquad (1)$$

Since the acceptorless dehydrogenation does not require the use of a sacrificial olefin, the overall process is potentially more economical from commercial perspective. One of the earliest notable examples for acceptorless dehydrogenation was reported by Crabtree in 1993, using $Ir(O_2CCF_3)(PCy_3)_2$ and cyclooctane (COA) as the substrate.[25] However, the initial rate (1.41 mM h^{-1}) and final turnovers (28.5 mM of cyclooctene after 48 h) were low, the catalyst also suffered from ligand degradation.

In 1997, our group first demonstrated that the high thermal stability of pincer-ligated iridium complexes (~200 °C)[26] could be exploited to efficiently carry out the acceptorless dehydrogenation of an alkane.[12a] For example, using complex **1d** (H-^{tBu}PCP)IrH_2, COA was dehydrogenated to give 144 mM and 190 mM of cyclooctene (COE) after 44 h and 120 h, respectively. The higher boiling point of cyclodecane (CDA, b.p. 201 °C) was even more advantageous in this respect. Accordingly, on refluxing a CDA solution of 1 mM **1d**, 170 mM and 360 mM of cyclodecenes (mixture of *cis* and *trans*) were obtained after 4 h and 24 h, respectively. The sterically less hindered complex (H-^{iPr}PCP)IrH_4, was found to give even higher turnover numbers for acceptorless dehydrogenation of CDA (total of 987 turnovers after 20 h).[12b]

With an aim to tune the electronic density at the iridium center, a more π-electron rich complex **2d**, (MeO-^{tBu}PCP)IrH_2, was synthesized and was found to be a more active and a stable catalyst as compared to **1d**. Under similar conditions, acceptorless dehydrogenation of CDA with complex **2d**, gave 820 turnover numbers after 48 h of reaction, which was more than double the concentration obtained with **1d** after the same reaction time.[16]

In this section we report the acceptorless dehydrogenation activity (with CDA and *n*-undecane as the substrates) of the π-electron rich iridium pincer complex **4d,** (Me_2N-^{tBu}PCP)IrH_2.

4.2.3.1 Acceptorless dehydrogenation of cyclodecane (CDA)

The high boiling point of cyclodecane (201 °C) allowed the acceptorless dehydrogenation to be carried out at a relatively good rate using the complexes **2d** and **4d**. In a typical experiment, 1 mL of a stock solution of CDA with 1 mM of catalyst was refluxed, under a stream of argon (to remove the H_2 produced), in an oil bath maintained at 250 °C and the product concentrations were determined by GC.

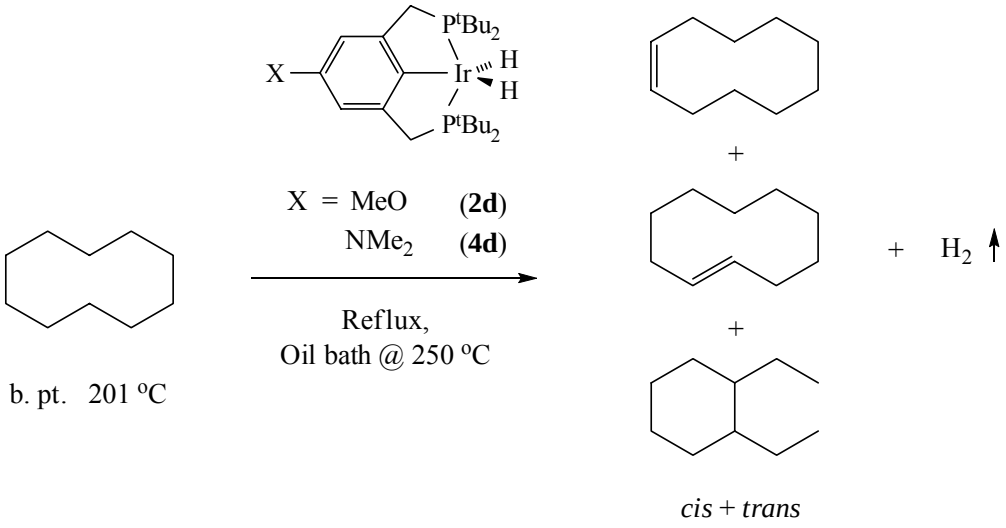

Scheme 4.12 Acceptorless dehydrogenation of cyclodecane catalyzed by (X-^{tBu}PCP)IrH$_2$

Total turnovers (which include concentrations for *cis* and *trans* cyclodecenes and diethylcyclohexanes) obtained with two catalysts are shown in Table 4.3. There was about 80 mM of difference in turnovers from the two complexes after 6 h; when the reactions were stopped after 96 h of heating there was a turnover difference of 400 mM between the two catalysts. Although it was apparent that from this point onwards the reaction seemed to level off, however, it could be due to either catalyst decomposition or product inhibition. There was a big drop in the reaction rate (95 to 33 for **2d** and 109 to 47 for **4d** after 6 and 24 h, respectively) and a very small increase in total turnover with both catalysts.

Table 4.3 Acceptorless dehydrogenation of CDA catalyzed by (X-^{tBu}PCP)IrH$_2$.

Catalyst	Time (h)	*cis* + *trans* DEC	*cis* + *trans* CDE	Total turnovers	Rate
2d (X = MeO)	1	4	150	154	154
	2	5	268	273	137
	3	6	351	356	119
	4	6	424	431	108
	6	9	564	572	95
	24	22	775	797	33
	48	25	813	838	17
	72	26	820	846	12
4d (X = NMe_2)	1	5	163	168	168
	2	6	297	303	152
	3	7	413	420	140
	4	8	493	501	125
	6	11	645	656	109
	24	27	1106	1133	47
	48	29	1182	1210	25
	72	31	1193	1224	17

All runs were conducted at 250℃ oil bath using 1 mM of catalysts in neat CDA. All concentrations are reported in mM. Rate = mM of total turnovers/h/mM of catalyst. DEC = diethylcyclohexane and CDE = cyclodecene.

Since these iridium-pincer complexes were known to decompose at a faster rate under high concentrations of olefinic substrates, in order to probe more into the difference in catalytic activity of the two complexes we decided to investigate their dehydrogenation behavior through continuous recycling of the catalysts. We felt, this

would give us more insight about whether the reaction leveling off was due to catalyst decomposition or because of product inhibition. To do this, cyclodecane solutions having 1 mM of either complex (**2d** or **4d**) was refluxed in an oil bath at 250 °C and the products were monitored continuously by GC. After six hours the reaction was stopped, volatiles (decenes and decane) were pumped off and a fresh batch of CDA was added; reflux was continued for another 6 h and the whole sequence was repeated for the second time. As suggested by the results (shown in Table 4.4) product inhibition (rather than just catalyst decomposition) was the key factor that led to lower turnovers and early reaction leveling-off, which was observed during the last experiment (Table 4.3).

A comparison of the data shown in Table 4.4 revealed that both catalysts were fairly stable after six hours of reaction at 250°C as indicated by a negligible drop in the reaction rate (141 to 134 for **2d** and 160 to 154 for **4d**) when the reactions were restarted with a fresh batch of CDA, after initial 6 h. After 12 h (6 h + 6 h) of heating, complex **4d** seemed to exhibit slightly better stability relative to **2d**, as shown by the comparison of individual rates at the end of two six-hour run (drop from 112 to 106 for **4d** *vs.* drop from 97 to 78 for **2d**). Results after 16 h (6h + 6h + 4h) of reaction indicated complex **2d** suffered significant decomposition at this point with a drop in the reaction rate from 71 to 46. However, **4d** was still relatively stable at this point, having a rate which was more than double that of **2** (46 of **2** *vs.* 97 of **4d**). When heating was ended after a combined reaction time of 22 h, catalyst **4d** had generated a total of about 1.8 M dehydrogenated product, by far the highest ever observed by a pincer complex in its category (bearing di-t-butyl groups on phosphines).

Table 4.4 Acceptorless dehydrogenation of CDA catalyzed by (X-^{tBu}PCP)IrH_2. Volatiles were pumped off and fresh CDA was added every 6h.

Catalyst	Run	Time (h)	*cis* + *trans* DEC	*cis* + *trans* CDE	Total turnovers	Rate
2d (X = MeO)	1	2	5	278	283	141
		4	6	422	428	107
		6	9	573	582	97
	2	2	4	266	270	135
		4	5	400	405	101
		6	5	465	470	78
	3	2	3	138	141	70
		4	2	183	185	46
		6	2	195	197	33
4d (X = NMe_2)	1	2	7	313	320	160
		4	10	511	521	130
		6	12	662	674	112
	2	2	6	302	308	154
		4	8	497	505	126
		6	10	624	634	106
	3	2	5	236	241	121
		4	6	382	388	97
		6	7	423	430	72
		10	8	475	483	48

All runs were conducted at 250℃ oil bath using 1 mM of catalysts in neat CDA. All concentrations are reported in mM. Rate = mM of total turnovers/h/mM of catalyst. DEC = diethylcyclohexane and CDE = cyclodecene.

4.2.3.2 Acceptorless dehydrogenation of n-undecane

The reaction of *n*-undecane (196 °C) was carried out with 1 mM of complexes **2d** and **4d** (scheme 4.13), under the same conditions used for dehydrogenation of cyclodecane (scheme 4.9). Product distributions were determined by GC, over a period of 24 h, the results are shown in Table 4.5.

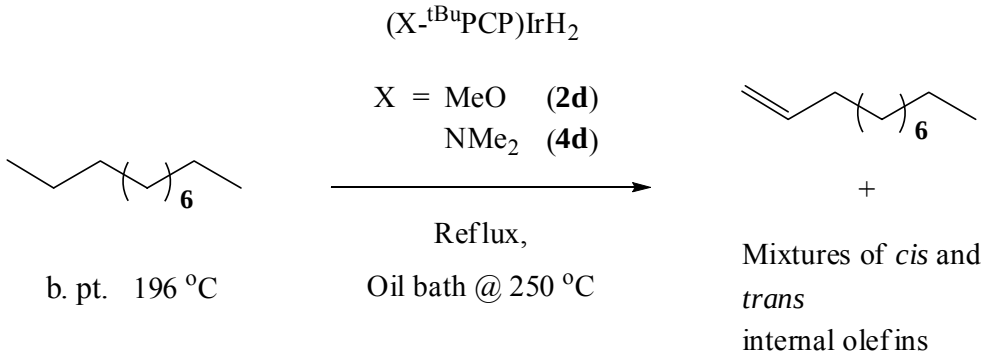

Scheme 4.13 Acceptorless dehydrogenation of n-undecane catalyzed by (X-^{tBu}PCP)IrH$_2$

As shown in Table 4.5 the concentrations at each point of time were fairly low as compared to the ones obtained with same catalysts using CDA. Although **4d** gave slightly higher turnovers and better initial and final rates, total turnovers achieved with the two catalysts after 24 h of heating were pretty small (108 and 131 with **2d** and **4d**, respectively).

Table 4.5 Acceptorless dehydrogenation of n-undecane catalyzed by (X-^{tBu}PCP)IrH$_2$.

Catalyst	Time (h)	1-undecene	Others	Total turnovers	Rate
2d (X = MeO)	1	22	16	38	38
	2	28	35	63	32
	4	33	51	84	21
	8	34	65	99	12
	24	31	77	108	5
4d (X = NMe$_2$)	1	32	15	47	47
	2	41	38	79	40
	4	43	57	100	25
	8	44	72	116	15
	24	42	89	131	6

All runs were conducted at 250℃ oil bath using 1 mM of catalysts in neat n-undecane. All concentrations are reported in mM. Rate = mM of total turnovers/h/mM of catalyst. Others = Mixtures of cis and trans internal olefins.

Very low turnovers as well as the poor rates obtained for *n*-undecane dehydrogenation are probably associated with the linear olefinic products, which are much less sterically hindered compared to cyclodecenes, and can bind to the iridium centers fairly strongly. Moreover the enthalpy of dehydrogenation of linear alkanes is much greater than that of CDA; this could potentially result in a much faster back-reaction of olefin product with the dissolved H_2.

An NMR study was conducted out in which complex **4d** (30 mM) was dissolved in two different NMR tubes containing 0.1 M solution of 1-undecene and *cis*-cyclodecene, respectively, in *p*-xylene. On heating the flame-sealed NMR tubes in an oven at 250 °C, the catalyst solution containing 1-undecene was found to decompose at a much faster rate, as indicated by ^{31}P NMR. The resulting spectra indicated the presence of complexes containing strongly coupled, inequivalent phosphorous atoms, possibly formed through cyclometallation of complexes bound to linear olefins.

4.2.3.3 Heterogeneous transfer dehydrogenation of cyclooctane

Ability to carry out transfer dehydrogenation under heterogeneous condition at a lower temperature may offer various advantages *e.g.* catalyst recycling, easy product separation from the catalyst etc. Using alumina as the support, iridium pincer complexes were used to investigate the heterogeneous transfer dehydrogenation of cyclooctane in presence of TBE as the hydrogen acceptor.

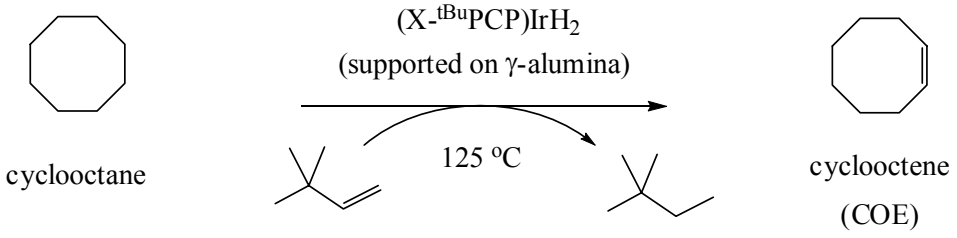

Scheme 4.14 Heterogeneous transfer dehydrogenation of cyclooctane catalyzed by (X-^{tBu}PCP)IrH$_2$

In a typical reaction, 5 mM solution of a catalyst was mixed with calcined γ-Al_2O_3. When the solution turned colorless (indicating complete adsorption of the catalyst onto the alumina surface) the solution was made 0.4 M with respect to TBE, heated at 125°C and monitored periodically using GC. The results are shown in Table 4.6.

Table 4.6 Heterogeneous transfer dehydrogenation of cyclooctane catalyzed by (X-^{tBu}PCP)IrH_2.

Catalyst	Time (min)	COE	Rate
1d (X = H)	30	2	0.8
	60	3	0.6
	120	4	0.4
	240	7	0.4
2d (X = MeO)	30	40	16
	60	60	12
	120	78	8
	240	84	4
4d (X = NMe_2)	30	68	27
	60	136	27
	120	207	21
	240	308	16

All runs were conducted at 125 ℃ oil bath using 5 mM of catalysts in neat cyclooctane. All concentrations are reported in mM. Rate = mM of total turnovers/h/mM of catalyst.

As shown in Table 4.6 complex **1d** suffered fast decomposition under the reaction condition compared to the other two catalysts. 4d was most stable under the heterogeneous condition, providing more than three times the turnover numbers as has been produced by 2d, after four hours of reaction. Higher stability of 4d relative to the other two is presumably due in part to its stronger binding to the alumina surface.

4.3 Conclusion

A new π-electron rich pincer ligand and its iridium hydride complex (Me_2N-^{tBu}PCP)IrH_2 (**4d**) were synthesized. Transfer dehydrogenation activity of complex **4d** was compared with those of **2d** and **1d** using different concentrations of NBE (acceptor) and *n*-octane as the substrate. A comparison of total turnover numbers and also the rates, suggested a superior performance of **4d** relative to the other two complexes. A comparison of the results, exhibited by two catalysts on conducting reactions with different NBE concentrations, revealed that the difference in selectivity between the catalysts increased with higher concentrations of NBE. Dehydrogenation of 4-propylheptane gave the similar results. The higher selectivity achieved by **4d** is presumably due to a combination of higher dehydrogenation rate and relatively lower isomerization activity.

Acceptorless dehydrogenation, under refluxing conditions, was carried out using complex **2d** and **4d** with cyclodecane (CDA) and *n*-undecane as the substrates. Three

days of continuous reflux of a solution of CDA with 1 mM of catalysts resulted in roughly 400 extra turnovers achieved with complex **4d**. Since the reaction seemed to level off after 24 h of heating, with either catalyst, it was repeated under a condition where the volatiles were pumped off every six hours, fresh batch of CDA was added, and refluxing resumed. After 26 h (6 h + 6 h + 10 h) of heating complexes **2d** and **4d** were found to accumulate about 1.2 M and 1.8 M, respectively, dehydrogenated products, indicating that the reaction leveling off in individual runs at longer times reaction was not due to catalyst decomposition but rather due to product inhibition.

Acceptorless dehydrogenation of *n*-undecane at 250 °C gave lower rates and yield than with CDA. Both **2d** and **4d** (1 mM) gave total turnovers which were slightly above 100. A study of the reaction by ^{31}P NMR indicated that the decomposition was probably due to reaction with linear olefinic products, which appeared to give cyclometalated products over course of the reaction.

4.4 Experimental

4.4.1 General procedures

All routine manipulations were performed at ambient temperature in an argon-filled glove box or under argon using standard Schlenk techniques. All NMR solvents (protiated or deuterated) were distilled from sodium/potassium alloy, vacuum transferred

under argon and stored in an argon-filled glove box. ^{1}H, $^{31}P\{^{1}H\}$ and $^{13}C\{^{1}H\}$ NMR spectra were obtained on a 400-MHz, Varian Inova-400 spectrometer or on a 300-MHz, Varian Mercury-300 spectrometer. ^{1}H chemical shifts are reported in ppm downfield from tetramethylsilane and were referenced to the residual protons of deuterated solvents. ^{31}P NMR chemical shifts were referenced to PMe_3/mesitylene (-62.6 ppm). Norbornene was purchased from Sigma-Aldrich, sublimed under vacuum and stored in an argon-filled glove box. All other chemicals were used as received from commercial suppliers.

4.4.2 Transfer Dehydrogenation

4.4.2.1 Transfer dehydrogenation of n-octane

n-Octane transfer dehydrogenation experiments were typically conducted as follows. A 5-mL reactor vessel was fitted with a Kontes high-vacuum stopcock, which allows freeze-pump-thaw cycling and addition of argon, and an Ace Glass "Adjustable Electrode Ace-Thred Adapter", which allows removal of 0.2-μL samples. In the argon-atmosphere glovebox, 0.5 mL of *n*-octane solution (1 mM catalyst, and acceptor) was charged into the reactor. The charged apparatus was removed from the glovebox, and additional argon was added on a vacuum line to give a total pressure of 800 Torr. The reactor was put into a GC oven 150 °C. Samples were periodically taken by microliter syringe for to analyze the product concentrations by GC, using 0.42 M hexamethyldisiloxane as the internal standard.

GC Method: Analysis of octenes was carried out with a Thermo Electron Corporation Focus gas chromatograph using Supelco Petrocol DH column (100 m length x 0.25 mm ID x 0.5 μm film thickness) with FID detector. Calibration curves were prepared using authentic samples. A method file (Inlet temperature: 230 °C, Detector temperature: 250 °C) having 60 °C isotherm and He flow rate of 1 mL/min was used.

4.4.2.2 Transfer dehydrogenation of 4-propylheptane

Since all the dehydrogenated products for this substrate could be easily detected using ^{1}H NMR, the reactions were carried out in flame-sealed NMR tubes. To a stock solution of 4-propylheptane (~ 2 M), NBE (0.3 M) and hexamethyldisiloxane (0.086 M, used as internal standard) in *p*-xylene-d_{10}, complexes **2d** or **4d** were added to make the solution 5 mM in catalyst. The solution was heated in a sealed tube immersed in an oil bath maintained at 150 °C and periodically monitored by both ^{1}H and ^{31}P NMR.

4.4.3 Acceptorless Dehydrogenation

In a typical experiment, in the argon-atmosphere glovebox, 1.0 mL of catalyst solution (1 mM) (in CDA or *n*-undecane) was charged into a reactor consisting of a 5-mL round-bottom cylindrical flask fused to a water-jacketed condenser (ca. 15 cm). The top of the condenser was fused to two Kontes high-vacuum valves and an Ace Glass "Adjustable Electrode Ace-Thred Adapter". The solution was refluxed in an oil bath held at 250 °C. H_2 was purged from the system by a continuous argon stream above the

condenser. The reactions were monitored by GC using 0.14 M mesitylene as the internal standard.

GC Method (**used for dehydrogenation of CDA**): Analysis of products was carried out with a Thermo Electron Corporation Focus gas chromatograph using Agilent HP-1 column (100% Methyl Silicone gum; 25 m length x 0.2 mm ID x 0.5 μm film thickness) with FID detector. A method file (Inlet temperature: 230 °C, Detector temperature: 250 °C) having a start temperature of 40 °C, 10 °C/min ramp and 200 °C final temperature with He flow rate of 1 mL/min was used.

GC Method (**used for dehydrogenation of *n*-undecane**): Analysis of octenes was carried out with a Thermo Electron Corporation Focus gas chromatograph using Supelco Petrocol DH column (100 m length x 0.25 mm ID x 0.5 μm film thickness) with FID detector. A method file (Inlet temperature: 230 °C, Detector temperature: 250 °C) having a start temperature of 130 °C, 0.5 °C/min ramp and 250 °C final temperature with He flow rate of 1 mL/min was used.

4.4.4 Synthesis of different pincer complexes (X-^{tBu}PCPIrH$_2$) and their precursors

*4.4.4.1 Synthesis of (H-^{tBu}PCP)IrH$_2$ (**1d**) and (MeO-^{tBu}PCP)IrH$_2$ (**2d**)*

These complexes were synthesized according to the reported procedures.[15,19]

*4.4.4.2 Synthesis of dimethyl 5-dimethylaminoisophthalate (**7**)*

This was prepared by a reported procedure for reductive alkylation of aromatic amines.[21] To a stirred solution of 5 g (23.4 mmol) dimethyl 5-aminoisophthalate (**6**) (98%) and 20 mL (269 mmol) of 37% aqueous formaldehyde in 150 mL of acetonitrile was added 5 g (75.6 mmol) of sodium cyanoborohydride. 3 mL of Glacial acetic acid was slowly added over 20 min to adjust the pH to 5-6, and the reaction was stirred at room temperature for 8 hr. TLC (Hexane : EtOAc = 1:1) of the clear yellow supernatant showed a single spot indicating pure product. The solution was transferred to a new flask and the solvent was removed under reduced pressure. The product obtained was washed thoroughly with distilled water and air-dried to give 5.39 g of **7** as a white solid in near quantitative yield (97%). ^{1}H NMR ($CDCl_3$): δ 8.01 (s, 1H, *Ar*), 7.56 (s, 2H, *Ar*), 3.94 (s, 6H, CO_2CH_3), 3.05 (s, 6H, $(CH_3)_2N$).

*4.4.4.3 Synthesis of 5-dimethylamino-1,3-benzenedimethanol (**8**)*

To a stirred suspension of 2.69 g (67.4 mmol) lithium aluminum hydride (95%) in anhydrous tetrahydrofuran (50 mL) at 0 °C under argon atmosphere was slowly added a solution of **7** (5 g, 21.1 mmol) in anhydrous tetrahydrofuran (100 mL). After the addition was complete, the resultant suspension was refluxed for 18 h, diluted with 100 mL tetrahydrofuran and cooled to 0 °C. Excess lithium aluminum hydride was quenched by slow addition of saturated sodium sulfate solution followed by water and the suspension was stirred at 0 °C - 5 °C for 1 h (until the gray color of lithium aluminum hydride disappeared completely). It was filtered through a pad of anhydrous magnesium sulfate

and washed subsequently with ethyl acetate (3 × 50 mL). The combined filtrates were concentrated under reduced pressure to give a clear colorless oil that crystallized upon standing. The product **8** was recrystallized from tetrahydrofuran/heptane as a white powder (3.49 g, 91% yield). ^{1}H NMR (DMSO-d_6): δ 6.58 (s, 1H, *Ar*), 6.56 (s, 2H, *Ar*), 5.03 (t, 2H, O*H*), 4.41 (d, 4H, CH_2), 2.87 (s, 6H, (CH_3)$_2$N).

*4.4.4.4 Synthesis of 1,3-bis(bromomethyl)-5-dimethylaminobenzene (**9**)*

PBr_3 (10.4 mL, 110 mmol) was added dropwise over a 30 min period to a solution of **8** (5.0 g, 27.6 mmol) in 140 mL of dry acetonitrile in a 250-mL flask under argon atmosphere at 0 °C. The solution was stirred at room temperature for 2 h and then heated to 70 °C for an additional 4 h. The reaction was quenched by pouring the solution onto ice, and saturated $NaHCO_3$ solution was added slowly to adjust pH to ~ 7. The solution was filtered and the white precipitate was dissolved in acetonitrile. Product **9** was recrystallized out from acetonitrile/water system to give 6.52 g of white powder in 77% yield. ^{1}H NMR ($CDCl_3$): δ 6.78 (s, 1H, *Ar*), 6.66 (s, 2H, *Ar*), 4.45 (s, 4H, CH_2), 2.99 (s, 6H, (CH_3)$_2$N).

*4.4.4.5 Synthesis of 1,3-bis[di(t-butyl)phosphinomethyl]-5-dimethylaminobenzene (NMe$_2$-^{tBu}PCP-H) (**4a**)*

To 1.0 g of **9** (3.25 mmol) in 20 mL of degassed acetone was added 1.36 mL (7.2 mmol) of di-tert-butylphosphine (98%) (Strem) at room temperature. The mixture was

heated under reflux with stirring for 24 h under an argon atmosphere, and the solvent was removed *in vacuo*. The solid was dissolved in degassed deionized water (15 mL) and treated with a solution of potassium carbonate (2.7 g, 19.5 mmol) in degassed deionized water (10 mL). The diphosphine ligand was extracted with degassed *n*-hexane (3 x 20 mL) and the solvent was evaporated under vacuum, giving 1.03 g (72%) of the ligand **4a** as a white solid. $^{31}P\{^{1}H\}$ NMR (C_6D_6): δ 31.03 (s). ^{1}H NMR (C_6D_6): δ 6.98 (s, 1H, *Ar*), 6.79 (s, 2H, *Ar*), 2.87 (d, J_{HP} = 2.4 Hz, 4H, C*H*$_2$), 2.78 (s, 6H, (C*H*$_3$)$_2$N), 1.18 (d, J_{HP} = 10.8 Hz, 36H, C*H*$_3$).

*4.4.4.6 Synthesis of (NMe$_2$-^{tBu}PCP)IrHCl (**4b**)*

To 0.51 g of **4a** (1.16 mmol) in 30 mL of toluene was added 0.38 g of $[Ir(COD)Cl]_2$ (0.57 mmol) at room temperature and stirred for 30 min under hydrogen atmosphere. (*note*: the solution changes color from yellow to deep red under hydrogen atmosphere at room temperature). This mixture was refluxed for three days with stirring, and the solvent was removed in vacuo giving 0.78 g of **4b** as dark-red solid in 94% yield. $^{31}P\{^{1}H\}$ NMR (C_6D_6): δ 67.03. ^{1}H NMR (C_6D_6): δ 6.65 (s, 2H, *Ar*), 3.16 (dvt, the left part of AB pattern $^{2}J_{HH}$ = 17.7 Hz, J_{HP} = 3.9 Hz, 2H, C*H*$_2$), 3.06 (dvt, the right part of AB pattern, $^{2}J_{HH}$ = 17.7 Hz, J_{HP} = 3.9 Hz, 2H, C*H*$_2$), 2.77 (s, 6H, (C*H*$_3$)$_2$N), 1.34 (vt, J_{HP} = 6.9 Hz, 18H, C*H*$_3$), 1.29 (vt, J_{HP} = 6.9 Hz, 18H, C*H*$_3$), - 43.11 (t, J_{HP} = 12.8 Hz, 1H, Ir-*H*).

*4.4.4.7 Synthesis of (NMe_2-^{tBu}PCP)IrH_4 (**4c**) and (NMe_2-^{tBu}PCP)IrH_4 (**4d**)*

A stream of hydrogen was passed through a solution of 0.73 g of (NMe_2-^{tBu}PCP)IrHCl (1.1 mmol) in 300 mL anhydrous pentane for about 30 min. A volume of 1.1 mL of 1 M $LiBEt_3H$ in THF (1.1 mmol) was added dropwise to this solution with continuous stirring under hydrogen atmosphere. The solution turned nearly colorless and some white precipitate was found at the bottom of the flask. After the addition of $LiBEt_3H$ was completed stirring was continued for 1 h and finally the solution was filtered under argon atmosphere. (*note*: on changing from H_2 to argon atmosphere the solution rapidly turned deep red). The solvent was removed *in vacuo,* giving 0.55 g (79%) of **4d** as reddish brown crystals containing ca. 10% of **4c**. NMR data for **4c**: $^{31}P\{1H\}$ NMR (C_6D_6): δ 72.42 (s). ^1H NMR (C_6D_6): δ 6.73 (s, 2H, *Ar*), 3.32 (vt, J_{HP} = 3.9 Hz, 4H, C*H*$_2$), 2.79 (s, 6H, (C*H*$_3$)$_2$N), 1.24 (vt, J_{HP} = 6.9 Hz, 36H, C*H*$_3$), - 9.09 (t, J_{HP} = 9.9 Hz, 4H, Ir*H*$_4$). NMR data for **4d**: $^{31}P\{1H\}$ NMR (C_6D_6): 85.48 (s). ^1H NMR (C_6D_6): δ 6.84 (s, 2H, *Ar*), 3.62 (vt, J_{HP} = 3.6 Hz, 4H, C*H*$_2$), 2.76 (s, 6H, (C*H*$_3$)$_2$N), 1.33 (vt, J_{HP} = 6.9 Hz, 36H, C*H*$_3$), -19.99 (t, J_{HP} = 8.7 Hz, 2H, Ir*H*$_2$).

4.5 References

1. (a) Tullo, A. H. *Chem. Eng. News*, **2001**, *79 (12)*, 18. (b) Goldman, A. S. *Encyclopedia of Catalysis*, **2002**, Horvath, I.; ed.; John Wiley & Sons.

2. Weckhuysen, B. M.; Schoonheydt, R. A. *Catalysis Today* **1999**, *51*, 223.

3. Crabtree, R. H.; Mihelcic, J. M.; Quirk, J. M. *J. Am. Chem. Soc.* **1979**,*101*, 7738.

4. (a) Baudry, D.; Ephritikhine, M.; Felkin, H. *J. Chem. Soc., Chem. Comm.* **1980**, 1243. (b) Baudry, D.; Ephritikhine, M.; Felkin, H.; Holmes-Smith, R. *J. Chem. Soc., Chem. Comm.* **1983**, 788.

5. (a) Burk, M. J.; Crabtree, R. H.; Parnell, C. P.; Uriarte, R. J. *Organometallics* **1984**, *3*, 816. (b) Burk, M. J.; Crabtree, R. H. *J. Am. Chem. Soc.* **1987**, *109*, 8025.

6. (a) Nomura, K.; Saito, Y. *Chem. Comm.* **1988**, 161. (b) Sakakura, T.; Sodeyama, T.; Tokunaga, M.; Tanaka, M. *Chem. Lett.* **1988**, 263.

7. Maguire, J. A.; Boese, W. T.; Goldman, A. S. *J. Am. Chem. Soc.* **1989**,*111*, 7088.

8. (a) Spillett, C. T.; Ford, P. C. *J. Am. Chem. Soc.* **1989**, *111*, 1932. (b) Maguire, J. A.; Goldman, A. S. *J. Am. Chem. Soc.* **1991**, *113*, 6706.

9. (a) Maguire, J. A.; Goldman, A. S. *J. Am. Chem. Soc.* **1991**, *113*, 6706. (b) Maguire, J. A.; Petrillo, A.; Goldman, A. S. *J. Am. Chem. Soc.* **1992**, *114*, 9492.

10. Wang, K.; Goldman, M. E.; Emge, T. J.; Goldman, A. S. *J. Organomet. Chem.* **1996**, *518*, 55.

11. (a) Gupta, M.; Hagen, C.; Flesher, R. J.; Kaska, W. C.; Jensen, C. M. *Chem. Commun.* **1996**, 2083. (b) Gupta, M.; Hagen, C.; Kaska, W. C.; Cramer, R. E.; Jensen, C. M. *J. Am. Chem. Soc.* **1997**, *119*, 840.

12. (a) Xu, W.; Rosini, G. P.; Gupta, M.; Jensen, C. M.; Kaska, W. C.; Krogh-Jespersen, K.; Goldman, A. S. *Chem. Comm.* **1997**, 2273. (b) Liu, F.; Goldman, A. S. *Chem. Comm.* **1999**, 655.

13. Liu, F.; Pak, E. B.; Singh, B.; Jensen, C. M.; Goldman, A. S. *J. Am. Chem. Soc.* **1999**, *121*, 4086.

14. (a) Gupta, M.; Hagen, C.; Kaska, W. C. and Jensen, C. M. *J. Chem. Soc., Chem. Commun.* **1997**, 461. (b) Morales-Morales, D.; Redon, R.; Wang, Z. H.; Lee, D. W.; Yung, C.; Magnuson, K.; Jensen, C. M. *Can. J. Chem.* **2001**, *79*, 823. (c) Gu,

X.-Q.; Chen, W.; Morales-Morales, D. and Jensen, C. M. *J. Mol. Cat. A*, **2002**, *189*, 119. (d) Zhang, X.; Fried, A.; Knapp, S.; Goldman, A. S. *Chem. Commun.* **2003**, 2060.

15. Krogh-Jespersen, K.; Czerw, M.; Zhu, K.; Singh, B.; Kanzelberger, M.; Darji, N.; Achord, P. D.; Renkema, K. B.; Goldman, A. S. *J. Am. Chem. Soc.* **2002**, *124*, 10797.

16. Zhu, K.; Achord, P. D.; Zhang, X.; Krogh-Jespersen, K.; Goldman, A. S. *J. Am. Chem. Soc.* **2004**, *126*, 13044.

17. "Isomerization of linear α-olefins catalyzed by iridium pincer complexes" Ray, Amlan; Zhu, Keming; Goldman, A. S. *Abstracts of Papers* 228th ACS National Meeting, Philadelphia, PA, August 22-26, **2004**, INOR-207.

18. Moulton, C. J.; Shaw, B. L. *J. Chem. Soc., Dalton Trans.* **1976**, 1020.

19. Gupta, M.; Hagen, C.; Flesher, R. J.; Kaska, W. C.; Jensen, C. M. *Chem. Commun.* **1996**, 2083.

20. Wolfe, J. P.; Tomori, H.; Sadighi, J. P.; Yin, J.; Buchwald, S. L. *J. Org. Chem.* **2000**, *65,* 1158.

21. Borch, R.F; Hassid, A. I. *J. Org. Chem.* **1972**, *37*, 1673.

22. Stang, S. L.; Meier, R.; Rocaboy, C.; Gladysz, J. A. *J. Fluorine Chem.* **2003**, *119*, 141.

23. Felder, D.; Nava, M. G.; Carreon, M. P.; Eckert, J.-F.; Luccisano, M.; Schall, C.; Masson, P.; Gallani, J.-L.; Heinrich, B.; Guillon, D.; Nierengarten, J.-F. *Helv. Chim. Acta* **2002**, *85*, 288.

24. Mao, Y.; Boekelheide, V. *J. Org. Chem.* **1980**, *45*, 2746.

25. Aoki, T.; Crabtree, R. H. *Organometallics* **1993**, *12*, 294.

26. McLoughlin, M. A.; Flesher, R. J.; Kaska, W. C. *Organometallics* **1994**, *13*, 3816.

27. Kundu, S; Ray, A; Goldman, A. S. *unpublished results.*

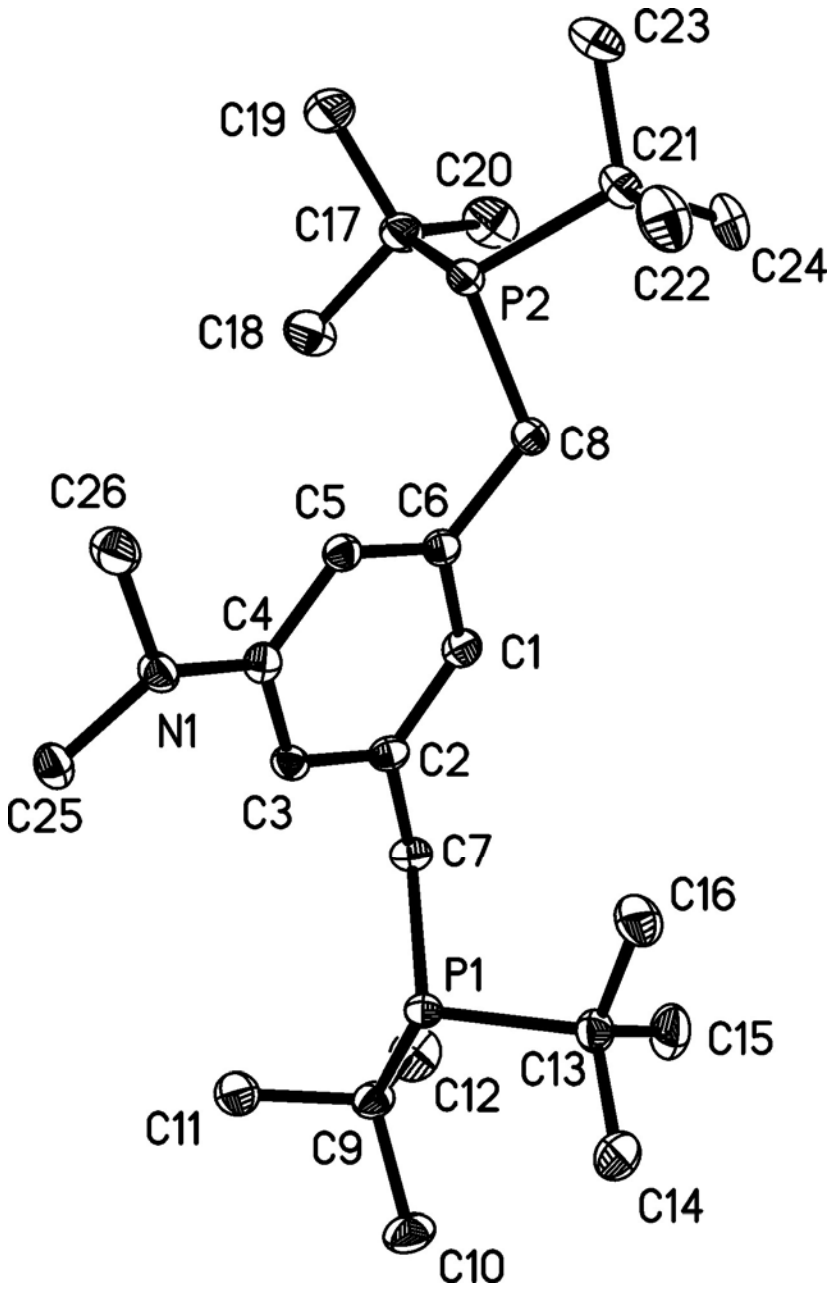

Figure 4.7 Crystal structure of complex ***4a***

*Table 4.7 Crystal data and structure refinement for complex **4a***

Empirical formula	$C_{26}H_{49}NP_2$	
Formula weight	437.60	
Temperature	173(2) K	
Wavelength	0.71073 Å	
Crystal system	Monoclinic	
Space group	P2(1)/c	
Unit cell dimensions	a = 7.4249(7) Å	α= 90°
	b = 29.668(3) Å	β= 95.443(2)°
	c = 12.7004(12) Å	γ = 90°
Volume	2785.0(4) $Å^3$	
Z	4	
Density (calculated)	1.044 Mg/m^3	
Absorption coefficient	0.168 mm^{-1}	
F(000)	968	
Crystal size	0.39 x 0.13 x 0.03 mm^3	
θ range for data collection	2.61 to 28.28°.	
Index ranges	-7<=h<=9, -39<=k<=21, -16<=l<=10	
Reflections collected	15099	
Independent reflections	6598 [R(int) = 0.0254]	
Completeness to theta = 28.28°	95.5 %	
Absorption correction	Semi-empirical from equivalents	
Max. and min. transmission	0.9999 and 0.7852	
Refinement method	Full-matrix least-squares on F^2	
Data / restraints / parameters	6598 / 0 / 276	
Goodness-of-fit on F^2	1.015	
Final R indices [I>2sigma(I)]	R1 = 0.0408, wR2 = 0.0970	
R indices (all data)	R1 = 0.0526, wR2 = 0.1028	
Largest diff. peak and hole	0.446 and -0.165 $e.Å^{-3}$	

*Table 4.8 Selected bond lengths [Å] and angles [°] for complex **4a***

P(1)-C(7)	1.8651(14)	C(9)-C(10)	1.535(2)
P(2)-C(8)	1.8578(14)	C(9)-C(12)	1.536(2)
C(1)-C(2)	1.3928(19)	C(13)-C(14)	1.536(2)
C(1)-C(6)	1.3956(19)	C(13)-C(16)	1.537(2)
C(2)-C(3)	1.3899(19)	C(17)-C(20)	1.528(2)
C(2)-C(7)	1.5138(19)	C(17)-C(19)	1.537(2)
C(3)-C(4)	1.4060(19)	C(17)-C(18)	1.539(2)
C(4)-N(1)	1.3903(17)	C(21)-C(24)	1.531(2)
C(4)-C(5)	1.4112(19)	C(21)-C(23)	1.534(2)
C(5)-C(6)	1.3896(19)	C(21)-C(22)	1.537(2)
C(6)-C(8)	1.5229(19)	N(1)-C(26)	1.4470(19)
C(13)-C(15)	1.529(2)	N(1)-C(25)	1.4595(18)

C(7)-P(1)-C(9)	100.17(7)	C(10)-C(9)-C(11)	107.46(13)
C(7)-P(1)-C(13)	103.45(7)	C(12)-C(9)-C(11)	108.87(13)
C(9)-P(1)-C(13)	110.44(7)	C(10)-C(9)-P(1)	109.36(10)
C(8)-P(2)-C(17)	102.04(7)	C(12)-C(9)-P(1)	117.21(11)
C(8)-P(2)-C(21)	99.32(7)	C(11)-C(9)-P(1)	104.11(10)
C(17)-P(2)-C(21)	110.20(7)	C(15)-C(13)-C(14)	109.70(13)
C(3)-C(2)-C(1)	119.76(13)	C(15)-C(13)-C(16)	109.15(13)
C(3)-C(2)-C(7)	119.59(12)	C(14)-C(13)-C(16)	107.52(13)
C(1)-C(2)-C(7)	120.65(12)	C(15)-C(13)-P(1)	117.08(11)
C(2)-C(3)-C(4)	121.13(12)	C(14)-C(13)-P(1)	107.28(10)
N(1)-C(4)-C(3)	121.03(12)	C(16)-C(13)-P(1)	105.68(10)
N(1)-C(4)-C(5)	120.96(13)	C(20)-C(17)-C(19)	109.64(13)
C(3)-C(4)-C(5)	117.98(12)	C(20)-C(17)-C(18)	108.75(14)
C(6)-C(5)-C(4)	121.12(13)	C(19)-C(17)-C(18)	107.05(13)
C(5)-C(6)-C(1)	119.59(12)	C(20)-C(17)-P(2)	117.58(11)
C(5)-C(6)-C(8)	121.69(13)	C(19)-C(17)-P(2)	108.29(12)
C(1)-C(6)-C(8)	118.67(12)	C(18)-C(17)-P(2)	104.99(10)
C(2)-C(7)-P(1)	113.95(9)	C(4)-N(1)-C(26)	118.12(12)
C(6)-C(8)-P(2)	117.21(10)	C(4)-N(1)-C(25)	118.68(12)
C(10)-C(9)-C(12)	109.34(13)	C(26)-N(1)-C(25)	115.10(12)

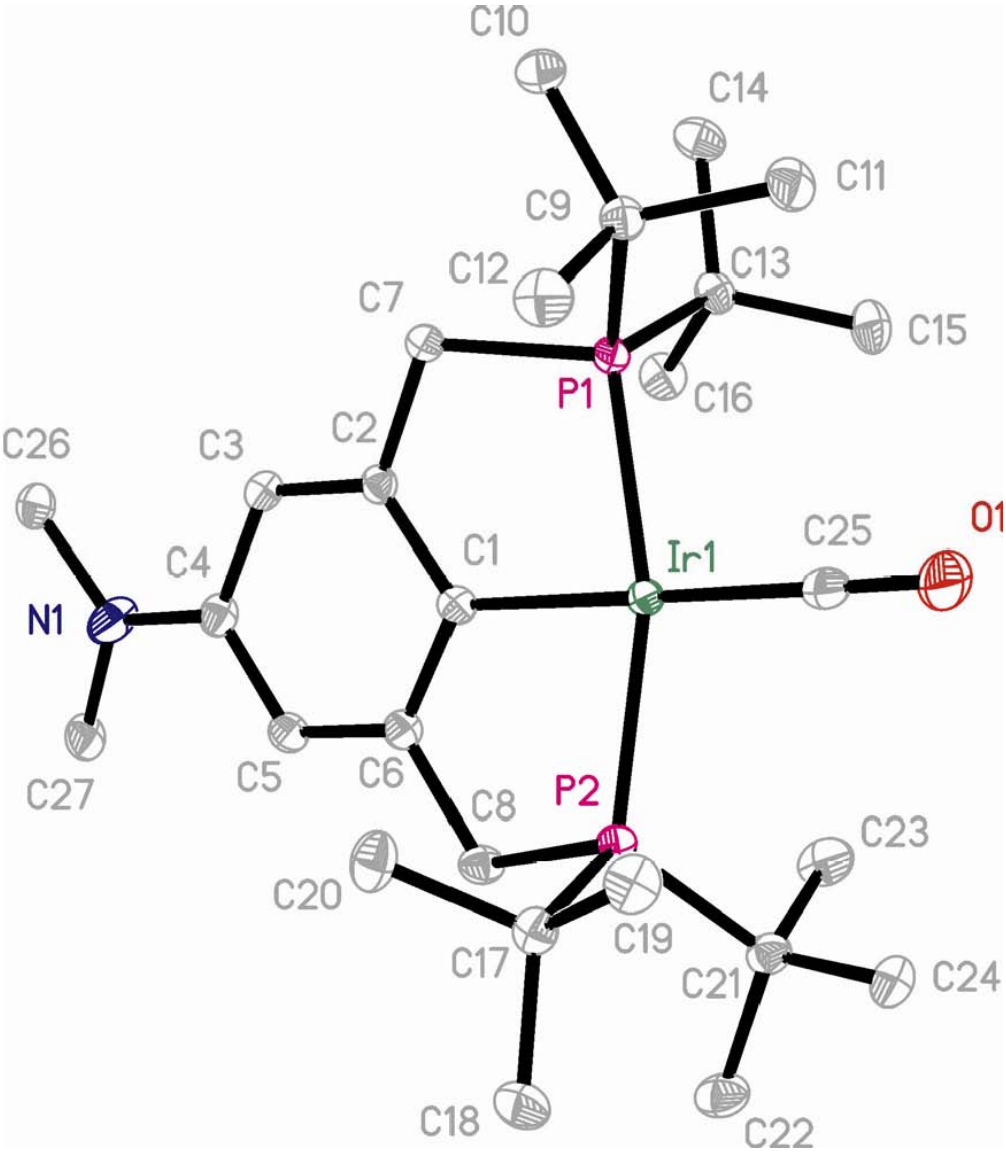

Figure 4.8 Crystal structure of complex (Me_2N-^{tBu}PCP)Ir(CO)

Table 4.9 Crystal data and structure refinement for (Me_2N-^{tBu}PCP)Ir(CO) co-crystallized with ortho-xylene

Empirical formula	$(C_{27}H_{48}NOP_2Ir)\cdot 0.5(C_8H_{10})$	
Formula weight	7.988	
Temperature	100(2) K	
Wavelength	Mo *K*α radiation 0.71073 Å	
Crystal system	triclinic	
Space group	P2(1)/c	
Unit cell dimensions	a = 8.3821(5) Å	α= 78.69°
	b = 10.5337(7) Å	β= 78.67(2)°
	c = 18.4541(12) Å	γ = 80.48°
Volume	1552.95 (17) $Å^3$	
Z	2	
Density (calculated)	1.518 Mg/m^3	
Absorption coefficient	0.168 mm^{-1}	
F(000)	722	
Crystal size	0.47 x 0.30 x 0.16 mm^3	
θ range for data collection	2.1 to 30.5°	
Index ranges	-11<=*h*<=11, -15<=*k*<=14, -26<=*l*<=25	
Reflections collected	18401	
Independent reflections	9275 [R_{int} = 0.019]	
Absorption correction	numerical Bruker SAINT	
Max. and min. transmission	0.192 and 0.468	
Refinement method	Primary atom site location: structure-invariant direct methods	
Data / restraints / parameters	6598 / 0 / 276	
Δρmax	2.15 e $e.Å^{-3}$	
Δρmin	−0.54 e $e.Å^{-3}$	
R indices (all data)	$R[F2 > 2\sigma(F2)]$ = 0.02, $wR(F2)$ = 0.050	

Table 4.10 Selected bond lengths [Å] and angles [°] for complex

(Me_2N-^{tBu}PCP)Ir(CO)

Ir1—C25	1.848 (2)	N1—C26	1.441 (3)
Ir1—C1	2.076 (2)	N1—C27	1.441 (3)
Ir1—P2	2.2857 (5)	C1—C6	1.415 (3)
Ir1—P1	2.2884 (5)	C1—C2	1.416 (3)
P1—C7	1.842 (2)	C2—C3	1.393 (3)
P1—C13	1.872 (2)	C2—C7	1.508 (3)
P1—C9	1.878 (2)	C3—C4	1.406 (3)
P2—C8	1.838 (2)	C3—H3	0.9300
P2—C17	1.877 (2)	C4—C5	1.405 (3)
P2—C21	1.881 (2)	C5—C6	1.391 (3)
O1—C25	1.167 (3)	C5—H5	0.9300
N1—C4	1.376 (3)	C6—C8	1.511 (3)

C25—Ir1—C1	179.38 (9)	C4—N1—C26	120.89 (18)
C25—Ir1—P2	98.73 (7)	C4—N1—C27	120.36 (19)
C1—Ir1—P2	81.79 (5)	C26—N1—C27	118.67 (18)
C25—Ir1—P1	97.79 (7)	C6—C1—C2	115.04 (17)
C1—Ir1—P1	81.70 (5)	C6—C1—Ir1	122.36 (14)
P2—Ir1—P1	163.473 (18)	C2—C1—Ir1	122.61 (14)
C7—P1—C13	105.31 (9)	C3—C2—C1	122.76 (18)
C7—P1—C9	103.40 (9)	C3—C2—C7	119.01 (17)
C13—P1—C9	111.44 (9)	C1—C2—C7	118.17 (17)
C7—P1—Ir1	104.37 (6)	C2—C3—C4	120.93 (18)
C13—P1—Ir1	112.63 (7)	N1—C4—C5	120.83 (19)
C9—P1—Ir1	118.13 (7)	N1—C4—C3	121.73 (19)
C8—P2—C17	105.36 (9)	C11—C9—P1	110.69 (14)
C8—P2—C21	102.91 (9)	C10—C9—P1	113.84 (14)
C17—P2—C21	111.25 (9)	C12—C9—P1	105.71 (14)
C8—P2—Ir1	104.64 (6)	C24—C21—P2	110.77 (14)
C17—P2—Ir1	112.29 (7)	C22—C21—P2	114.28 (15)
C21—P2—Ir1	118.78 (7)	C23—C21—P2	104.84 (14)

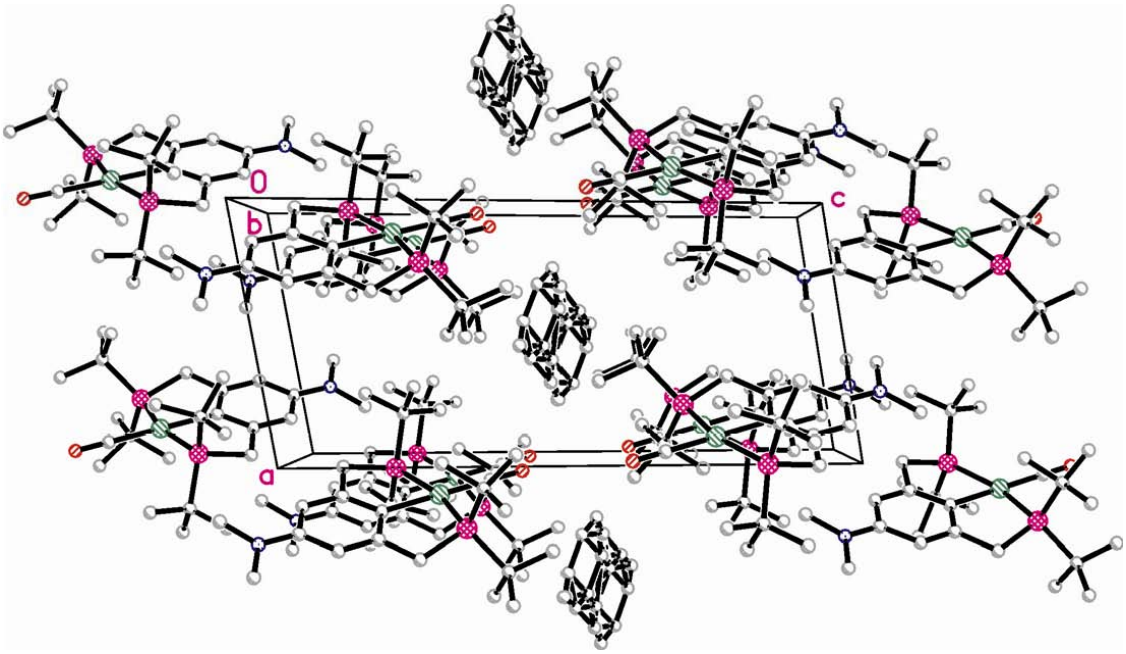

Figure 4.9 Crystal structure of complex (Me_2N-^{tBu}PCP)Ir(CO) co-crystallized with ortho-xylene

Chapter 5

Study of olefin insertion into the Ir-H bonds of pincer complexes of the type (PCP)Ir(H)(Y)

Abstract

As an extension of the earlier work reported in chapter three related to isomerization of 1-octene by (X-^{R}PCP)IrH_2 complexes, we have investigated the effects of varying "Y" on the rate of insertion of an olefin into the Ir-H bonds of complexes (PCP)Ir(H)(Y). Although we intended to study a series of (PCP)Ir(H)(Y) complexes, due to the labile nature of some of these complexes, in the presence of the olefin (1-octene), detailed kinetic study could be carried out with only four complexes with Y = Cl, CCPh, OH and OPh. Both rates of 1,2- and 2,1-insertion, of the substrate *cis*-1,2-dideutero-1-octene into the Ir-H bonds, were found to increase in the in the following sequence Y = Cl < CCPh < OH < OPh. DFT calculations predicted an insertion pathway in which olefin binds to the metal center in the position *trans* to the PCP-aryl ring. An olefin bound 14-electron complex, (PCP)Ir(1-octene), often speculated to be the resting state of (X-^{R}PCP)IrH_2 catalysts in the dehydrogenation cycles, was characterized by low temperature ^{1}H and ^{31}P NMR.

5.1 Introduction

Insertion of an olefin into a metal-hydride bond and the microscopic reverse, β-hydrogen elimination, are critically important elementary transformations in organometallic chemistry. These reactions are of interest due to their fundamental importance, as well as their widespread occurrence in various transition-metal-catalyzed processes such as olefin polymerization, isomerization, hydroformylation and hydrogenation. Therefore, a detailed understanding of the mechanism of the olefin insertion/elimination and elucidation of the factors that influence the rates of these processes are of importance in both organometallic chemistry and catalysis.

Early results by other workers with several transition metal alkyl complexes indicated a number of stereochemical features associated with the olefin insertion/β-H elimination processes. Whitesides *et al.* have shown that five and six membered Pt-metallocycles are much more resistant to thermal decomposition via β-H elimination compared to their, slightly more flexible, seven membered analogues.[1] In a similar study Bower and Tennent have found that a number of transition metal norbornyl complexes are also unusually stable towards β-H elimination even at a fairly high temperature (>100 °C).[2] These initial results have strongly suggested the requirement of a planar arrangement of the M-C-C-H unit involved in the bond making (for olefin insertion) or bond breaking (for β-H elimination) process. Additionally, when the stereochemistry of the product has been established, following an olefin insertion into a M-H bond, a net *cis* addition was observed.[3]

It is now generally believed that olefin insertion is a two step process. Coordination of the olefin to a vacant site on the metal center, with a *cis* relationship to the hydride ligand, is followed by insertion of the olefin into the metal-hydride bond involving a planar cyclic transition state with overall *cis* addition of M-H to the olefin double bond (Scheme 5.1).

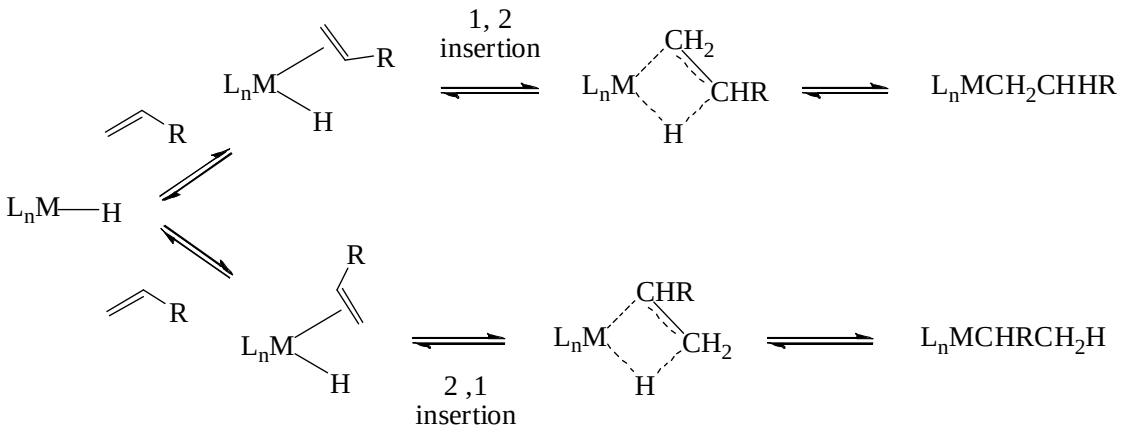

Scheme 5.1 Generic steps for insertion of an olefin into a M-H bond

In a catalytic cycle involving olefin insertion as one of the steps, there were a number of reports with different transition metals (Mo, Fe, Ru, Pt) indicating that the insertion/elimination step was fast and reversible relative to other steps (*e.g.* ligand loss, C-H elimination) of the catalytic cycle.[4] For example, Whitesides has shown that thermal decomposition of di-*n*-butyl-*2,2-d*$_2$-bis (triphenylphosphine)-platinum(II) at 60 °C results in the formation of an equimolar mixture of 1-butene and *n*-butane (Scheme 5.2).[4a]

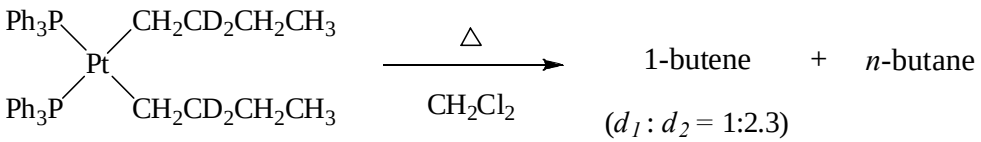

Scheme 5.2 Product distribution from thermal decomposition of di-n-butyl-2,2-d_2-bis (triphenylphosphine)-platinum(II)

Isotopic composition of the 1-butene was found to be 29% d_1 and 67% d_2. A mechanism involving slow β-D elimination to give 1-butene followed by fast C-D elimination giving *n*-butane would result in about 100% d_1 in the product butene. However, significant scrambling of deuterium (67% d_2 product presumably formed *via* fast 2,1 insertion of the product d_1 butene into Pt-D bond followed by β-H elimination) indicated that both 1-butene elimination and its readdition to platinum deuteride are faster than the reductive C-D elimination giving *n*-butane. However, the reverse situation has also been observed when, after detailed kinetic analysis, it was found that the insertion step is the rate-limiting of the overall process.[5] Clark and Jablonski have shown that ethylene insertion into the Pt-H bond of the complex *trans*-$Pt(H)(NO_3)(PEt_3)_2$ goes via initial rapid equilibrium to give *trans*-$Pt(H)(C_2H_4)(PEt_3)_2^+$ followed by a slower rate-determining insertion.

One of the earliest reports of the elucidation of substituent electronic effects, on the kinetic parameters of the rate of olefin insertion, was provided by Halpern and Okamoto.[6] Investigating the rates of insertion of *para* substituted styrenes into the Rh-H bonds of $RhH_2Cl(PPh_3)_3$ they showed that there is a clear correlation between the

strength of binding of an olefin onto the metal center and their subsequent insertion into the metal-hydride bonds (Scheme 5.3).

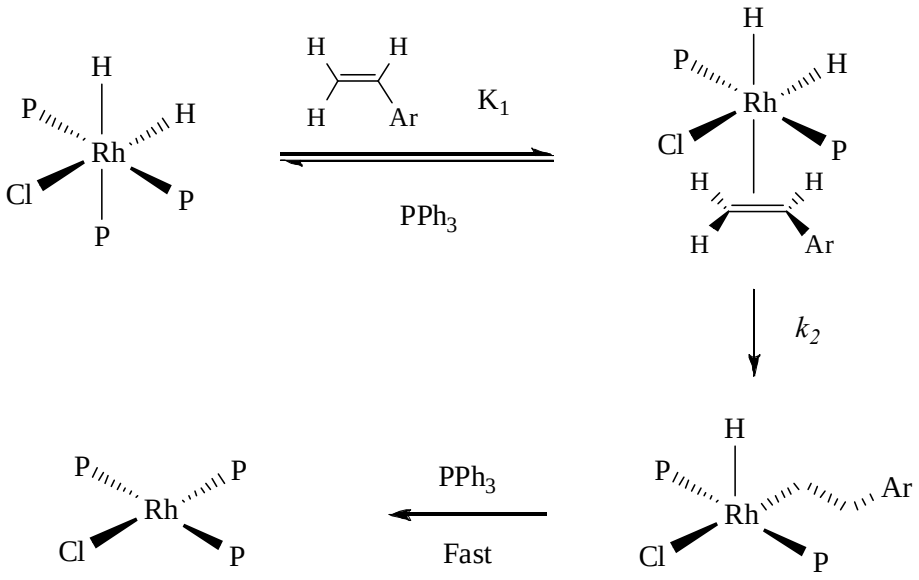

Scheme 5.3 Insertion steps and kinetic parameters for styrene insertion into the Rh-H bond of $RhH_2Cl(PPh_3)_3$ ($P = PPh_3$, Ar = p-X-C_6H_4 where X = Cl, H, Me, OMe)

In accordance with the Dewar-Chatt-Duncanson model for binding of an olefin onto a transition metal center, electron-withdrawing groups at the *para* position of the styrene led to strong binding of the olefin onto the rhodium center [equilibrium constant, K_1, varies in the following order 2.53 (*p*-Cl) > 1.72 (*p*-H) > 0.69 (*p*-Me) > 0.34 (*p*-OMe)] and this was found to result in a slower rate of insertion, with insertion rate constant k_2 (s^{-1}) increasing in the reverse direction [0.097 (*p*-Cl) < 0.11 (*p*-H) < 0.23 (*p*-Me) < 0.50 (*p*-OMe)].

However for the same system, results obtained from tuning the electronic effects at the metal center (by changing R groups on phosphines) were irregular and did not follow a consistent trend. The binding equilibrium constant (K_1) was found to be maximum for PPh_3 (1.75) and decreasing in both directions with electron-withdrawing (0.47 for P(*p*-Cl-C_6H_4)$_3$) and electron-donating groups (0.57 for P(*p*-OMe-C_6H_4)$_3$). The rate of insertion, on the other hand, was found to slowly increase with increasing electron-donating ability of the phosphines. The authors have argued that this could be due to electron-donating ligands stabilizing the electron deficient, co-ordinatively unsaturated (16e) product of the insertion step [RhH(alkyl)Cl(PR_3)$_2$], thereby increasing the rate of the reaction.

One of the most notable examples of detailed investigation of steric and electronic effects on the rates of olefin insertion into metal-hydride bonds was provided by Bercaw and Doherty.[7] Using magnetization transfer technique they have measured the insertion rate constant (k_1 for the forward reaction shown in Scheme 5.4) for a variety of olefinic substrates into the Nb-H bond of the complex $Cp^*_2Nb(CH_2=CHR)(H)$.

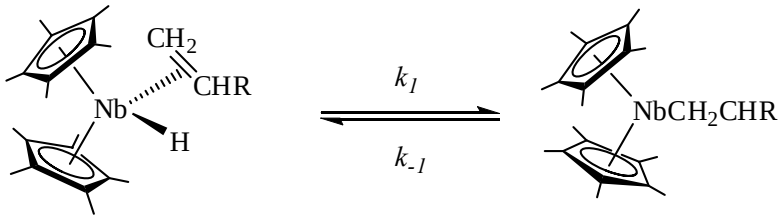

Scheme 5.4 Insertion of olefins into niobium-hydride bonds

Early results indicated that the insertion rate increased in the following order with different 'R' groups on the olefin - k_1, s^{-1} = 2.62 (R = H) < 3.18 (R = Ph) < 890 (R = Me) which correlated with relative binding of these complexes onto the niobium center as indicated by an increase in K_{eq} in the reverse direction (Scheme 5.5, K_{eq} = 1 (R = H) > 0.047 (R = Ph) > 0.0069 (R = Me)). For propene (R = Me) the binding is weakest due to both steric and electronic factors. Styrene (R = Ph) showed an intermediate binding because although the steric factor destabilized the olefin bound ground state, due to electronic withdrawing effect of the phenyl ring overall binding was stronger than what would be expected from the steric factor alone.

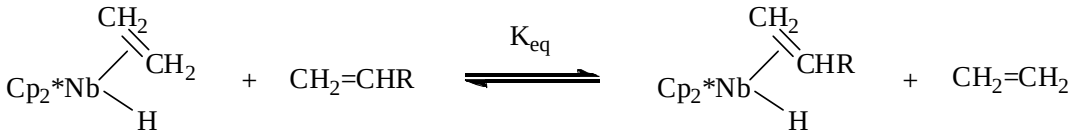

K_{eq} R = H > R = Ph > R = Me

Scheme 5.5 Comparative binding of olefins onto the niobium center relative to ethylene

Although these initial observations suggested that slower insertion rate of an olefin, roughly correlated with its stronger binding to the metal center, study of insertion kinetics of *para*-substituted styrenes did not fully conform to this theory. K_{eq} values (Scheme 5.5) were found to be fairly insensitive to electronic effects exerted by the substituents at the *para* position of styrenes (K_{eq} = 0.41 for *p*-MeO-C_6H_4 and 0.40 for *p*-CF_3-C_6H_4) whereas, the insertion rate was found to increase with stronger electron donating substituents [k_1, s^{-1} = 6.8 (*p*-Me_2N-C_6H_4) > 4.81 (*p*-MeO-C_6H_4) > 3.47 (*p*-Me-C_6H_4) > 0.91 (*p*-CF_3-C_6H_4)]. They have reasoned that there was a partial positive charge

developed at the β-carbon of the olefin in the insertion transition state and hence the electron donating substituents enhance the rate of the reaction (Scheme 5.6).

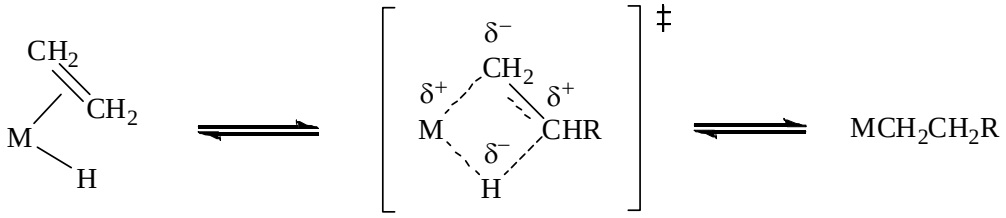

Scheme 5.6 Schematic representation of the transition state of olefin insertion

In a more recent report the same group has investigated the steric and electronic effects exerted by different alkyl substituents on the cyclopentadienyl rings.[8] Fig. 5.1 and 5.2 below depict the structures of different complexes studies and the rates associated with them for insertion of the bound ethylene into the Nb-H bonds.

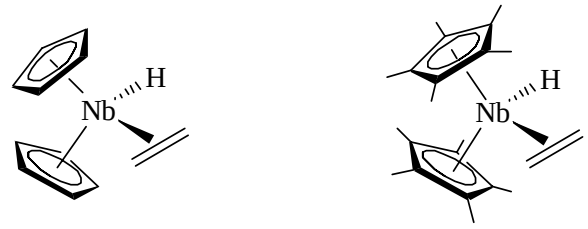

(A) $k = 9.3\ s^{-1}$ **(B)** $k = 1.9\ s^{-1}$

Fig 5.1 Olefin insertion rates at 318 K for unbridged niobocene ethylene hydride complexes

A comparison between complexes **A** and **B** suggested that increasing electron density at the metal center was translated to a stronger binding of ethylene to the Nb, thereby reducing the rate of insertion. The dramatic increase in insertion rate was observed on going from the unbridged (**A** or **B**) to the bridged complex (**C**) was attributed to lower electron density at the metal center for singly bridged ansa metallocene fragments. This reduction in electron density was indeed found to be true for a number of metallocene systems.[9] For example, Parkin *et al*. have shown that the barrier to PMe_3 dissociation for singly bridged $[Me_2\text{-}Si(\eta 5\text{-}C_5Me_4)_2]ZrH_2(PMe_3)$ is much larger than that for the unbridged analogue $Cp^*_2ZrH_2(PMe_3)$, with $k_{Cp^*} > 500k_{ansa}$ at 25 °C.[9a] The effect has been attributed to the silyl bridge, in the *ansa* complex, pulling the Cp rings back to $\eta^3{:}\eta^3$ hapticity, making the Zr center more electrophilic and binding the PMe_3 more tightly. Presumably, for similar reasons, the sharp increase in insertion rate was observed on moving from unbridged to the bridged metallocenes.

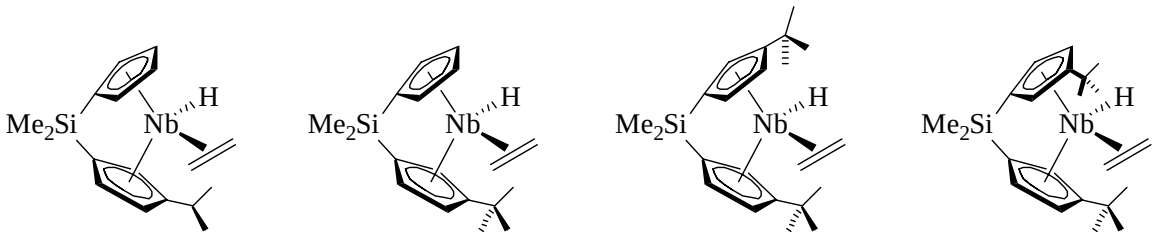

(C) $k = 1250\ s^{-1}$ **(D)** $k = 161\ s^{-1}$ **(E)** $k = 4.8\ s^{-1}$ **(F)** $k = 1220\ s^{-1}$

Fig 5.2 Olefin insertion rates at 318 K for various bridged niobocene ethylene hydride complexes with alkyl substituents on the Cp rings

The reduction in rate observed in the series from **C** to **E** was believed to be a combination of both steric and electronic factors. While electron density increased slowly at the metal center, insertion transition state also involved bringing the bound ethylene towards the hydride ligand thereby increasing its steric interaction with alkyl substituents on the Cp ring(s). This factor along with the electronic effects makes the insertion process more and more unfavorable. For complex **F**, presumably close proximity of the ^{t}butyl groups led to enhanced ^{t}butyl/ethylene steric interaction which destabilized the olefin bound ground state, reducing the barrier for insertion.

When used as an acceptor or used to study the rate of isomerization, different olefinic compounds (1-olefins, norbornene, 3,3-dimethyl-1-butene) have been found to undergo insertion into the Ir-H bond of pincer-ligated iridium dihydride complex (PCP)IrH_2. Depending on the steric and electronic factors, these insertions rates have been found to vary with the substrate as well as on changing the substituents on the iridium-pincer complexes.

Additionally Iridium-pincer-hydride complexes of the type (PCP)Ir(H)(Y) can also provide us with an excellent opportunity to study the rate of olefin insertion into the Ir-H bond and also to observe the effect of different ancillary ligands Y on the barrier to insertion. As shown in Fig 5.3 these complexes tend to have an approximately square pyramidal geometry with the hydride ligand in the apical position. There are several advantages associated with this system, which make it an attractive model for studying the olefin insertion reactions.

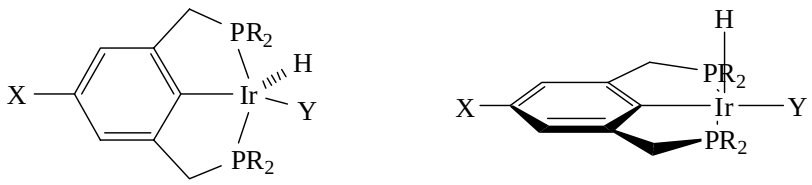

X = H, OMe, NMe_2

R = ^{i}Pr, ^{t}Bu

Y = Cl, Ph, CCPh, OH, NH_2

Fig 5.3 (X-PCP)Ir(H)(Y) complexes indicating possible sites for steric and electronic tuning

i. (PCP)Ir(H)(Y) are 16e complexes with a vacant coordination site on the metal center, thus obviating the need for any ligand dissociation to occur before olefin coordination, thereby simplifying the overall reaction kinetics.

ii. There is ample opportunity for steric modification (through R groups) and electronic tuning (through modification of X on the pincer ligand backbone or coordinated Y) in the system to observe their effects on the barrier of insertion.

iii. Starting with (PCP)$IrH_{2/4}$ it is possible to easily synthesize a series of these complexes with varying Y groups.

In Chapter 3 we have already investigated (implicitly) the steric and electronic effects exerted by the R and X groups, respectively, on the rate of olefin isomerization reaction. Therefore, in this chapter we will limit the discussion to studying the effects of varying Y on the rate of insertion of 1-octene into the Ir-H bonds of the complexes (PCP)Ir(H)(Y).

5.2 Results and discussions

5.2.1 Experimental Results of Olefin Insertion

5.2.1.1 Synthesis of (PCP)Ir(H)(Y) complexes and the olefin

It has been observed that the presumed 14-electron intermediate of the dehydrogenation cycle, "(PCP)Ir", undergoes oxidative addition to a variety of C-H, O-H and N-H bonds providing an easy access to a series of (PCP)Ir(H)(Y) complexes[10] (Scheme 5.7) which could be used to measure the effect of Y on the insertion barrier of an olefin into the Ir-H bonds.

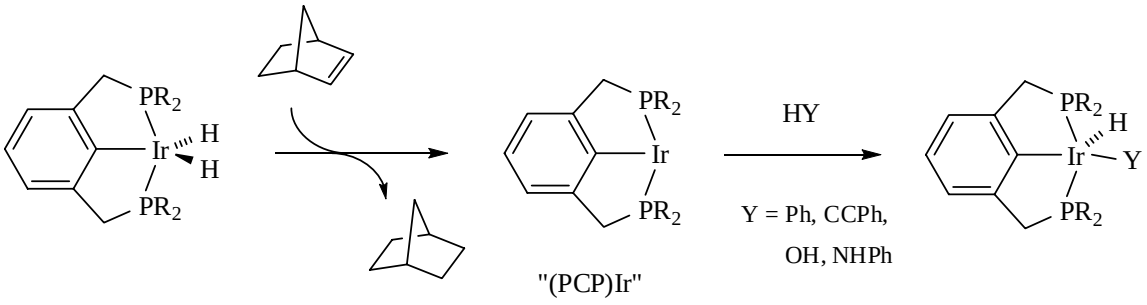

Scheme 5.7 Synthesis of various (PCP)Ir(H)(Y) complexes starting from the (PCP)IrH_2

To differentiate between the products and to measure their respective concentrations, in order to evaluate the rates of insertions, we chose *cis*-1,2-dideutero-1-octene as the substrate. This was synthesized according to a literature procedure by partial reduction of 1-octyne using Lindlar Catalyst (~5% palladium on calcium

carbonate; poisoned with lead) and deuterium gas. ^{2}H NMR of the product indicated complete consumption of the starting material; however, along with the desired product about 6-7% of 1-octene was found to be all-proteo.

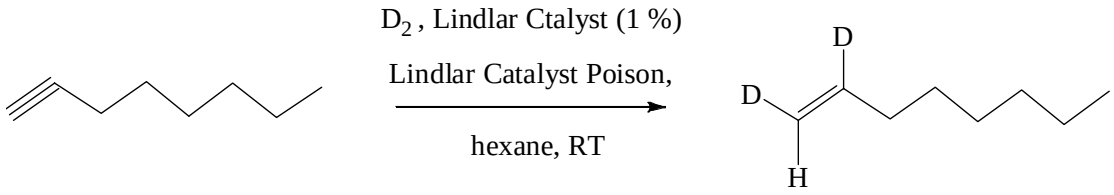

Scheme 5.8 Synthesis of cis-1,2-dideutero-1-octene by catalytic deuteration

5.2.1.2 General insertion schemes with (PCP)Ir(H)(Y) and cis-1,2-dideutero-1-octene

Insertion of an olefin into a M-H bond can be a 1,2 or 2,1 type (shown in Scheme 5.9 and 5.10). In the case of 1,2 insertion the primary alkyl product can then undergo β-H elimination, to give back the starting olefin. Alternatively, it can do a β-H elimination following metal alkyl bond rotation. Depending on the composition and stereochemistry of the starting olefin the latter β-H elimination pathway may lead to an exchanged product.

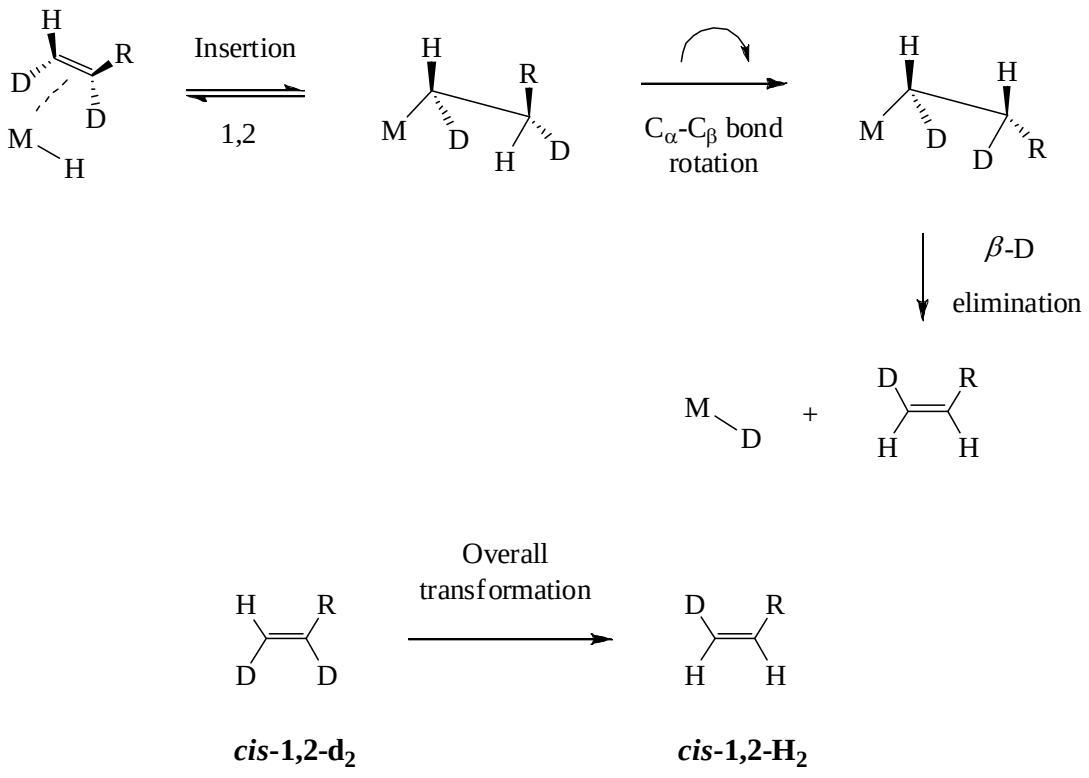

Scheme 5.9 Generic scheme for 1,2 insertion of cis-1,2-dideutero-1-octene (cis-1,2-d_2) into an M-H bond and product (cis-1,2-H_2) formation via subsequentβ-D elimination. R = "n-hexyl" ; for reaction with (PCP)Ir(H)(Y) complex, M = "(PCP)Ir(Y)"

As shown in the above scheme, the only possible product from 1,2 insertion of the starting deuteron octene and following β-D elimination, is the *cis*-1-deutero-1-octene (referred to as *cis-1,2-H_2* for simplicity). Comparison of the starting octene *(cis-1,2-d_2)* and the product *(cis-1,2-H_2)* reveals that there is a loss of deuterium at the β carbon and stereochemical inversion at the α carbon. By a combination of ^{1}H, ^{2}H and ^{13}C NMR we hoped it would be possible to differentiate the product from the starting compound and

measure its concentration, which would indicate the rate of 1,2 insertion with a given (PCP)Ir(H)(Y) complex.

A 2,1 insertion followed by β-H/D elimination, on the other hand can give us a mixture of different products. The possible product composition and their respective stereochemistries from 2,1 insertion pathway are shown in Scheme 5.10. Both *gem-1,1-H_2* and *trans-1,2-d_2* could be formed via similar, rotation around the C_α-C_β bond. The third product, *2-octene-d_2* is a result of conventional double bond isomerization.

Out of the three different products from 2,1 isomerization route, *2-octene-d_2* could be distinguished very easily from the others by either ^{1}H or ^{2}H NMR. However, *trans-1,2-d_2* because of its very close structural similarity with the starting material would be hard to distinguish in a mixture of other products. The third product, *gem-1,1-H_2* could also be easily followed by ^{13}C NMR as the terminal carbon, bearing two hydrogens, would exhibit a splitting pattern distinct from all the rest.

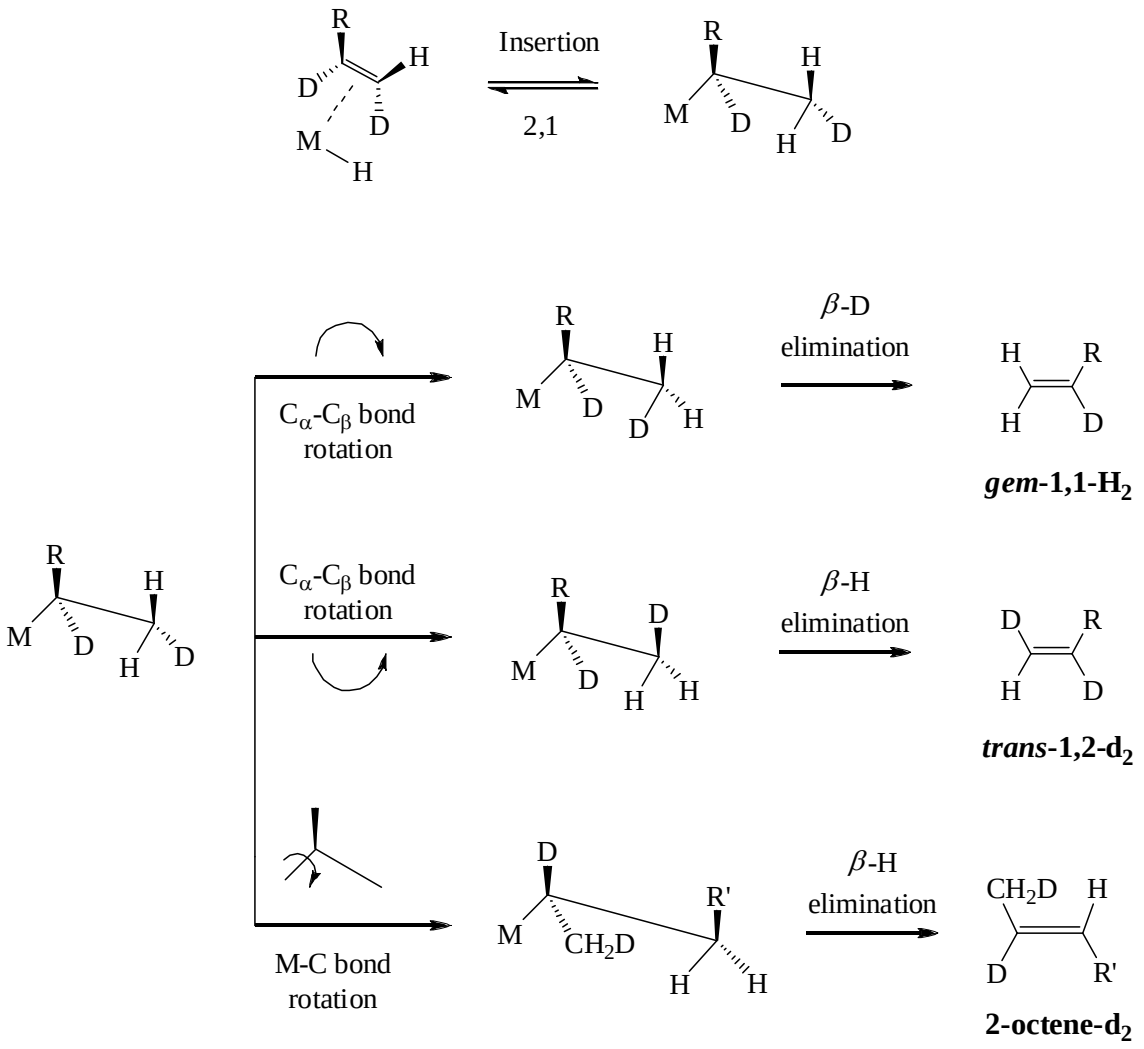

Scheme 5.10 Generic scheme for 2,1 insertion of cis-1,2-dideutero-1-octene (cis-1,2-d_2) into an M-H bond and possible product distribution (gem-1,2-H_2, trans-1,2-d_2, 2-octene-d_2) via C-C/M-C bond rotation and β-H/D elimination. R = "n-hexyl" and R′ = "n-pentyl" ; for reaction with (PCP)Ir(H)(Y) complex, M = "(PCP)Ir(Y)".

When the insertion reactions were investigated using different (PCP)Ir(H)(Y) complexes, and followed by ^{1}H, ^{2}H, ^{31}P and ^{13}C NMR, it was found that *cis-1,2-H_2* and *2-octene-d_2* were the major species formed in the reaction. As explained earlier

characterizing the *trans-1,2-d_2* and estimating its concentration was difficult in the presence of the starting *cis-1,2-d_2*. However, the concentration of *gem-1,2-H_2* was found to be very small compared to that of *2-octene-d_2*, indicating that the 2,1 insertion pathway leads mainly to isomerization. This was further confirmed by comparing the loss of β-D signal from the starting octene which matched very closely with the sum of 1,2 exchanged product (*cis1,2-H_2*) and the isomerized product (*2-octene-d_2*). Therefore we decided to evaluate the 1,2 and 2,1 insertion rates primarily by looking at the concentrations of *ci-1,2-H_2* and *2-octene-d_2* over time.

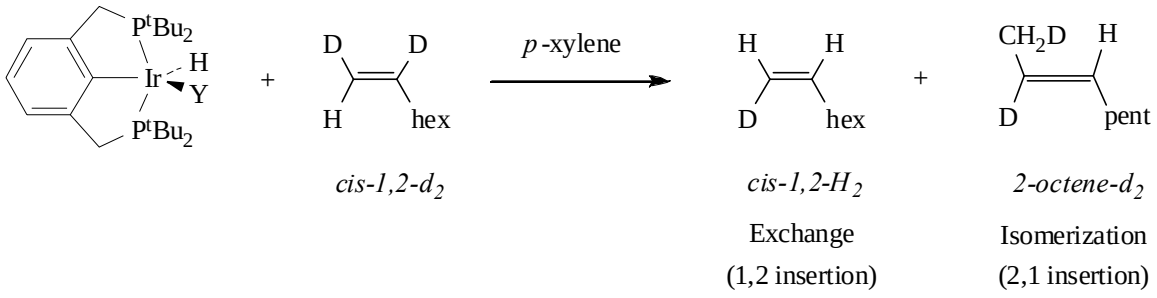

Scheme 5.11 Distribution of products used to measure the 1,2 and 2,1 insertion rates

5.2.1.3 Labile nature of certain (PCP)Ir(H)(Y) complexes

In order to study the rate of olefin insertion into the Ir-H bond of a certain (PCP)Ir(H)(Y) complex, the primary requirement is that the complex needs to be stable under the reaction condition, and should not get converted to a species that can give rise to products expected from the insertion reaction. However, during the course of the study

we have found that there were a number of (PCP)Ir(H)(Y) complexes which were present in the solution only in equilibrium concentrations along with other pincer-iridium complex capable of effecting exchange and isomerization reactions with the substrate octene. For example, when one equivalent of *cis-1,2-d_2* was added to a solution of (PCP)Ir(H)(Ph) in *p*-xylene, ^{31}P NMR of the solution indicated a small peak at 67.44 (having ~8-10% of the total phosphorus intensity) due to the Ir-phenyl hydride, along with four other peaks (doublet of doublets) arising from the olefin bound 14-electron "(PCP)Ir" complex (characterization and dynamic NMR behavior of the complex is described in section 5.2.3). ^{2}H NMR spectra of the solution, after adding the deuterated octene, also showed two peaks of the bound olefin deuteriums (at 2.8 and 5.8 ppm) – indicating that PhH was partially displaced by 1-octene from the (PCP)Ir(H)(Ph) complex to give the olefin bound (PCP)Ir(1-octene) (Scheme 5.12).

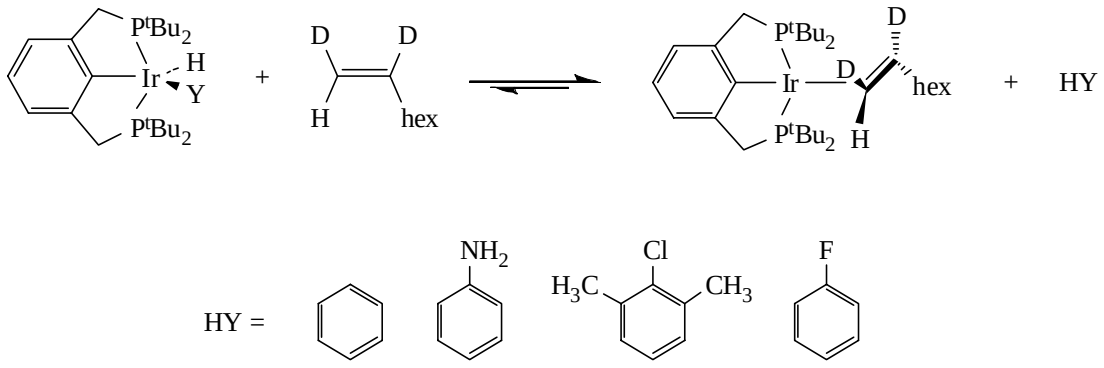

Scheme 5.12 Equilibrium between (PCP)Ir(H)(Y) and (PCP)Ir(1-octene) in solution for certain HY

Of the several complexes considered for a study of their insertion behavior, four of them (HY = PhH, $PhNH_2$, PhF and $(CH_3)_2C_6H_3Cl$) were found to be displaced by the 1-octene (in varying extents, as indicated by the resulting ^{31}P NMR of the solution). Consequently we could not use any of these HY to measure olefin insertion rates into the Ir-H bonds of the corresponding (PCP)Ir(H)(Y) complexes.

5.2.1.4 Study of olefin insertion using stable (PCP)Ir(H)(Y) complexes (Y = Cl, CCPh, OH, OPh)

Four (PCP)Ir(H)(Y) complexes (Y = Cl, CCPh, OH, OPh) did not show any labile behavior (*i.e.* HY was not displaced by the substrate octene) under the reaction condition when heated for an extended period of time. Therefore we initially limited our insertion study only to these stable (PCP)Ir(H)(Y) complexes. In a typical experiment, one equivalent each of 1-octene (*cis-1,2-d_2*) and a (PCP)Ir(H)(Y) complex (30 mM) was dissolved in *p*-xylene-d_{10} and was heated in a sealed tube in a GC oven and was monitored periodically by both ^1H and ^{31}P NMR. Solutions of $CHCl_3$ in *p*-xylene-d_{10} and PMe_3 in mesitylene-d_{12} were used as the external standards for quantification and referencing purpose, respectively. When the reaction was monitored by ^2H NMR, *p*-xylene-d_{10} was replaced by proteo *p*-xylene as the solvent and a solution of $CDCl_3$ in proteo *p*-xylene was used as the internal standard for quantification purpose.

The first complex that was used for study, (PCP)Ir(H)(Cl), was found to be extremely unreactive in its insertion behavior. The reaction was first attempted at 50 °C and there was no change in either ^{1}H or ^{2}H NMR spectra even after one week. On raising the temperature to 80 °C, although some visible change could be observed after 12 h, the reaction was still fairly slow (half-life on the order of 3-4 days). Finally the reaction was carried out at 120 °C and was monitored over a period of 60 h. While following the reaction by ^{2}H NMR it was found that the internal deuterium signal (δ 5.86 ppm) of the starting 1-octene, *cis-1,2-*d_2 , was lost at a faster rate compared to the terminal deuterium signal (appearing at 5.08 ppm), thereby indicating that the 1,2 insertion (leading to exchange) was going at a faster rate than the 2,1 insertion (leading to isomerization) (see Scheme 5.11) (Note: as shown in Scheme 5.10 and 5.11, 1,2 insertion followed by *β*-H elimination would result in the loss of only internal deuterium of the substrate *cis-1,2-*d_2. A 2,1 insertion leading to isomerization, on the other hand, would result in the loss of both terminal and internal deuterium signal of the substrate). Throughout the course of the reaction ^{31}P NMR of the solution showed only one peak (at 67.7 ppm) indicating (PCP)Ir(H)(Cl) was the only species present in the solution.

The reactions with the other complexes (Y = CCPh, OH and OPh) were significantly faster than that of (PCP)Ir(H)(Cl); the insertion with these complexes was carried out at 50 °C.

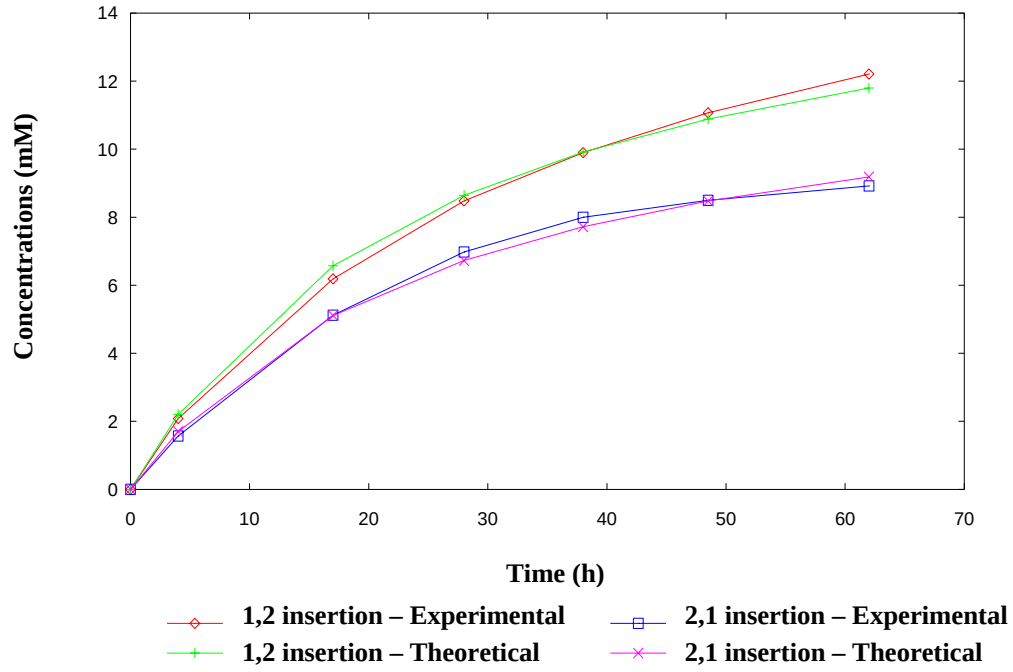

Fig. 5.4 Kinetic plot for insertion of cis-1,2-d_2 into Ir-H bond of (PCP)Ir(H)(Cl)

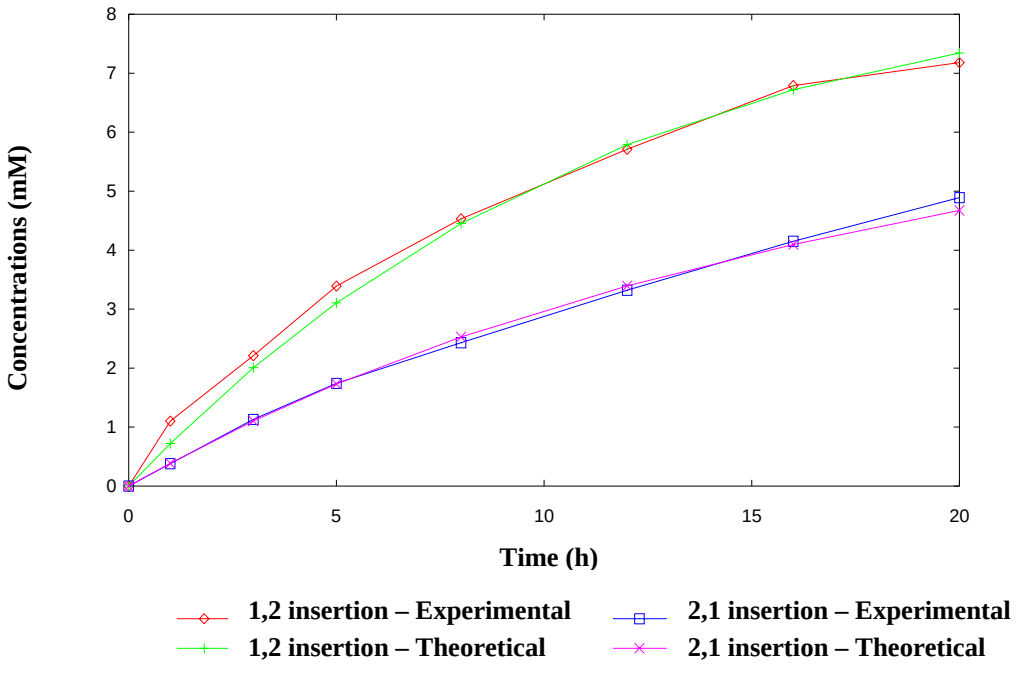

Fig. 5.5 Kinetic plot for insertion of cis-1,2-d_2 into Ir-H bond of (PCP)Ir(H)(CCPh)

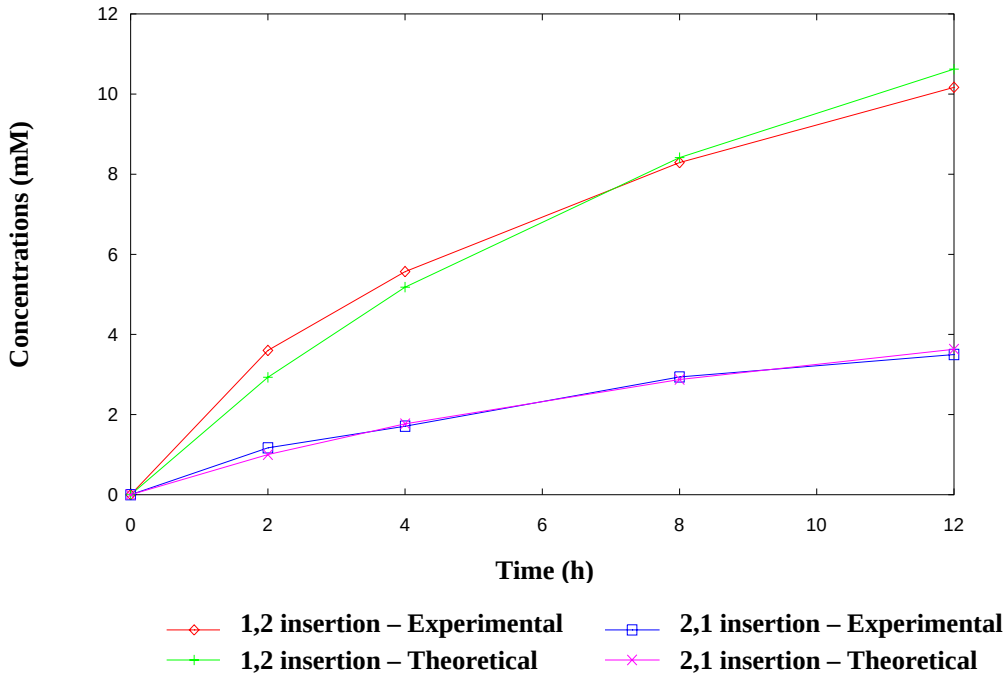

Fig. 5.6 Kinetic plot for insertion of cis-1,2-d_2 into Ir-H bond of (PCP)Ir(H)(OH)

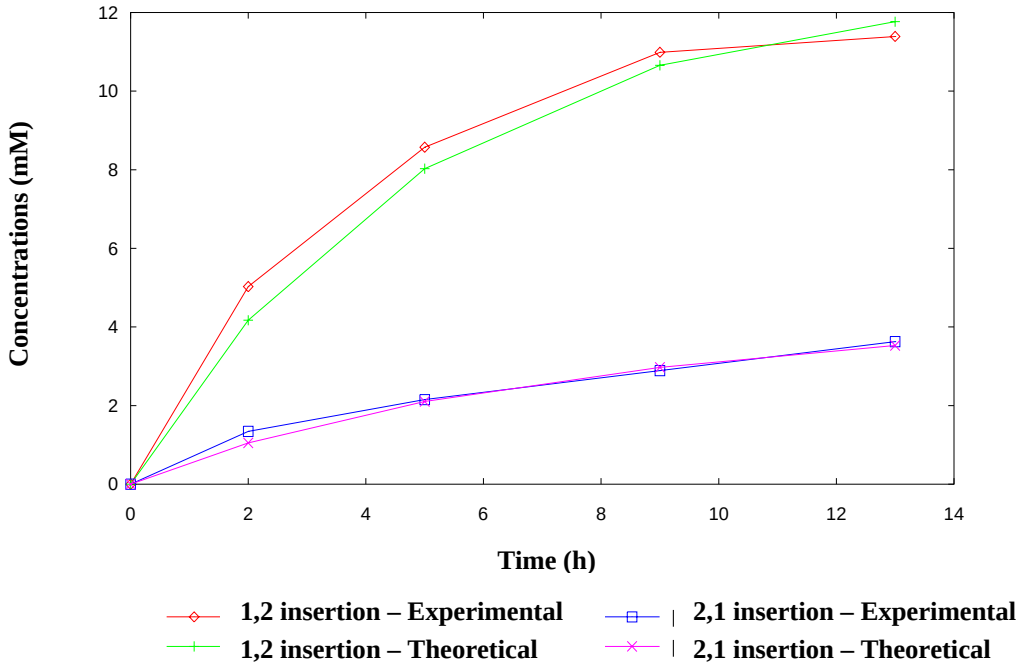

Fig. 5.7 Kinetic plot for insertion of cis-1,2-d_2 into Ir-H bond of (PCP)Ir(H)(OPh)

Additionally, the ^{31}P spectra indicated the (PCP)Ir(H)(Y) complexes were the only species present in the solution throughout the reaction time. The kinetic data for all complexes were fit using the program Gepasi[11] and are shown in the Fig 5.4 to 5.7. Corresponding rate constants and activation free energies are reported in Table 5.1.

Table 5.1 Rates of 1-octene insertion into the Ir-H bonds of (PCP)Ir(H)(Y) (50 °C, p-xylene)

	k_{12} (10^{-4}) ($mole^{-1}s^{-1}$)	$\Delta G^{\neq}_{12}$ (kcal/mole)	k_{21} (10^{-4}) ($mole^{-1}s^{-1}$)	$\Delta G^{\neq}_{21}$ (kcal/mole)
(PCP)Ir(H)(Cl)[a]	7.04	28.89	5.93	29.02
(PCP)Ir(H)(CCPh)	12.8	23.23	4.7	23.88
(PCP)Ir(H)(OH)	19.7	22.96	6.4	23.68
(PCP)Ir(H)(OPh)	33.3	22.62	7.29	23.59

[a] *Measured at120 °C*

Although the data in Table 5.1 apparently indicates that the electron-withdrawing groups tend to reduce the rate of insertion of 1-octene into the Ir-H bonds, the trend is not rigorously followed in the series. A comparison between (PCP)Ir(H)(Cl) and (PCP)Ir(H)(CCPh) shows that although the rate is much slower with the former, the *sp* hybridized carbon in the latter is expected to have similar electron withdrawing ability compared to the "Cl" in the former complex; the "Cl" has a significant π-donating ability,

which is absent in the “CCPh” system. During the course of the reaction, no olefin bound 18-electron species of the type (PCP)Ir(H)(Y)(1-octene) was detected by ^{1}H, ^{2}H or ^{31}P with either of the complexes. Therefore no conclusion can be drawn in terms of any extra stabilization of the olefin bound ground state (and subsequent slower insertion rate) with either (PCP)Ir(H)(Cl) or (PCP)Ir(H)(CCPh).

In explaining the results obtained from measurement of the rates of insertion of *para* substituted styrenes in the Nb-H bonds of $Cp^{*}_{2}Nb(H)$(styrene) complexes, Bercaw commented that in the insertion transition state a mild positive was developed at the metal center as well as on the olefin β-carbon (Scheme 5.6).[7] It is possible that a similar effect has resulted in an increase in insertion rate in the (PCP)Ir(H)(Y) systems, on going from (PCP)Ir(H)(CCPh) to either (PCP)Ir(H)(OH) or (PCP)Ir(H)(OPh). Although an oxygen atom is know to be more electron withdrawing compared to the "CCPh" fragment, it is also much more π-donating relative to the phenylacetylide. Consequently a positive charge developed on the Ir center in the TS, would be much more stabilized with either "OH" or "OPh" compared to the "CCPh". Similarly between (PCP)Ir(H)(OH) and (PCP)Ir(H)(OPh), the latter complex because of the phenyl ring attached to oxygen could show a slightly better π-donating behavior. A phenyl ring is known to be electron withdrawing by inductive effect but at the same time, when attached to an oxygen atom it can exhibit electron-releasing effect by stabilizing a positive charge via resonance. It is possible that this due to this +R effects the phenoxy complex, (PCP)Ir(H)(OPh), has shown the highest insertion rate among the four studied here.

5.2.1.5 Study of olefin insertion using (PCP)Ir(H)(Ph) and 3,3-dimethyl-1-butene (TBE)

Although, during the study of olefin insertion, as indicated by both ^{1}H and ^{31}P NMR, no species other than (PCP)Ir(H)(Y) was found to be present in the solution, in order to confirm that the exchange or isomerization observed wad due to insertion/β-hydride elimination reaction and not due C-H addition/elimination mechanism *via* Ir(I)-Ir(III) or Ir(III)-Ir(V) couple, two more experiments were carried out.

To test if the reaction was going *via* Ir(I)-Ir(III) the reaction was carried out with (PCP)Ir(H)(OPh) and the same octene (*cis-1,2-*d_2) in the presence of free PhOH (20 mM). No change in product distribution or rate of either insertion was observed and therefore it was very unlikely that the exchanged or isomerized products were actually formed though the C-H addition/elimination mechanism *via* Ir(I)-Ir(III).

A second experiment was carried out where TBE was used as the substrate to investigate its insertion into the Ir-H bond of (PCP)Ir(H)(Ph). Due to the absence of any γ-H, TBE cannot isomerize and its internal olefinic proton (β proton) has a better resolution compared to the internal proton of 1-olefins. Additionally, unlike 1-octene, due to its bulky nature TBE does not displace benzene from the (PCP)Ir(H)(Ph) (to form a π-bound complex), thus allowing insertion reaction to be carried out. As shown in Scheme 5.13 there are three exchanged products possible from the reaction. An internal exchanged product **A** is possible only through 1,2 insertion/β-H elimination mechanism (the site is too crowded for exchange via oxidative addition). Both **B** and **C** can form via

oxidative addition/C-H elimination mechanism (involving an Ir(III)-Ir(V) couple); due to the steric factors terminal exchange (formation of both **B** or **C**) *via* 2,1 insertion/*β*-H elimination would be too improbable.

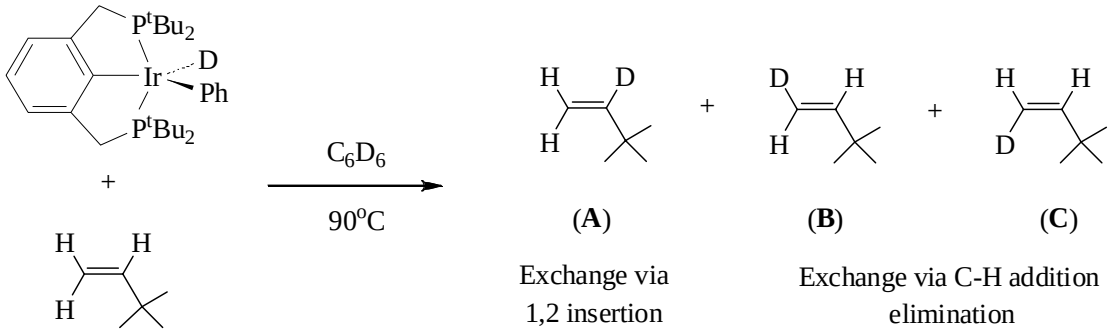

Scheme 5.13 Possible exchanged products on reaction of 3,3-dimethy-1-butene (TBE) with (PCP)Ir(H)(Ph)

To a solution of 10 mM PCPIrH_2 in neat benzene-d_6 0.2 M TBE was added, the tube was sealed under argon and monitored by both ^{1}H and ^{31}P NMR until the full formation of (PCP)Ir(H)(Ph) was observed. The tube was then heated in a GC oven at 90°C. After 8 h of reaction roughly 5% of exchange was observed at both terminal (**B** + **C**) and internal position. After overnight heating, there was slightly more exchange at the internal position compared to the terminal, along with roughly 1:1 ratio of **B** to **C**. From the point of view of steric crowding, it was obvious that **B** has a lower barrier of formation relative to **C**. It could be possible that the 2,2-dimethylbutane (formed *via* hydrogenation of TBE) was dehydrogenated by a very small amount of "(PCP)Ir" present into the system producing catalytic amount of active (PCP)IrH_2. This iridium-

dihydride complex can then hydrogenate and dehydrogenate the initial exchanged products (**A**, **B** or **C**) giving a mixture of products (Scheme 5.14).

To examine, if the results discussed above was really due to the exchange *via* (PCP)IrH_2 the reaction was repeated under two different conditions – a "neutral" and a "hydrogen deficient" environment.

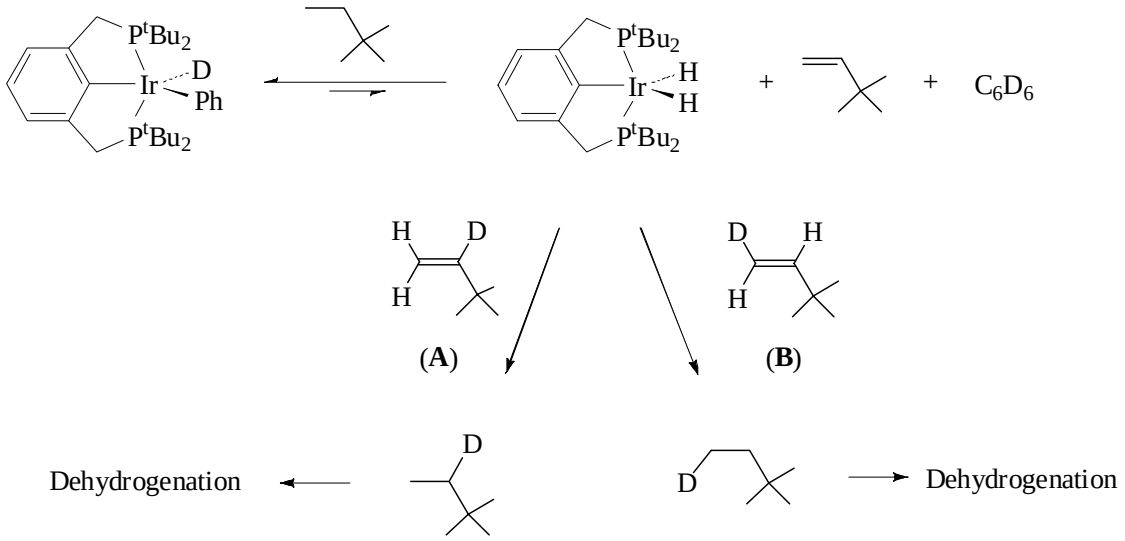

Scheme 5.14 Distribution of exchanged products via hydrogenation-dehydrogenation sequence through catalytic amount of (PCP)IrH_2

In the first case, to a solution of 10 mM PCPIrH_2 in neat benzene-d_6 was added excess TBE and the solution was pumped down to about 90% of its initial volume to remove the 2,2-dimethylbutane (hydrogenated TBE) along with any unreacted TBE. The solution was then made 0.2 M *w.r.t.* fresh TBE and heated at 90°C in a sealed tube. After

20 h, about 5% of 1,2 exchanged product (**A**, Scheme 5.13) was observed along with ~15% of **B**. Moreover, the ratio of **B** to **C** was roughly 8:1 - indicating that part of the earlier results was due to hydrogenation-dehydrogenation mechanism shown in Scheme 5.14. To simulate a "hydrogen deficient" environment, the reaction was carried out (after pumping off the 2,2-dimethylbutane and unreacted TBE) in presence of 0.1 M norbornene (NBE). Since NBE known to be a good acceptor, carrying out the reaction in presence of an excess amount of NBE would minimize any unreacted $PCPIrH_2$ (if at all there) being left in the solution and catalyzing the actual exchange reaction. After heating at 90°C for 20 h, the product yield got reduced by a small amount, although the relative ratios remained the same (2-3% internal exchanged product **A**; 10% of combined **B** and **C**). No evidence was found for hydrogenation activity of NBE (intensity of olefinic peaks remained unchanged) and the **B** to **C** ratio was also similar to what was found in the "neutral" environment.

This served as the confirmed that the exchange was not due to any unreacted $(PCP)IrH_2$ but was rather *via* insertion into Ir-D bond of PCPIr(D)(Ph). Small drop in the yield of exchanged products under "hydrogen deficient" condition, relative to the "neutral" condition could be explained *via* relative competition between benzene and NBE to trap the 14e intermediate, "PCPIr" (Scheme 5.15).

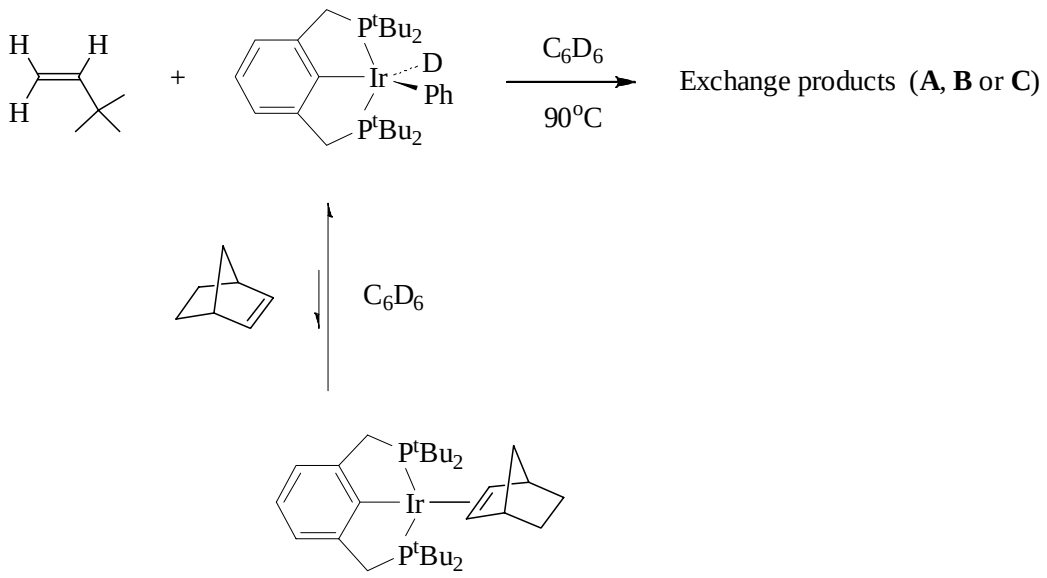

Scheme 5.15 Equilibrium between (PCP)Ir(Ph)(D) and (PCP)Ir(NBE) leading to slower rate of exchange

5.2.2 DFT Calculations for Olefin Insertion

DFT calculations were conducted on four complexes ((PCP)Ir(H)(Y) - Y = Cl, OH, CCH and H) relating insertion and a cycle (hypothetical, except Y = H) for X-H addition to olefin, by Yuriy Choliy, Karsten Krogh-Jespersen. All calculations were done with full ^{tBu}PCP ligands. It has been attempted to dissect the process into a hypothetical rearrangement of H and Y, which opened a site that allowed olefin to coordinate *cis* to H, followed by insertion, and then elimination of alkyl-Y. The two possible pathways for insertion and subsequent (hypothetical, except Y = H) elimination are shown in Scheme 5.16 and 5.17.

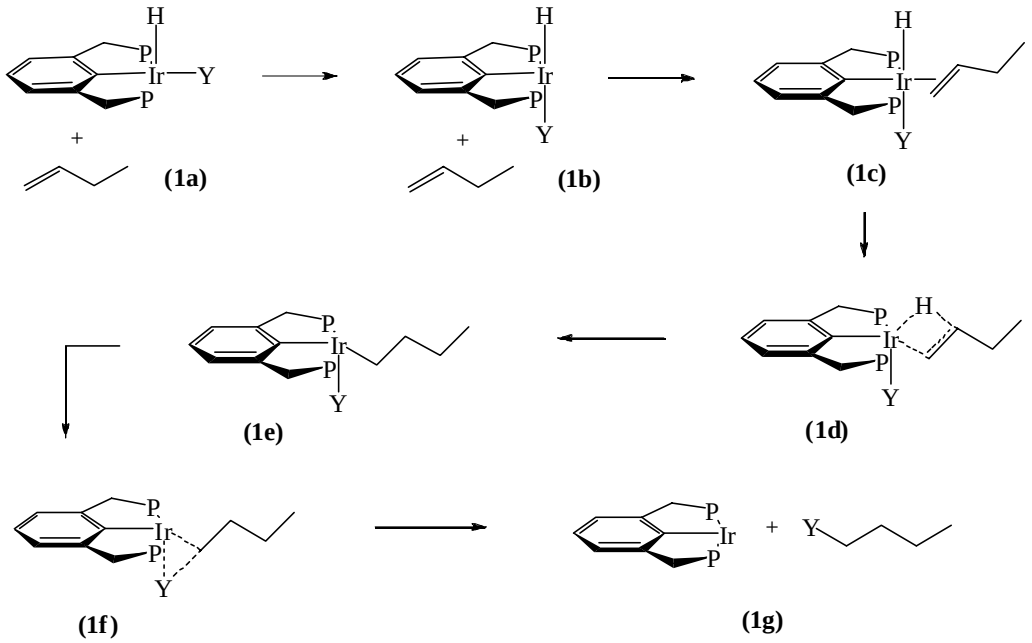

Scheme 5.16 Olefin insertion/alkyl-Y elimination with olefin trans to PCP-aryl ring - pathway ***olefin-trans*** *- (*^{t}*Butyl groups on phosphines are omitted for clarity)*

The (PCP)Ir(H)(Y) complexes are known to exist in a square pyramidal geometry with hydride ligand in the apical position, *cis* to the PCP-aryl ring. As shown in Scheme 5.16, in the **olefin-*trans*** pathway Y moves in a position *trans* to the hydride, opening up a vacant co-ordination site *cis* to the hydride, where incoming olefin can bind and undergo insertion. In the **olefin-*cis*** pathway, both the hydride and Y rearrange to move the hydride *trans* to the PCP-aryl ring, and the incoming olefin binds onto Ir center in the vacant site earlier occupied by the hydride ligand (Scheme 5.17).

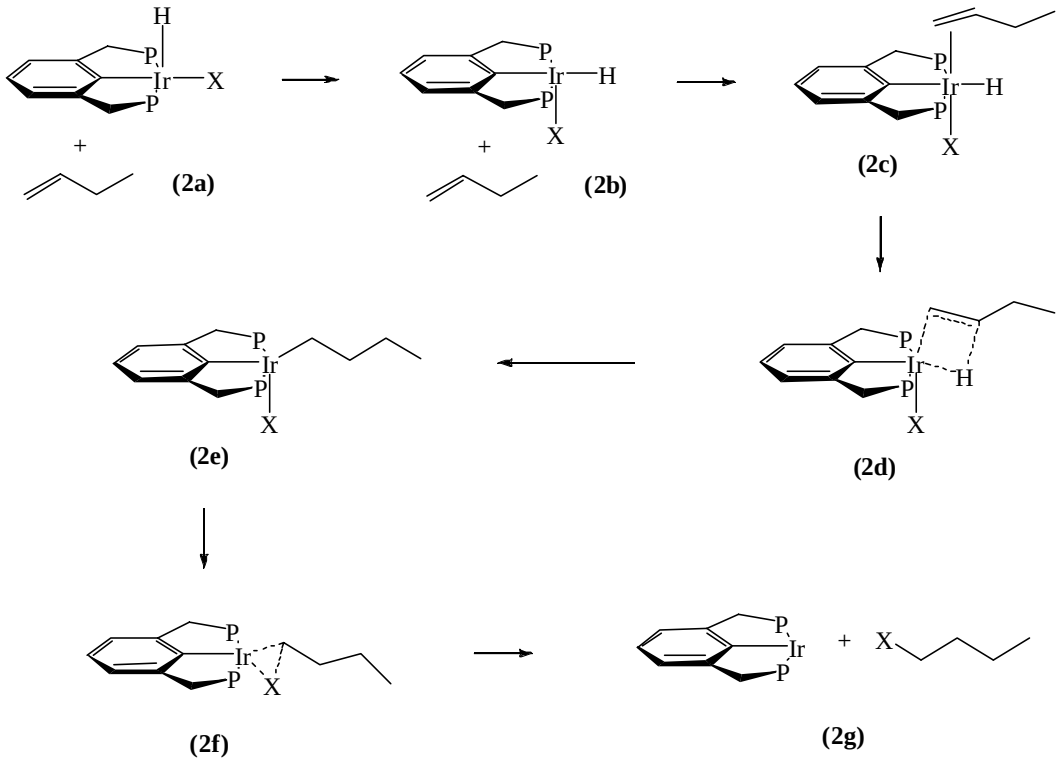

Scheme 5.17 Olefin insertion/alkyl-Y elimination with olefin cis to PCP-aryl ring - pathway ***olefin-cis*** *- (ᵗButyl groups on phosphines are omitted for clarity)*

The results from calculations, for two different pathways and for four complexes (Y = Cl, OH, CCH and H) are shown in Table 5.2 and 5.3.

*Table 5.2 Relative energies (kcal/mole) of different species involved in the insertion/alkyl-Y elimination along pathway **olefin-trans**. TS-I = Transition State for olefin insertion, TS-E = Transition State for alkyl-Y elimination.*

Y = Cl	**H**	**G**
(PCP)Ir(Cl)(H) + butene (**1a**)	0.00	0.00
(PCP)Ir(Cl)(H-cis) + butene (**1b**)	15.91	17.95
(PCP)Ir(Cl)(H-cis)(butene) (**1c**)	-2.04	13.41
(PCP)Ir(Cl)(H-cis)(butene)-TS-I (**1d**)	16.50	48.29
(PCP)Ir(Cl)(butyl) (**1e**)	1.43	16.52
(PCP)Ir(Cl)(butyl)-TS-E (**1f**)	41.53	55.52
(PCP)Ir + butyl-Cl (**1g**)	33.15	30.7

Y = OH	**H**	**G**
(PCP)Ir(OH)(H) + butene (**1a**)	0.00	0.00
(PCP)Ir(OH)(H-cis) + butene (**1b**)	17.13	17.79
(PCP)Ir(OH)(H-cis)(butene) (**1c**)	-1.81	12.78
(PCP)Ir(OH)(H-cis)(butene)-TS-I (**1d**)	23.70	39.18
(PCP)Ir(OH)(butyl) (**1e**)	2.83	16.48
(PCP)Ir(OH)(butyl)-TS-E (**1f**)	35.70	48.30
(PCP)Ir + butyl-OH (**1g**)	12.44	8.96

Y = CCH	**H**	**G**
(PCP)Ir(CCH)(H) + butene (**1a**)	0.00	0.00
(PCP)Ir(CCH)(H-cis) + butene (**1b**)	17.26	19.40
(PCP)Ir(CCH)(H-cis)(butene) (**1c**)	-1.06	14.86
(PCP)Ir(CCH)(H-cis)(butene)-TS-I (**1d**)	17.18	34.61
(PCP)Ir(CCH)(butyl) (**1e**)	1.63	16.21
(PCP)Ir(CCH)(butyl)-TS-E (**1f**)	18.30	33.01
(PCP)Ir + butyl-CCH (**1g**)	9.17	6.97

Y = H	**H**	**G**
(PCP)Ir(H)(H) + butene (**1a**)	0.00	0.00
(PCP)Ir(H)(H-cis) + butene (**1b**)	12.34	15.06
(PCP)Ir(H)(H-cis)(butene) (**1c**)	-11.82	4.86
(PCP)Ir(H)(H-cis)(butene)-TS-I (**1d**)	2.71	19.41
(PCP)Ir(H)(butyl) (**1e**)	-9.33	4.68
(PCP)Ir(H)(butyl)-TS-E (**1f**)	-4.93	9.66
(PCP)Ir + butyl-CCH (**1g**)	-6.78	-7.66

Table 5.3 Relative energies (kcal/mole) of different species involved in the insertion/alkyl-Y elimination along pathway ***olefin-cis****. TS-I = Transition State for olefin insertion, TS-E = Transition State for alkyl-Y elimination*

Y = Cl	**H**	**G**
(PCP)Ir(Cl)(H) + butene (**2a**)	0.00	0.00
(PCP)Ir(Cl)(H-trans) + butene (**2b**)	49.82	49.82
(PCP)Ir(Cl)(H-trans)(butene) (**2c**)	28.27	44.42
(PCP)Ir(Cl)(H-trans)(butene)-TS-I (**2d**)	27.78	44.94
(PCP)Ir(Cl)(butyl) (**2e**)	1.43	16.52
(PCP)Ir(Cl)(butyl)-TS-E (**2f**)	41.53	55.52
(PCP)Ir + butyl-Cl (**2g**)	33.15	30.7

Y = OH	**H**	**G**
(PCP)Ir(OH)(H) + butene (**2a**)	0.00	0.00
(PCP)Ir(OH)(H-trans) + butene (**2b**)	38.72	38.72
(PCP)Ir(OH)(H-trans)(butene) (**2c**)	20.23	37.46
(PCP)Ir(OH)(H-trans)(butene)-TS-I (**2d**)	23.38	39.17
(PCP)Ir(OH)(butyl) (**2e**)	2.83	16.48
(PCP)Ir(OH)(butyl)-TS-E (**2f**)	35.70	48.30
(PCP)Ir + butyl-OH (**2g**)	12.44	8.96

Y = CCH	**H**	**G**
(PCP)Ir(CCH)(H) + butene (**2a**)	0.00	0.00
(PCP)Ir(CCH)(H-trans) + butene (**2b**)	22.73	22.73
(PCP)Ir(CCH)(H-trans)(butene) (**2c**)	19.97	36.65
(PCP)Ir(CCH)(H-trans)(butene)-TS-I (**2d**)	24.17	40.08
(PCP)Ir(CCH)(butyl) (**2e**)	1.63	16.21
(PCP)Ir(CCH)(butyl)-TS-E (**2f**)	18.30	33.01
(PCP)Ir + butyl-CCH (**2g**)	9.17	6.97

Y = H	**H**	**G**
(PCP)Ir(H)(H) + butene (**2a**)	0.00	0.00
(PCP)Ir(H)(H-trans) + butene (**2b**)	2.54	2.54
(PCP)Ir(H)(H-trans)(butene) (**2c**)	-3.04	13.52
(PCP)Ir(H)(H-trans)(butene)-TS-I (**2d**)	2.84	19.73
(PCP)Ir(H)(butyl) (**2e**)	-9.33	4.68
(PCP)Ir(H)(butyl)-TS-E (**2f**)	-4.93	9.66
(PCP)Ir + butyl-CCH (**2g**)	-6.78	-7.66

It was surprisingly difficult to get a transition state for insertions (TS-I) with Y = Cl and OH. The current numbers for Y = Cl seem to favor the **olefin-*cis*** pathway (44.94 over 48.29) whereas, for Y = OH there is no indication for a strong preference of one over the other (39.17 with 39.18). However, since the TS-I for either of these two species could not be fully located, for a comparison between the two pathways (**olefin-*cis* or olefin-*trans*)**, it is probably more meaningful to look at the numbers of other two complexes. Tables indicate **olefin-*trans*** route would be favored strongly for Y = CCH (34.61 over 40.08) and marginally for Y = H (19.41 over 19.73) - suggesting that this pathway is presumably of lower energy route for olefin insertions involving (PCP)Ir(H)(Y) systems.

A comparison of these results with experimental observations indicate that insertion and subsequent elimination is strongly favored for Y = H (both experimentally and computationally). Experimentally, the kinetics of insertion are strongly disfavored by Y = Cl; no evidence for intermediates was found using DFT calculations.

5.2.3 Study of 1-olefin bound ″(PCP)Ir″ fragment – the (PCP)Ir(1-octene) complex

As mentioned in section 5.2.1.3 addition of 1-octene into a solution of complexes (PCP)Ir(H)(Y) (Y = Ph, NHPh, *o*-F-Ph and 4-Cl-3,5-$(CH_3)_2$Ph) in *p*-xylene resulted an equilibrium between the (PCP)Ir(H)(Y) and (PCP)Ir(1-octene) complex at 25 °C. (PCP)Ir(1-olefin) is supposedly the catalyst resting state during the transfer dehydrogenation of *n*-alkanes (PCP)IrH_2. Since it is believed to be a key intermediate in the catalytic cycle we wanted to characterize the complex by both ^{31}P and ^{1}H NMR.

The complex, (PCP)Ir(1-octene), can be synthesized and isolated in a fairly straight forward manner by adding and excess of 1-octene into a solution of (PCP)IrH_2 in p-xylene and then removing the excess octene, along with the solvent and *n*-octane formed.

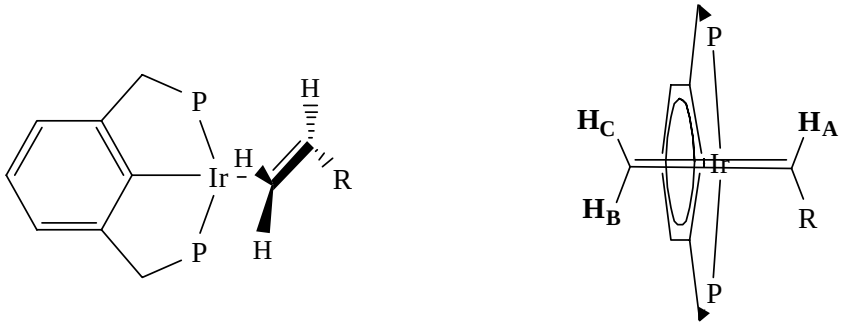

Fig. 5.8 (PCP)Ir(1-octene) complex – planar and perpendicular view. ^{t}butyl groups on phosphines are omitted for clarity. R = hexyl.

1H NMR signal of a solution of the complex in mesitylene-d_{12} at 25 °C showed three distinct multiplets in a ratio of 1:1:1 for the olefinic protons $\mathbf{H_A}$ (4.53 ppm), $\mathbf{H_B}$ (3.80 ppm) and $\mathbf{H_C}$ (3.88 ppm). The assignments were confirmed by comparing ^{1}H and ^{2}H NMR spectra of (PCP)Ir(*cis*-1,2-d_2) complex, where, either only $\mathbf{H_A}$ & $\mathbf{H_C}$ or only $\mathbf{H_B}$ are/is observed depending on the NMR nuclei used. ^{31}P NMR of the complex at 25 °C showed four broad peaks (centered at 58.2 ppm) with a second order pattern due to two inequivalent phosphorous atoms. A ^{1}H NMR spectra recorded in presence of 1:1 excess of free octene exhibited sharp olefinic signal for free as well as the bound octene – indicating there was no external exchange between the free and the bound olefin. This observation, along with broad ^{31}P NMR signals strongly suggested the presence of an intramolecular process.

On slowly cooling the solution from 25 °C, ^{31}P signals started getting sharp, finally becoming static at -40 °C. The methylenes on the pincer backbone were also

resolved into three sets of multiplets, in the ^{1}H NMR. On warming the solution, both methylenes, in the ^{1}H NMR, and the ^{31}P signals got broad and finally coalesced to a single peak at +10 °C and +60 °C, respectively. During this period, the free and bound olefin peaks remained sharp until +50 °C, allowing measurement of kinetic and thermodynamic parameters for the "intramolecular only" processes within a temperature rage of -40 °C to +50 °C.

A closer look at the methylene protons (on the PCP-ligand backbone) in the ^{1}H NMR indicated a number of interesting observations. At -40 °C the methylenes showed three separate multiplets for the four protons (one, presumably due to overlapping $\mathbf{H_Q}$ and $\mathbf{H_S}$ which were in fairly similar chemical environment and the other two were due to $\mathbf{H_R}$ and $\mathbf{H_T}$). On warming the sample, the sets due to $\mathbf{H_R}$ and $\mathbf{H_T}$ were found to coalesce together and also the peak due to overlapping $\mathbf{H_Q}$ and $\mathbf{H_S}$ started becoming broad, and could be identified as three different sets until 10 °C. This observation suggested an olefin flipping process, possibly *via* de-coordination of the π-bound olefin to form a metal olefin σ-complex, which can reattach itself as a π-complex in either direction, ′R′ facing up or down. As shown in Fig 5.9, this would make the methylenes, $\mathbf{H_R}$ and $\mathbf{H_T}$ equivalent.

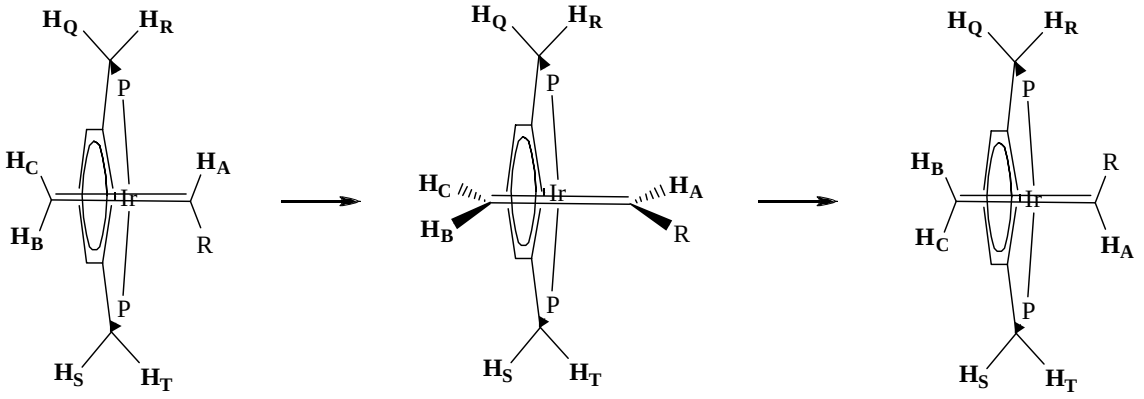

Fig. 5.9 Flipping of the π-bound olefin. ^{t}butyl groups on phosphines are omitted for clarity. R = hexyl.

On warming beyond 10 °C, all four methylenes coalesce to a single broad peak. As mentioned above, a simple flipping process would account for equivalency of only $\mathbf{H_R}$ and $\mathbf{H_T}$ and of all four protons. Therefore it was apparent that either a rotation of the σ-bound olefin or formation of a vinyl-hydride intermediate which, during the C-H activation/elimination did a rotation was responsible for making all the four methylene protons equivalent above 10 °C (Note: A rotation of the π-bound olefin in combination with the flipping process would also result in equivalency of all methylene protons, however, rotation of the π-bound olefin would be too improbable due to steric hindrance offered by the large ^{t}butyl groups on the phosphines). Interestingly, since, either an olefin flipping or a combination of flipping and olefin-rotation resulted in the phosphorus atoms getting equivalent, the full Eyring plot (-40 °C to +50 °C) obtained from the ^{31}P line-

shape analysis also indicated the presence of two different processes below and above 10 °C (Fig 5.10).

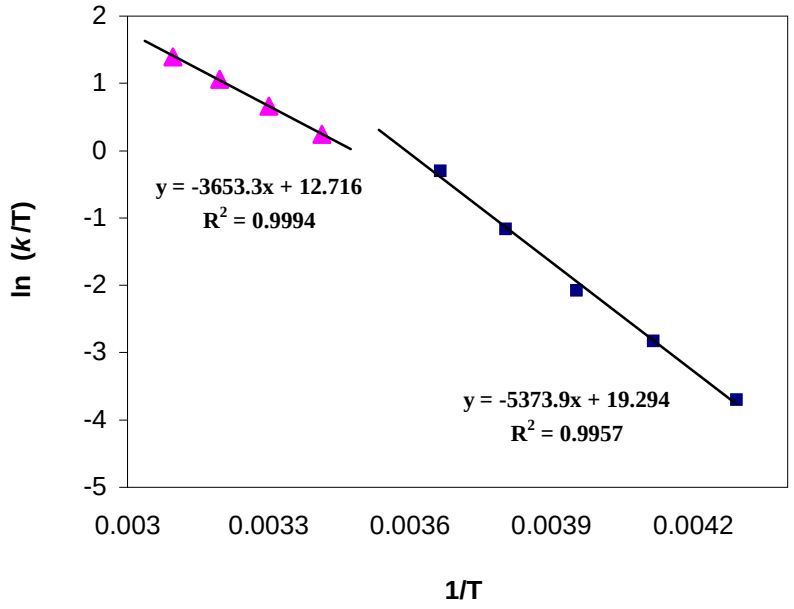

Fig. 5.10 Eyring plot obtained from the ^{31}P line-shape analysis for olefin flipping (■) and a combination of flipping and rotation (▲) processes in the (PCP)Ir(1-octene) complex

Using the Eyring equation -

$$\ln\frac{k}{T} = \frac{-\Delta H^{\neq}}{R}\cdot\frac{1}{T} + \ln\frac{k_b}{h} + \frac{\Delta S^{\neq}}{R}$$

$\Delta H^{\neq}$ and $\Delta S^{\neq}$ for the olefin flipping only process (occurring until 10 °C and indicated by a solid square above) were found to be 10.68 kcal/mole and -8.88 cal/K/mole, respectively. For the processes above 10 °C (presumably a combination

flipping and rotation) the respective values are 7.26 kcal/mole and -21.94 cal/K/mole. Much higher $\Delta S^{\neq}$ value associated with the latter pathways clearly indicated that it was a more hindered one, which was obvious since rotation of the olefin would cause steric interactions with the ^{t}butyl groups on phosphines as compared to a simple flip. On heating the sample, the olefinic protons in both bound and free 1-octene started getting broad at 55 °C, indicating the onset of intermolecular exchange and the ^{31}P signals finally merge onto a singlet at 60 °C.

5.3 Conclusion

Olefin insertion into the Ir-H bonds of different pincer complexes (PCP)Ir(H)(Y) were investigated using *cis*-1,2-dideutero-1-octene (*cis-1,2-d*$_2$) as the substrate. At least four systems (Y = Cl, CCPh, OH and OPh) were found to be stable under the reaction conditions, allowing detailed kinetic experiments to be carried out on them. A number of other (PCP)Ir(H)(Y) complexes (Y = Ph, *o*-F-Ph etc) were stable in solution only in the absence of 1-octene. Addition of 1-octene resulted in displacement of HY (*e.g.* PhH, PhF) from these complexes, producing a stable olefin bound product - (PCP)Ir(1-octene).

1,2 insertion of (*cis-1,2-d*$_2$) followed by β-D elimination resulted in the formation of *cis*-1-deutero-1-octene as the only product. 2,1 insertion primarily led to isomerization of the double bond. The insertion and β-H/D elimination products were characterized by

^{1}H, ^{2}H and ^{13}C NMR. As indicated by ^{2}H NMR – in cases when β-D elimination took place, the resulting Ir-D exchanged rapidly with the C-H of ^{t}Bu groups on phosphines. Both 1,2 and 2,1 insertion rates were found to increase in the in the following sequence Y = Cl < CCPh < OH < OPh. (PCP)Ir(H)(Cl) was found to be strongly resistant to insertions, as the reaction showed some reasonable kinetic rate (half-life in the order of 2-3 days) only at 120°C. The sequence apparently showed a minor indication of reduction in rate by strong σ-withdrawing/low π-donating effect, although an extreme unreactivity for Y = Cl relative to CCPh could not be fully reconciled.

Using DFT calculations were performed involving the insertion and subsequent C-Y elimination from the iridium center. Computationally it was hard to locate an insertions transition state with Y = Cl, OH and the results indicated a slight preference for pathway in which olefin binds to the metal center in between H and Y with a *trans* arrangement to the PCP-aryl ring.

Finally, the olefin bound 14-electron complex - (PCP)Ir(1-octene) was characterized by ^{1}H and ^{31}P NMR. The complex showed a clean intermolecular only dynamic behavior in the ^{31}P NMR from 50 °C to -35°C. $\Delta S^{\neq}$ and $\Delta H^{\neq}$ for the intramolecular processes were calculated from the Eyring plot.

5.4 Experimental

5.4.1 General procedures

All routine manipulations were performed at ambient temperature in an argon-filled glove box or under argon using standard Schlenk techniques. Kinetic experiments were carried out in flame-sealed NMR tubes and were heated in a GC oven maintained at a constant temperature. All NMR solvents (protiated or deuterated) were distilled from sodium/potassium alloy, vacuum transferred under argon and stored in an argon-filled glove box. ^{1}H, $^{31}P\{^{1}H\}$ and $^{13}C\{^{1}H\}$ NMR spectra were obtained on a 400-MHz, Varian Inova-400 spectrometer or on a 300-MHz, Varian Mercury-300 spectrometer. ^{2}H NMR spectra were obtained in 300-MHz, Varian Mercury-300 spectrometer. ^{1}H and ^{2}H chemical shifts were reported in ppm downfield from tetramethylsilane and were referenced to residual $^{1}H/^{2}H$ of protiated/deuterated solvents. ^{31}P NMR chemical shifts were referenced to PMe_3. Norbornene was purchased from Sigma-Aldrich, sublimed under vacuum and was stored in an argon-filled glove box. All other chemicals were used as received from commercial suppliers.

5.4.2 Synthesis of *cis*-1,2-dideutero-1-octene (*cis-1,2-d*$_2$)

This was done using the literature reported procedure used for hydrogenation of phenylacetylene.[12] A 500 mL reaction flask is charged with 25 mL (0.17 mole) of 1-octyene, 0.88 g of Lindlar Catalyst (~5% palladium on calcium carbonate; poisoned with lead), 8.8 mg of 2,2'-(Ethylenedithio)diethanol (Lindlar Catalyst Poison) and 150 mL of

n-hexane. The apparatus is evacuated, and deuterium (99.9% D) is admitted to a pressure slightly above 1 atm. Stirring is started, causing rapid absorption of deuterium. The deuterium pressure is kept close to 1 atm. throughout the reaction and composition of the reaction mixture was periodically monitored by GC. Reaction was stopped when complete consumption of the 1-octyne was indicated. Solution was filtered through a pad of Celite and *n*-hexane was distilled off. The product was distilled from sodium/potassium alloy, vacuum transferred under argon and stored in an argon-filled glove box. ^{1}H and ^{2}H NMR indicated about 95% purity. ^{2}H NMR (*p*-xylene): δ 5.08 (s, 1D, *internal*), 5.89 (d, 1D, J_{HD} = 1.54 Hz, *terminal*).

5.4.3 Synthesis of (PCP)Ir(H)(Y) complexes

5.4.3.1 Synthesis of (PCP)Ir(H)(Y) (Y = Cl, OH, Ph, NHPh, CCPh)

(PCP)Ir(H)(Cl) was synthesized according to the literature reported procedure *via* cyclometalation of the pincer ligand pincer ligand, ^{tBu}PCP, using $[Ir(COD)Cl]_2$.[13] For Y = Ph,[10a] OH,[10b] NHPh[10c] and CCPh[10d] the general procedure was followed which included reacting (PCP)IrH_2 with excess of an hydride acceptor (NBE, TBE or 1-olefin) in presence of the corresponding HY, followed by pumping off the excess/hydrogenated acceptor along with the solvent to isolate the pure complex, (PCP)Ir(H)(Y).

5.4.3.2 Synthesis of (PCP)Ir(H)(OPh)

To 0.5 mL of *p*-xylene was added 8.83 mg of (PCP)IrH_2 (0.015 mmol) and 2.8 mg of NBE (0.03 mmol). The solution was shaken vigorously and allowed to stand at RT

for 15 min. 1.5 mg of phenol (0.016 mmol) was then added to the solution and the color changed to bright orange. After keeping it at RT for 30 min, the solution was evacuated to dryness at 50°C, removing the solvent, norbornane and any unreacted norbornene and phenol. The solid product was redissolved in *p*-xylene and a single peak (at 63.05 ppm) in ^{31}P NMR indicated pure product.

5.5 References

1. McDermott, J. X.; White, J. F.; Whitesides, G. M. *J. Am. Chem. Soc.* **1976**, *98*, 6521.

2. Bower, B. K.; Tennent, H. G. *J. Am. Chem. Soc.* **1972,** *94,* 2512.

3. Labinger, J. A,; Hart, D. W.; Seibert, W. E., III; Schwartz, J. *J. Am. Chem. Soc.* **1975,** *97,* 3851. (b) Nakamura, A,; Otsuka, S. *J. Am. Chem. Soc.* **1973,** *95,* 7262.

4. (a) Whitesides, G. M.; Gaasch, J. F.; Stredonsky, E. R. *J. Am. Chem. Soc.* **1972**, *94*, 5258. (b) Reger, D. L.; Culbertson, E. C. *J. Am. Chem. Soc.* **1976**, *98*, 2789. (c) Kazlauskas, R. J.; Wrighton, M. S. *J. Am. Chem. Soc.* **1982**, *104*, 6005; (d) Watson, P. L.; Roe, D. C. *J. Am. Chem. Soc.* **1982**, *104*, 6471. (e) Komiya, *S.;* Morimato, Y.; Yamamoto, A.; Yamamoto, T. *Organometallics* **1982**, *11*, 1528. (f) Ozawa, F.; Ito, T.; Yamamoto, A. *J. Am. Chem. Soc.* **1980**, *102*, 6457.

5. Clark, H. C.; Jablonski, C. R. *Inorg. Chem.* **1974**, *13*, 2213.

6. Halpern, J.; Okamoto, T. *Inorg. Chim. Acta,* **1984**, *89*, L53.

7. Doherty, N. M.; Bercaw, J. E. *J. Am. Chem. Soc.* **1985**, *107*, 2670.

8. Ackerman, L. J.; Green, M. L. H.; Green, J. C.; Bercaw, J. E. *Organometallics* **2003,** *22,* 188.

9. (a) Lee, H.; Desrosiers, P. J.; Guzei, I.; Rheingold, A. L.; Parkin, G. *J. Am. Chem. Soc.* **1998**, *120*, 3255. (b) Shin, J. H.; Parkin, G. *Chem. Commun.* **1999**, 887.

10. (a) Kanzelberger, M.; Singh, B.; Czerw, M.; Krogh-Jespersen, K.; Goldman, A. S. *J. Am. Chem. Soc.* **2000**, *122*, 11017. (b) Morales-Morales, D.; Lee, D. W.; Wang, Z. H.; Jensen, C. M. *Organometallics* **2001**, *20*, 1144. (c) Kanzelberger, M.; Zhang, X.; Emge, T. J.; Goldman, A. S.; Zhao, J.; Incarvito, C.; Hartwig, J. F. *J. Am. Chem. Soc.* **2003**, *125*, 13644. (d) Ghosh, R.; Zhang, X.; Achord, P.; Emge, T. J.; Krogh-Jespersen, K.; Goldman, A. S. *J. Am. Chem. Soc.* **2007**, *129*, 853.

11. (a) Mendes, P. *Comput. Appl. Biosci.* **1993**, *9*, 563-571. (b) Mendes, P. *Trends Biochem. Sci.* **1997**, *22*, 361-363. (c) Mendes, P.; Kell, D. *Bioinformatics* (Oxford) **1998**, *14*, 869-883.

12. Lindlar, H.; Dubuis, R *Organic Syntheses* **1973**, *Coll. Vol. 5*, 880.

13. Moulton, C. J.; Shaw, B. L. *J. Chem. Soc., Dalton Trans.* **1976**, 1020.

CURRICULUM VITA

Amlan Ray

Education:

1996	B.Sc. Chemistry, University of Calcutta, Calcutta, India.
1998	M.Sc. Chemistry, Indian Institute of Technology Kharagpur, Kharagpur, India
2000	M.Tech. Materials Science, Indian Institute of Technology Bombay, Mumbai, India
2007	Ph.D. Chemistry, Rutgers, The State University of New Jersey, New Brunswick, NJ

Publications:

- "Catalytic post-modification of alkene polymers: Chemistry and kinetics of dehydrogenation of alkene polymers and oligomers with Ir complexes" **Ray, Amlan**; Kissin, Yury V.; Zhu, Keming; Goldman, Alan S.; Cherian, Anna E.; Coates, Geoffrey W. *J. Mol. Cat. A: Chemical* **2006**, *256(1-2)*, 200-207.

- "Dehydrogenation of aliphatic polyolefins catalyzed by pincer-ligated iridium complexes" **Ray, Amlan**; Zhu, Keming; Kissin, Yury V.; Cherian, Anna E.; Coates, Geoffrey W.; Goldman, Alan S. *Chem. Commun.* **2005**, *27*, 3388-3390.

- “Investigation on T_c tuned nanoparticles of magnetic oxides for hyperthermia applications” Giri, Jyotsnendu; **Ray, Amlan**; Dasgupta, S.; Datta, D.; Bahadur, D. *Bio-Med. Mater. Engg.* **2003**, *13(4)*, 387-399.

- "Compaction and sintering behavior of glass alumina composites", **Ray, Amlan**; Tiwari, A.N. *Mater. Chem. Phys.* **2001**, *67(1-3)*, 220-225.